THE UNIVERSITY *of* LIVERPOOL

Residential Demand Side Scheduling Considering Users' Concerns and Uncertainties

Thesis submitted in accordance with the
requirements of the University of Liverpool
for the degree of Doctor of Philosophy

in

Electrical Engineering and Electronics

by

Yuefang Du, B.Sc.(Eng.)

July 2017

Residential Demand Side Scheduling Considering Users' Concerns and Uncertainties

by

Yuefang Du

Acknowledgements

I would like to express my great appreciation to my supervisor, Dr. Lin Jiang, for his valuable help, inspiration, and encouragement in my research work. The research methods and the writing and presenting skills he taught me will benefit me throughout my life.

I am particularly grateful to all the colleagues in the Smart Grid Control and Renewable Energy Group, the Department of Electrical Engineering and Electronics, the University of Liverpool, for their kind help in my work and life. Thanks for all the meetings and talks we had together, and these meetings and talks broaden my mind and horizon on both research and living. I would like to offer my special thanks to Dr. Yuanzheng Li and Mr. Chao Duan for their recommendation of relevant papers and books and technical support in realizing my research ideas.

I would like to thank China Scholarship Council and the University of Liverpool for funding my study in the United Kingdom.

Thanks go to my friends, Ms. Pei Zhang and Ms. Yi Fang, for their support and friendship.

Finally, I would like to express my deep gratitude to my beloved family for giving me strength and support during these years.

Abstract

In the residential demand side scheduling (RDSS), the energy consumption of home appliances should be scheduled with users' concerns satisfied and uncertain factors should be taken into account as they affect users' concerns. The operational safety of appliances is of great concern to users especially when appliances are scheduled in periods when users are not at home or are asleep. In these periods, appliances are in operation without users' monitoring. The energy consumption of manually operated appliances (MOAs) is uncertain when the energy consumption of schedulable appliances is scheduled and this uncertainty will affect users' electricity cost. The uncertainty of outdoor temperature has impact on the energy consumption scheduling of the heating, ventilation and air conditioning system which is one of the main RDSS sources, and it affects both the electricity cost and users' comfort.

The appliances' operational safety is formulated based on whether users are at home and awake to monitor appliances' operations. The approach of finding the Pareto-optimal front is adopted to solve the multi-objective RDSS with the consideration of the operational safety of appliances. The uncertainties of MOAs and the outdoor temperature are dealt with through the robust optimization approach and the distributionally robust optimization approach, respectively. With the consideration of the operational safety of appliances and uncertainties of MOAs and the outdoor temperature, the RDSS is further improved with the electricity cost reduced and users' concerns satisfied.

Declaration

The author hereby declares that this thesis is a record of work carried out in the Department of Electrical Engineering and Electronics at the University of Liverpool during the period from October 2013 to July 2017. The thesis is original in content except where otherwise indicated.

Contents

List of Figures

List of Tables

List of Abbreviations

DR	Demand response
RDSS	Residential demand side scheduling
MORDSS	Multi-objective residential demand side scheduling
ESS	Energy storage system
RES	Renewable energy source
HEMS	Home energy management system
EMC	Energy management controller
MOA	Manually operated appliance
SA	Schedulable appliance
HVAC	Heating, ventilation and air conditioning
LOT	Length of operation time
OTI	Operation time interval
UTR	Unsafety time rate
PAR	Peak-to-average ratio
TOUP	Time-of-use pricing
RTP	Real-time pricing
IBR	Inclining block rate
ROA	Robust optimization approach
SOA	Stochastic optimization approach
DROA	Distributionally robust optimization approach
GA	Genetic algorithm
PSO	Particle swarm optimization
IP-EA	Intergeneration projection evolutionary algorithm
NSGA	Nondominated sorting genetic algorithm
SDP	Semidefinite programming
LP	Linear programming

Notations

Chapter 3

a	Index of appliance.
n	The number of appliances.
t	Index of time slot.
x_a	The start time slot of the operation of appliance a.
T	The horizon of energy consumption scheduling.
X	The vector of appliances' start time slots.
i, j	Index of X.
k	The number of X of the Pareto-optimal front.
I	The set of indexes of X of the Pareto-optimal front.
$\mathbf{\Omega}$	The set of all feasible X.
$\mathbf{X}$	The set of X of the Pareto-optimal front.
α	The earliest start time of appliance's operation.
β	The deadline of appliance's operation.
γ	The length of operation time.
s_a	The number of time slots in which users are at home and awake when appliance a is in operation.
S_a	The indication of the on-off status of appliance a.
$M(t)$	Users' at-home status at time slot t.
$N(t)$	Users' awake status at time slot t.
e_a^t	The energy consumption of appliance a at time slot t.
E_a	The energy consumption vector of appliance a in the scheduling horizon T.
l_t	The total energy consumption of appliances at time slot t.
prc_t	The electricity price at time slot t.
$f_1(X)$	The appliances' operational unsafety.
$f_2(X)$	The appliances' electricity cost.
$f_3(X)$	The appliances' operational delay.
$F(X)$	The vector of multiple objectives.
ρ_a	The unsafety parameter of appliance a.
σ_a	The delay parameter of appliance a.
UTR_a	The unsafety time rate of appliance a.

DTR_a	The delay time rate of appliance a.
w_1, w_2, w_3	The importance factor of f_1, f_2, f_3.
η_1, η_2, η_3	The constraint factor of f_1, f_2, f_3.
$\underline{f_1}, \underline{f_2}, \underline{f_3}$	The minimum value of f_1, f_2, f_3 in $\mathbf{\Omega}$.
$f_1^{\min}, f_2^{\min}, f_3^{\min}$	The minimum value of f_1, f_2, f_3 in $\mathbf{X}$.
$f_1^{\max}, f_2^{\max}, f_3^{\max}$	The maximum value of f_1, f_2, f_3 in $\mathbf{X}$.
$f_1^{\mathrm{P}}, f_2^{\mathrm{P}}, f_3^{\mathrm{P}}$	The value of f_1, f_2, f_3 of the final solution of the Pareto approach.
$f_2^{\mathrm{W}}, f_3^{\mathrm{W}}$	The value of f_2, f_3 of the final solution of the Weight approach.
F^{P}	The vector of values of f_1, f_2, f_3 of the final solution of the Pareto approach.
N	The number of objectives.
m	Index of objective.
δ_m	The importance rank of objective m.
w_m	The importance factor of objective m.

Chapter 4

t, θ	Index of time slot.
l_t	The total energy consumption of home appliances at time slot t.
prc_t	The electricity price at time slot t based on the pricing scheme with the combination of RTP and IBR.
e_t	The real-time electricity price at time slot t.
c	The threshold of energy consumption.
P	The power vector of an appliance.
p_θ	The power consumption of an appliance at time slot θ.
α	The earliest start time of appliance's operation.
β	The deadline of appliance's operation.
γ	The length of operation time.
ϵ	The multiplier of electricity price when l_t exceeds c.
s	Scenario index.
ρ_s	The probability of scenario s.
NS	The number of scenarios.
i, j	Index of SA,MOA.
m, n	The number of MOAs,SAs.
b, d	Index of non-interruptible,interruptible SA.

f, g	Index of non-suspendable,suspendable MOA.
x_i^t	The energy consumption of SA i at time slot t.
u_j^t	The energy consumption of MOA j at time slot t.
x_b^t	The energy consumption of non-interruptible SA b at time slot t.
x_d^t	The energy consumption of interruptible SA d at time slot t.
u_f^t	The energy consumption of non-suspendable MOA f at time slot t.
u_g^t	The energy consumption of suspendable MOA g at time slot t.
t_b	The start time slot of the operation of non-interruptible SA b.
t_f	The start time slot of the operation of non-suspendable MOA f.
$\gamma_f^{\min}$	The minimum LOT of non-suspendable MOA f.
$\gamma_f^{\max}$	The maximum LOT of non-suspendable MOA f.
$\gamma_g^{\min}$	The minimum LOT of suspendable MOA g.
$\gamma_g^{\max}$	The maximum LOT of suspendable MOA g.
T	The horizon of energy consumption scheduling.
H	The set of time slots in the scheduling horizon.
X_b	The energy consumption schedule of non-interruptible SA b.
X_d	The energy consumption schedule of interruptible SA d.
U_f	The energy consumption case of non-suspendable MOA f.
U_g	The energy consumption case of suspendable MOA g.
$\mathbf{X}$	The energy consumption schedule of SAs.
$\mathbf{U}$	The energy consumption case of MOAs.
$\mathbf{U}_s$	The energy consumption case of MOAs in scenario s.
$\mathbf{\Omega}$	The set of energy consumption schedules of SAs.
$\mathbf{\Gamma}$	The set of energy consumption cases of MOAs.
$\mathbf{\Gamma}_s$	The set of energy consumption cases of MOAs in scenario s.
c_1, c_2	The acceleration constants in PSO.
r_1, r_2	The randomly generated numbers in range of [0,1] in PSO.
w	The inertia weight factor in PSO.
k	Iteration index in PSO.
v_ζ^k, p_ζ^k	The velocity,position of the particle ζ at the kth iteration in PSO.
$pbest_\zeta^k$	The best position of the particle ζ among k iterations in PSO.
$gbest^k$	The best position of the particle swarm among k iterations in PSO.

Chapter 5

t	Index of time slot.
i	Index of subinterval of the maximum interval of the outdoor temperature.
m	The total number of temperature subintervals.
U_t^i	The ith subinterval of the outdoor temperature at time slot t.
U_t^m	The maximum interval of the outdoor temperature at time slot t.
B_t^i	The ith sub-zone of the outdoor temperature and the effect of users' activities at time slot t.
B_t^m	The maximum zone of the outdoor temperature and the effect of users' activities at time slot t.
$\mathcal{P}_t^0$	The set of all the probability distributions of uncertain variables.
$\mathcal{P}_t^1, \mathcal{P}_t^2$	The ambiguity set of the probability distribution of the outdoor temperature.
$\mathcal{P}_t^3$	The ambiguity set of the probability distribution of the outdoor temperature and the effect of users' activities.
$\mathbb{P}_t$	The probability distribution of uncertain variables.
ξ_t	The actual outdoor temperature at time slot t.
μ_t	The forecast outdoor temperature at time slot t.
σ_t^2	The variance of the outdoor temperature at time slot t.
l_t^i	The lower bound of U_t^i.
u_t^i	The upper bound of U_t^i.
p_t^i	The probability of $\xi_t \in U_t^i$.
C	The thermal capacity of HVAC.
R	The thermal resistance.
η	The coefficient of performance of HVAC.
q_t	The real-time power consumption of HVAC.
q_t^{ref}	The reference power consumption of HVAC.
$q^{\max}$	The upper limit of power consumption of HVAC.
ε	The probability of exceeding the limits of power consumption of HVAC.
θ_t	The indoor temperature at time slot t.
$\theta^{\min}$	The lower bound of the indoor temperature.
$\theta^{\max}$	The upper bound of the indoor temperature.

θ^{best}	Users' preferred indoor temperature.
κ	The penalty factor of the deviation of users' preferred temperature.
φ_t	The effect of users' activities on the indoor temperature.
ϕ_t	The forecast effect of users' activities on the indoor temperature.
φ_t^{max}	The maximum effect of users' activities on the indoor temperature.
φ_t^{min}	The minimum effect of users' activities on the indoor temperature.
w_1	The importance factor of Cost (electricity cost).
w_2	The importance factor of Num_VioTem (number of violations of comfortable temperatures).
w_3	The importance factor of Time (computation time).
Δt	The time period in a time slot.
e_t	The electricity price at time slot t.
T	The horizon of energy consumption scheduling.
s_e	Index of scenario of the electricity price.
S_e	The total number of scenarios of the electricity price.
β, h, y	
$\boldsymbol{y}, \lambda_i, \lambda$	Auxiliary variables.
τ_0, τ_1	

Chapter 1

Introduction

1.1 Background

1.1.1 Smart grid

Traditional power grid was designed to supply energy produced by a small number of large-scale generators to match users' demand on electric energy [1–3]. The installed generation, transmission and distribution capacities must be able to meet the peak of the demand, and a sufficient additional capacity is meanwhile required to deal with the uncertainty in generation and consumption. Therefore, grid resources are under utilized for most of the time [4]. Moreover, traditional power grid has now been challenged by the remarkable grid penetration of renewable energy sources (RESs) [5–8]. The capacity of RESs excluding hydroelectric energy accounted for 10.3% of the global power generation and took up 53.6% of the global capacity of newly installed power generators in 2015 [9]. RESs are variable, uncertain and just partially dispatchable, and these features of RESs bring a great challenge to the real-time balancing between the demand and the supply [5].

Smart grid is a new generation of power grid [4, 10–12], and it has been introduced to address the main issues of traditional grid with advances from the information and communication technology, and control and optimization methodologies [13–15]. With the penetration of RESs, the participation of demand response (DR) from the user side, and the deployment of energy storage systems (ESSs),

smart grid helps reduce the consumption of fossil fuels and the emission of greenhouse gases, lower the peak demand and the investment of additional capacity of power generation, and improve the economical efficiency and the reliability of grid operations [1, 16].

1.1.2 Demand response

DR is an essential characteristic of smart grid [1]. DR is defined as changes in electric usage by end-use customers from their normal consumption patterns in response to changes in the electricity price over time, or to incentive payments designed to induce lower electricity use at times of high wholesale market prices or when the system reliability is jeopardized [13, 17–19]. DR encourages the reduction of the electricity consumption in the periods with peak demand and it motivates the consumption when the generation is surplus, e.g. at night when the wind power exceeds the electricity demand.

DR is categorized into an incentive-based program and a price-based program [1] and most works in DR are designed according to the price-based program [20–24]. In the incentive-based program, the energy consumption of certain appliances is controlled based on the requirements of the power utility [25], and users are provided with load modification incentives. In the price-based program, the power utility induces users to change their energy consumption according to the variance of the electricity price [26–30], and many electricity pricing schemes are proposed, e.g. time-of-use pricing (TOUP) [31], real-time pricing (RTP) [32] and inclining block rate (IBR) [33]. TOUP and RTP vary the electricity price based on the time of day and IBR sets the electricity price based on a threshold of the total energy consumption of home appliances during a certain period. According to the IBR, the electricity price will increase to a higher value when the threshold is exceeded.

Users can obtain economic benefits from DR [34]. Meanwhile DR is an effective means of reducing the whole market price, as it reduces the expense of operating generators through rescheduling the users' energy consumption and defers the cost of additional capacity of generation, transmission and distribution [5]. Moreover, DR helps improve the reliability of power grid and the penetration of RESs in smart

grid as it can make quick response to meet the balancing between the supply and the demand [35–40]. [41] demonstrates that DR is an effective way to integrate more wind power in the power system and to reduce the generation cost.

Residential, commercial and industrial users can actively contribute to the DR, and residential users are expected to play an important role [13]. The residential consumption constitutes one of the major parts of the energy demand, and it is responsible for nearly one third of the electricity consumption in the United Kingdom and is the largest contributor to the winter peak demand [42]. With the increase of household electric vehicles and other appliances, the residential consumption will probably exceed 40% of the total yearly consumption in most of the Western countries in the near future [4,43]. Residential users usually participate in the DR through the demand side scheduling in which the energy consumption of residential users is scheduled based on the electricity price information [44, 45].

1.2 Motivation and objectives

Based on the electricity price information, the energy consumption of residential users is scheduled taking into account users' concerns and uncertainties. The motivation and objectives of the research work in this thesis are presented from two aspects including users' concerns and uncertainties considered in the residential demand side scheduling (RDSS). Users' concerns are objectives users care about, e.g. the electricity cost and their convenience. Uncertainties, e.g. the uncertainty of the weather, are factors which are not certainly known when the energy consumption of home appliances is scheduled and these uncertainties affect users' concerns.

1.2.1 Users' concerns in residential demand side scheduling

Several users' concerns have been considered in the RDSS, such as the minimization of the electricity cost [46], the reduction in the delay of appliances' operations [47], and the improvement of users' convenience level [44]. However, to the best knowledge of the author, improving the operational safety of appliances has not been considered in the RDSS, and it should be paid more attention. 1083 fires

caused by washing machines and tumble driers, and 475 fires caused by dishwashers had happened in the United Kingdom in $2011/2012$ [48]. 8500 fires caused by home appliances had resulted in a 265 million dollar loss in the United States in 2010 [49]. These accidents arouse users' perception of risk and users would like appliances to be operated in periods when they are at home and awake to monitor appliances' operations. In case of operation faults of appliances, users can give quick response when they are at home and awake. For example, users can cut off the power immediately when an operation fault of the washing machine happens, otherwise the operation fault may cause fire and more serious consequence when users are not at home or are asleep [50]. In the previous work of RDSS, appliances are scheduled without the consideration of users' perception of risk and the possible faults of appliances' operations when they are scheduled in periods when users are not at home or are asleep. As the safety risk is of great concern to users, it is worth taking into account the operational safety in the RDSS. The relationships among the operational safety and other objectives need clarified with the consideration of the operational safety as a new objective.

When multiple objectives are taken into account in the RDSS simultaneously, it is usually solved by converting these objectives to a single objective including the approach that weights the importance of objectives [33, 47] and the approach that confines objectives within certain ranges in constraints [51]. Compared with these two approaches, the Pareto approach does not depend on the predefined weights and ranges of objectives. It simultaneously optimizes all the objectives and directly shows the relationships between different objectives, and it is more complex to be achieved. The approach of finding the Pareto-optimal front is adopted to optimize the electricity cost and users' comfort in [52].

In this thesis, the multi-objective residential demand side scheduling (MORDSS) is investigated with the consideration of the appliances' operational safety as a new objective. The approach of finding the Pareto-optimal front is adopted to deal with the MORDSS and to investigate the relationships between the operational safety and other objectives. This approach is compared with the approach that weights the importance of objectives and the approach that sets constraints to the deviations of

objectives from their optimal values.

1.2.2 Uncertainties in residential demand side scheduling

Though several uncertainties, i.e. the electricity price [53] and the outdoor temperature [45], have been considered in the RDSS as these uncertainties affect users' concerns such as the electricity cost and their comfort, the uncertainty of manually operated appliances (MOAs) has not been considered to the author's best knowledge. Home appliances are categorized into schedulable appliances (SAs) and MOAs [47]. MOAs, e.g. lights and TV, are manually controlled by users in real time and cannot be scheduled ahead. Depending upon users' real-time demands, the usage of MOAs is affected by many random external factors. SAs, e.g. washing machine and dishwasher, can be scheduled since their energy consumption is shiftable and flexible. In [33, 46, 54, 55], the fixed energy consumption is assumed for MOAs when the energy consumption of SAs is scheduled, and the optimal schedules obtained for SAs will degrade when the energy consumption of MOAs differs from the assumed consumption. In [47], MOAs are not considered when the energy consumption of SAs is scheduled based on the electricity pricing scheme with the combination of RTP and IBR. The energy consumption threshold set by the IBR and the lack of the consideration of MOAs' energy consumption make users confront the risk of a high electricity cost as the total energy consumption of home appliances may exceed the consumption threshold when the energy consumption of MOAs is accidentally involved. As MOAs make up around 30% to 40% of the total energy consumption of home appliances [33, 46, 47, 54, 55] and they affect the performance of the energy consumption scheduling of home appliances, the uncertainty of MOAs is worth considering in the RDSS.

The heating, ventilation and air conditioning (HVAC) system is one of the main RDSS resources because of its relatively large energy consumption and its ability to potentially adjust power usage without much compromise to users' comfort [56]. The uncertainty of the outdoor temperature should be considered in the energy consumption scheduling of HVAC, otherwise the indoor temperature may violate the comfortable temperature zone [57]. Many studies have been carried

out to deal with this uncertainty when the energy consumption of HVAC is scheduled [45, 58, 59]. [45] takes into account the uncertainty of the outdoor temperature through the stochastic optimization approach (SOA) with a certain probability distribution, and [59] conservatively adopts the robust optimization approach (ROA) considering the uncertainty only with a temperature interval. The distributionally robust optimization approach (DROA) combines the advantages of both the SOA and the ROA [60]. The conservativeness of the DROA is reduced with the probabilistic information observed from historical data and the exact probability distribution of the uncertain variable is not required [60]. With the mean and the variance extracted from historical data, this approach has been applied in the reserve scheduling problem in the power system with the consideration of the uncertainty of renewable energy [60].

In this thesis, the uncertainty of MOAs is considered in the RDSS to reduce the electricity cost. To better deal with the uncertainty of the outdoor temperature, a newly proposed DROA is adopted to schedule the energy consumption of HVAC to reduce the electricity cost whilst maintaining users in the comfortable temperature zone. The newly proposed DROA is different from the DROA based on the mean and the variance as it extracts more information from historical weather data. The proposed DROA takes into account the probabilistic information of subintervals of the outdoor temperature, i.e. the maximum interval of the outdoor temperature is partitioned into subintervals and the proposed DROA makes use of the probabilistic information of these subintervals of historical weather data.

1.3 Research contributions and thesis outline

1.3.1 Research contributions

In the RDSS, the energy consumption of home appliances should be scheduled to satisfy users' concerns and uncertain factors should be taken into account as they affect users' concerns. The operational safety of appliances is of great concern to users especially when the appliances are in operation without users' monitoring. The uncertainty of the energy consumption of MOAs affects users' electricity cost, and

the uncertainty of outdoor temperature has impact on both the electricity cost and users' comfort when the energy consumption of HVAC is scheduled. To further meet users' concerns and reduce the electricity cost, the operational safety of appliances and uncertainties of MOAs and the outdoor temperature are taken into account in the RDSS. The MORDSS with the consideration of the operational safety of appliances is dealt with through the approach of finding the Pareto-optimal front. The ROA and the DROA are adopted to tackle uncertainties of MOAs and the outdoor temperature, respectively.

The safe operation of appliances is of great concern to users and it has not been considered in the RDSS to the best knowledge of the author. When users are not at home or are asleep and appliances are in operation, users will care more about the operational safety as appliances are without users' monitoring. The formulation of appliances' operational safety is proposed based on whether users are at home and awake to monitor appliances' operations. The MORDSS is investigated with the consideration of the appliances' operational safety together with the electricity cost and the operational delay. The relationships between the operational safety and the other two objectives are investigated through the approach of finding the Pareto-optimal front. Moreover, the Pareto approach is compared with the approach that weights the importance of multiple objectives and the approach that sets constraints to objectives. Taking into account the appliances' operational safety, the Pareto approach is proved effective in presenting comprehensive optimal solutions of the MORDSS with relationships among objectives presented.

The energy consumption of MOAs is manually controlled based on the real-time demands of users and it is uncertain when SAs are scheduled. The ROA is adopted to solve the RDSS under the uncertainty of the MOAs as the probabilistic information of the energy consumption of MOAs is usually unknown and not easily estimated. Among all the possible energy consumption cases of the MOAs, the ROA takes into account the worst case to reduce the electricity cost of all home appliances based on the electricity pricing scheme with the combination of RTP and IBR. The RDSS with the consideration of the uncertainty of MOAs through the ROA is solved by the intergeneration projection evolutionary algorithm, which is a nested heuristic

algorithm with the inner genetic algorithm and the outer particle swarm optimization algorithm. Case studies are based on one day case, and one month cases with various combinations of SAs and MOAs. Simulation results prove that the ROA is effective in reducing the electricity cost compared with the approach without considering the uncertainty of MOAs and the approach considering MOAs with the fixed energy consumption.

With the consideration of the uncertainty of the outdoor temperature, a DROA is proposed to schedule the energy consumption of the HVAC system. With the maximum interval of the outdoor temperature partitioned into subintervals, the newly proposed DROA constructs the ambiguity set of the probability distribution of the outdoor temperature according to the probabilistic information of these subintervals of historical weather data. The actual energy consumption will be adjusted based on the deviation of the outdoor temperature from the forecast and the scheduled consumption in real time. The energy consumption scheduling of HVAC through the proposed DROA is formulated as a nonlinear problem with distributionally robust chance constraints, and this nonlinear problem is solved via linear programming after these distributionally robust chance constraints are reformulated to be linear. The proposed DROA is compared with the DROA based on the mean and the variance of historical data and the traditional ROA. Simulation results demonstrate that the proposed DROA effectively reduces the electricity cost whilst maintaining the users in the comfortable temperature zone, and that the proposed DROA approximately takes only 10% of the computation time of the DROA based on the mean and the variance to solve the energy consumption scheduling of HVAC.

The publications produced from all the research work are listed as follows:

1. Y. F. Du, L. Jiang, C. Duan, Y. Z. Li, and J. S. Smith, Energy consumption scheduling of HVAC considering weather forecast error through the distributionally robust approach, published in IEEE Transactions on Industrial Informatics, May 2017.

2. Y. F. Du, L. Jiang, Y. Z. Li, J. Counsell, and J. S. Smith, Multi-objective demand side scheduling considering the operational safety of appliances, published in Applied Energy, July 2016.

3. Y. F. Du, L. Jiang, Y. Z. Li, and Q. H. Wu, A robust optimization approach for demand side scheduling under energy consumption uncertainty of manually operated appliances, published in IEEE Transactions on Smart Grid, May 2016.

4. Y. F. Du, L. Jiang, Y. B. Bi, and Y. Z. Li, Smooth energy consumption for demand side scheduling using heuristic optimization, published in IEEE PES Innovative Smart Grid Technologies Conference Europe, Oct. 2014.

1.3.2 Thesis outline

Chapter 2 presents a survey on the RDSS, and the problems and methods in the RDSS are reviewed, respectively.

Chapter 3 shows the MORDSS taking into account the operational safety of appliances. After the introduction on the operational safety of appliances, the system model is presented. With the users' multiple concerns including the operational safety, the electricity cost and the operational delay of appliances formulated, the adopted approach of finding the Pareto-optimal front is introduced to tackle MORDSS. As the Pareto-optimal front consists of a set of optimal solutions, a method of making the final scheduling decision is proposed based on the relationships among users' multiple concerns. The comparison between the adopted Pareto approach and other two approaches is illustrated in simulation results. Finally, the conclusion of this chapter is presented.

Chapter 4 shows the RDSS considering the uncertainty of MOAs through the ROA. The uncertainty of MOAs is introduced at first. With the home energy management system and the impact of the uncertainty of MOAs presented, the ROA is introduced to tackle MOAs' uncertainty. After the effectiveness of the ROA is justified in simulation results, conclusions are presented.

Chapter 5 proposes a DROA to schedule the energy consumption of the HVAC system with the consideration of the uncertainty of the outdoor temperature. Firstly, the justification of the importance of the energy consumption scheduling of HVAC, the reason why the uncertainty of the outdoor temperature should be taken into

account, and the reason why the DROA is adopted are illustrated. Then the complete problem formulation and the proposed DROA are introduced. Conclusions are given after the simulation results on the comparison between the proposed DROA and other two approaches are presented.

Chapter 6 demonstrates conclusions of this thesis and future research.

Chapter 2

A survey on residential demand side scheduling

2.1 Introduction

As shown in Fig. 2.1 [61], the traditional power grid supplies energy produced by bulk generators to meet users' energy demand, and there is a lack of communication between the supply side and the demand side. Besides, facilities and equipment in the traditional grid are usually under utilized since the additional capacity of generation, transmission and distribution should be reserved to ensure the reliability of the system. Moreover, to reduce greenhouse gas emissions and diminish the dependence on fossil fuels, renewable energy sources (RESs) are integrated in the power grid. The remarkable usage of RESs brings great challenge to the power grid due to their intermittency and uncertainty. Smart grid is the new generation of power grid and it is introduced to deal with the problems in the traditional power grid with the development of the information and communication technology, the advanced control and optimization methodologies and the newly introduced equipment in the power grid such as the energy storage equipment and devices of power electronics [13–15]. Compared with the traditional power grid, it is shown in Fig. 2.2 [1] that RESs, energy storage systems (ESSs), the advanced metering infrastructure and the two-way communication between the supply side and the demand side have been

integrated in the smart grid. The penetration of RESs, the deployment of ESSs and the participation of demand response (DR) based on the advanced metering and the two-way communication constitute the main characteristics of smart grid [16].

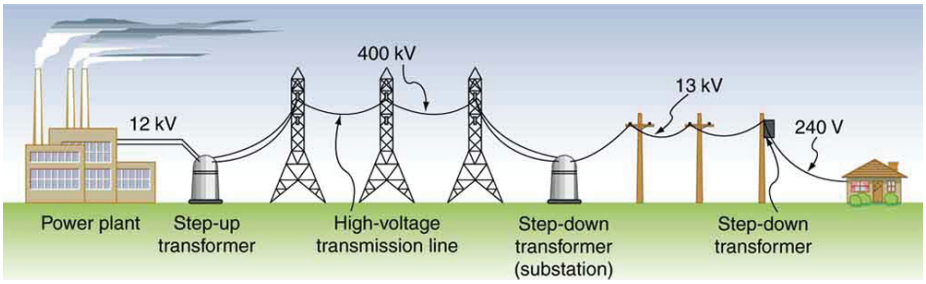

Figure 2.1: An example of the framework of traditional power grid

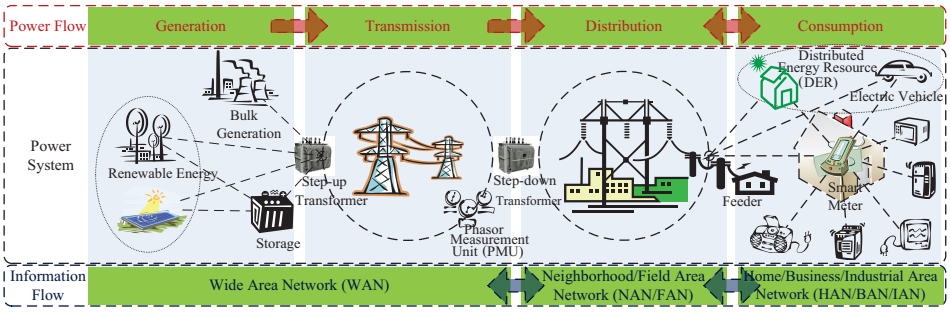

Figure 2.2: The framework of smart grid

Though the penetration of RESs brings great challenge to the power grid, they will be widely utilized. It is illustrated in Fig. 2.3 that the capacity of RESs excluding hydroelectric energy made up 53.6% of the global capacity of newly installed power generators, and accounted for 10.3% of the global power generation in 2015 [9]. The capacity of RESs is increasing for the reasons that the development of technology, e.g. the advanced control methodology, will meet the challenge brought by RESs and that substantial socio-economic advantages can be obtained including the reduction of greenhouse gas emissions and the increase of the employment in manufacturing, installation and management of equipment of RESs [4].

ESSs convert electrical energy into a form that can be stored for converting back

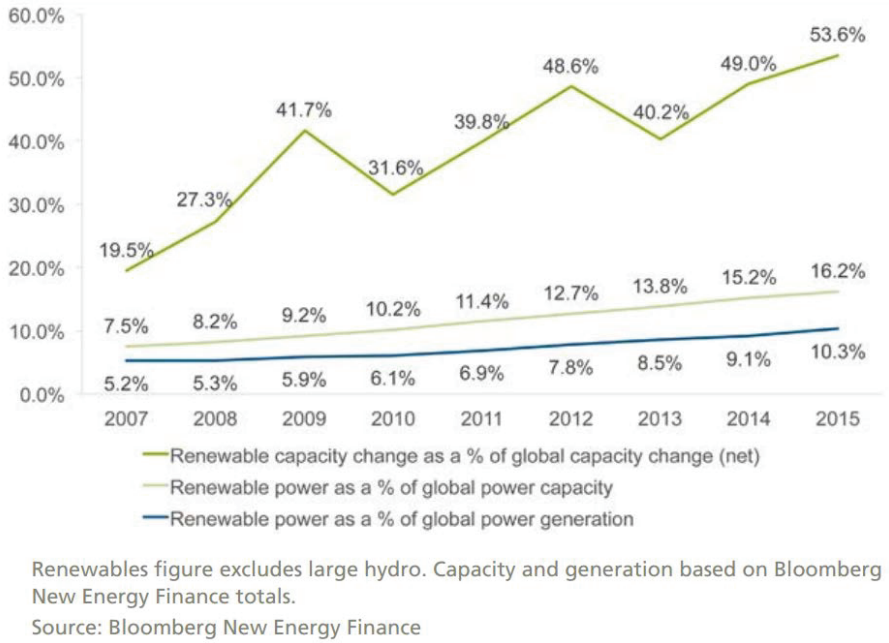

Figure 2.3: The penetration of renewable energy in power grid

to electrical energy when needed. ESSs can provide numerous benefits including load following and standby reserve, and they are important to the power system with the penetration of RESs. ESSs are classified into the mechanical energy storage, e.g. the pumped hydroelectric storage, the chemical energy storage, e.g. batteries, the thermal energy storage, e.g. hot rocks, and the electrical energy storage, e.g. capacitors [62]. The pumped hydroelectric storage is the most widely implemented large-scale ESS, and large-scale batteries are expected to be gradually implemented with their price decreased and their cycle life increased [62].

As an essential characteristic of the smart grid, DR is able to shape users' energy consumption in a convenient fashion through the smart metering infrastructure and the two-way communication [1]. DR is defined as changes in electric usage by end-use customers from their normal consumption patterns in response to changes in the electricity price over time, or to incentive payments designed to induce lower electricity use at times of high wholesale market prices or when the system reliability is jeopardized [13, 17]. Smart metering infrastructure and the two-way communi-

cation play key roles in the implementation of DR. The smart metering measures users' energy usage and not only the total energy consumption but also the energy consumption in time slots is measured. Based on the energy consumption in each time slot and the electricity price, the smart metering calculates the electricity cost [33]. The information of users' energy consumption is transmitted to the power utility and the electricity price information is transmitted to users through the two-way communication. Since DR can adjust users' energy consumption according to the requirements of the supply side and can respond quickly to the imbalance between the supply and the demand, it helps enhance the reliability of the power system, improve the penetration of RESs and reduce the investment of ESSs.

DR reduces the peak-to-average ratio (PAR) of energy demand and contributes to the improvement of the reliability of the power system. [33, 47] demonstrate that users pay less and the PAR is drastically reduced with a more balanced energy demand through DR.

DR is demonstrated to be an effective way to help integrate more renewable energy in the power system and decrease emissions of greenhouse gases [35, 38]. As RESs are variable, uncertain and just partially dispatchable and they are now largely integrated into the power grid, the real-time balancing between the demand and the supply is enormously challenged in the power grid [5]. [38] illustrates that imbalances between the demand and the supply are lowered as a direct consequence of the strategy of pairing the wind energy and the DR. To manage the variability of RESs, [35] considers the forecast error of RESs and incorporates DR, and [63] proposes a pool-based DR exchange model in which DR is traded among participants. [64] investigates a demand side scheduling problem for a house equipped with a solar assisted heating, ventilation, and air conditioning (HVAC) system.

DR helps reduce the investment of ESSs. [40] proposes a theoretical framework for the joint optimization of batteries, RESs and the DR, and demonstrates the advantage of DR in reducing the investment cost of batteries. [65] deals with the optimal capacity of batteries for the smart grid operation and shows that the capacity of batteries and the power generation cost are reduced through the participation of DR sources, e.g. electric vehicles and heat pumps in households. [66] adopts a dis-

tributed algorithm to schedule the energy consumption of home appliances with the consideration of batteries and demonstrates that more economically viable batteries will reap more benefits from DR.

DR is categorized into industrial, commercial and residential DR based on users who participate in it. As the residential energy consumption takes up a large percentage in the energy demand, for example, the residential consumption makes up nearly one third of the electricity consumption in the United Kingdom and contributes most to the winter peak demand [42], the residential DR plays an important role in achieving the benefits of the DR in smart grid. Most work in the residential DR is focused on the residential demand side scheduling (RDSS) in which the energy consumption of residential users is scheduled based on the electricity price information [44, 45, 67–69].

2.2 Framework of residential demand side scheduling

Fig. 2.4 shows the framework of RDSS [1]. Based on the price information provided by the supply side, the energy consumption of the demand side is adjusted with benefits to both supply and demand sides. The price information can be the contracted payment that induces lower electricity consumption or the varying electricity price that motivates users to shift the consumption [34], and the information of the varying electricity price is mostly adopted in the RDSS [67, 70–72]. With the knowledge of the price information and the installation of the home energy management system (HEMS), home appliances are automatically controlled based on users' requirements for appliances' operations.

The illustration of electricity pricing schemes is shown in Fig. 2.5 [1]. Time-of-use pricing (TOUP) and real-time pricing (RTP) vary the electricity price at different time intervals of a day and typically each time period is longer than one hour for TOUP and less than one hour for RTP [73–76]. For example, TOUP has been adopted by some utility companies in the United Kingdom with higher electricity price for daytime and lower price at night [31] and hourly based RTP has been adopted by the Illinois Power Company in the United States [32]. The ener-

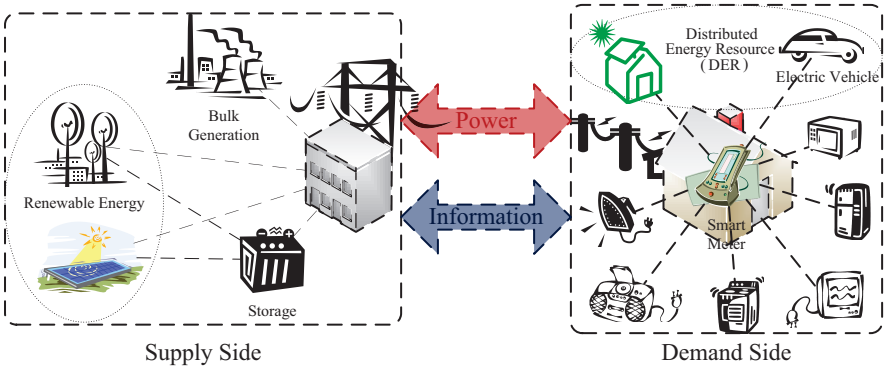

Figure 2.4: The framework of residential demand side scheduling

gy consumption of home appliances is scheduled based on RTP and TOUP in [53] and [46], respectively. The inclining block rate (IBR) designs a two-level rate structure, i.e. when the total energy consumption in a certain period such as one hour in Fig. 2.5 exceeds a certain threshold, the electricity price will climb up to a higher value [33]. Compared with other pricing schemes, RTP reflects more real-time information of the power system and brings more economic benefits to the power system [53], but it may aggregate energy consumption in periods with lower prices to cause peak demands [47]. The electricity pricing scheme with the combination of RTP and IBR can reserve the economic benefits of RTP and meanwhile avoid the possible aggregation effect as the electricity price will increase to a higher value when users' total energy consumption exceeds a threshold [33]. The pricing scheme that combines RTP and IBR is adopted in [47] and its effectiveness in reducing the PAR is demonstrated in the comparison with RTP.

Home appliances are categorized into manually operated appliances (MOAs) and schedulable appliances (SAs). MOAs, e.g. lights and TV, are manually operated based on users' real-time demands and cannot be scheduled ahead. SAs, e.g. the washing machine and the dishwasher, are appliances whose energy consumption is shiftable and can be scheduled based on the electricity price information [66,77–80]. For example, after users put clothes in the washing machine and set the time period of the operation, e.g. the deadline of the washing, the HEMS will work out a start time slot to help users reduce the electricity cost and will automatically start

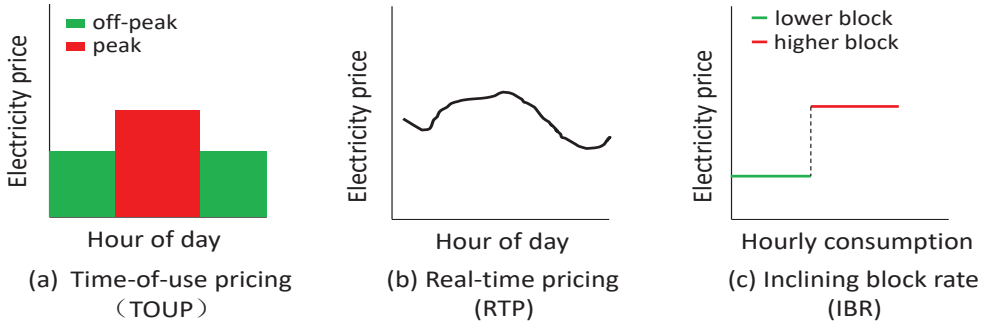

Figure 2.5: The illustration of electricity pricing schemes

the washing machine at the scheduled time slot, so is the case for the dishwasher. [53] further classifies SAs as interruptible and non-interruptible ones according to whether the operations of SAs can be interrupted or not. The operations of interruptible SAs, e.g. the washing machine, can be suspended, while non-interruptible SAs cannot be paused until their operations are finished, e.g. the oven.

When the energy consumption of home appliances is scheduled by the HEMS, it should meet users' requirements for the appliances' operations. [81, 82] define deadlines of appliances' operations, [47] specifies operation lengths of appliances and [83] confines the total energy consumption of appliances in the scheduling horizon. The power of home appliances can be considered with a fixed value or a value within a range. [45] considers the air conditioning system with the on-off operation mode, i.e. the power consumption of the system can be either its maximum power or 0. The power consumptions of home appliances are taken into account as continuous variables in [84–86].

[87, 88] demonstrate the implementation of the HEMS. [87] introduces the design of the HEMS equipped with sensors, a controller, smart appliances and home networks, and [88] achieves the RDSS based on a real-house environment with a personal computer as the controller, smart appliances and home networks. The sensors detect the general physical sensing measurements to assist the controller to schedule the energy consumption of home appliances. The sensing measurements and the control signals are transmitted through home networks, and several communication protocols have been proposed for the HEMS [89, 90]. Smart appliances

indicate appliances can be automatically controlled. In [88], the ordinary appliances with their electronic switches connected to the relay switch modules are used to simulate smart appliances. The smart appliances with the function of automatic control have been realized in practice [91] and they are being utilized in households.

2.3 Optimization problems in residential demand side scheduling

The RDSS is usually formulated to optimize users' concerns under the condition that the requirements of the operations of appliances are satisfied. In the optimization of the RDSS, there may exist uncertain factors and these uncertain factors affect users' concerns. In this section, the optimization problems in the RDSS are presented from aspects of users' concerns and uncertainties.

2.3.1 Problems of users' concerns

Several users' concerns have been considered in the RDSS including the electricity cost, users' convenience and comfort and their privacy.

The electricity cost is the concern that is mostly considered in the RDSS [67, 70–72, 92]. [67] proposes a two-level framework in the RDSS. The electricity price information is decided by the upper level (the aggregator, the utility, or the market) and the home appliances at the lower level are controlled to minimize the electricity cost. [70] directly minimizes users' electricity cost with the knowledge of the electricity price information. [72] presents a simulation model to generate household load profiles under a flat tariff, and it simulates changes in these profiles when the energy consumption of home appliances is scheduled to minimize the electricity cost under time-based electricity prices. Based on the RTP, the electricity cost of HVAC is minimized in [71]. [92] pays customers rewards to shift the energy consumption of home appliances.

Apart from the electricity cost, users care about their convenience and comfort. [44] takes into account users' convenience level according to whether appliances

are operated in users' preferred time periods. For convenience, users would not like to delay the operations of appliances too long and wish them to be finished as soon as possible. The reduction in the delay of appliances' operations is usually formulated based on how long the operations of appliances are finished before the deadlines [33, 47]. [47] geometrically increases the penalty of the appliances' delay with the increase of the delay time. [33] introduces parameters to indicate different effects of appliances' delays and reduces the total effect of the operational delay of home appliances. When the heating and cooling systems are included in the RDSS, users' thermal comfort is always taken into account [44].

With the penetration of the information collection and transmission in the smart grid, it is possible to identify users' activities through the profiles of users' energy consumption, which raises users' concern on privacy. As appliances' usage patterns could be extracted from the fluctuation of the aggregated energy consumption profile, [93] introduces metrics to quantitatively measure the fluctuation of the metered energy profile and schedules the energy consumption of home appliances to disguise the fluctuation. [68] addresses users' concern on privacy by using energy storage devices to mask the original energy consumption profile. Except the energy storage devices, RESs reduce users' dependence on the power grid and it is shown in [94] they protect users' privacy by diversifying energy sources.

Though several users' concerns have been considered in the RDSS, improving the operational safety of appliances has not been considered in the RDSS to the best knowledge of the author. Since the safety risk of appliances' operations exists, for example, 1083 fires happened in washing machines and tumble driers' operations in the United Kingdom in $2011/2012$ [48], and the consequences in the cases of the appliances' faults will deteriorate if the appliances are in operation during periods when users are not at home or are asleep, the operational safety is worth considering in the RDSS to further optimize the energy consumption of home appliances. The relationships among the operational safety and other uses' concerns need clarified with the operational safety taken into account as users' new concern.

2.3.2 Problems of uncertainties

Uncertain factors may exist in the RDSS, e.g. the electricity price, the renewable energy, and the outdoor temperature. These uncertainties have impacts on users' concerns, and they should be taken into account in the RDSS. In [53], the electricity price is announced every 5 minutes, and the price for the time after 5 minutes is unknown and uncertain. [53] takes into account the price uncertainty to schedule the energy consumption of home appliances every 5 minutes to minimize the electricity cost. [69] takes into account the uncertainty of solar insolation to reduce the electricity cost when the solar energy is considered in the RDSS. The uncertainty of the outdoor temperature is considered in the energy scheduling of HVAC to satisfy users' thermal comfort in [45].

Though several uncertainties have been taken into account in the RDSS, the uncertainty of MOAs' energy consumption has not been considered to the best knowledge of the author. Home appliances are classified into SAs and MOAs. The energy consumption of SAs is shiftable and schedulable, such as the washing machine. The energy consumption of MOAs is manually controlled by users in real time and their energy consumption cannot be scheduled in advance, such as TV. Therefore, the energy consumption of MOAs is uncertain when SAs' energy consumption is scheduled ahead. In [33, 46, 54, 55], the energy consumption of SAs is scheduled with the assumed MOAs' energy consumption. Since the usage of MOAs is dependent upon users' real-time demands and is affected by many random external factors, their optimal schedules for SAs will be degraded when the energy consumption of MOAs differs from the assumed consumption. In [47], MOAs are not considered when the energy consumption of SAs is scheduled based on the electricity pricing scheme that combines RTP with IBR, which would make users confront the risk of a high electricity cost due to the excess of the energy consumption threshold set by IBR when the energy consumption of MOAs is accidentally involved. As MOAs usually consume around 30% to 40% of the total energy consumption of home appliances [33, 46, 47, 54, 55], it is necessary and worth to consider the uncertainty of MOAs' energy consumption so as to further improve the performance of the scheduling scheme of home appliances.

2.4 Methods in residential demand side scheduling

In this section, the methods of dealing with users' multiple concerns simultaneously and the methods of tackling uncertainties in the RDSS are reviewed, respectively. When only one concern of users is considered, the energy consumption scheduling of home appliances is usually solved through an optimization algorithm, such as genetic algorithm, linear programming and mixed integer linear programming. [33] and [47] schedule the energy consumption of home appliances to minimize the electricity cost through genetic algorithm and linear programming, respectively. [53] introduces integer variables to indicate the on-off states of appliances and the RDSS aiming at the minimization of the electricity cost is solved through mixed integer linear programming.

2.4.1 Methods of tackling multiple concerns

When users' multiple concerns, i.e. multiple objectives of the RDSS are taken into account simultaneously, it is usually solved by converting these objectives to a single objective. [33, 47] weight the importance of the electricity cost and the operational delay and sum the two objectives with their corresponding importance factors as the final objective function. The formulation of the method that weights the importance of objectives is illustrated via an example with the consideration of two objectives

$$\min_{x} \quad w_1 f_1(x) + w_2 f_2(x) \tag{2.4.1}$$

where x is the decision variable, w_1 and w_2 are the importance weights of objectives $f_1(x)$ and $f_2(x)$, respectively, and $w_1 + w_2 = 1$. The magnitude of objectives can be taken into account in determining the weights and the weights make the objectives expressed with approximately the same numerical values [47, 95]. For example, the values of objectives can be divided by their optimal values in the final objective function, respectively [95], when the weights are determined. When both the electricity cost and users' convenience are considered, [51] minimizes the electricity cost with the constraint that confines the convenience violation within a certain range. With the constraint that limits the indoor temperature within the comfortable zone, [58]

schedules the energy consumption of HVAC to minimize the electricity cost. The formulation of the method that optimizes one objective with the constraints of other objectives is illustrated via an example with the consideration of two objectives

$$\begin{aligned} &\min_{x} f_1(x) \\ &\mathrm{f}_2^{\min} \leq f_2(x) \leq \mathrm{f}_2^{\max} \end{aligned} \tag{2.4.2}$$

where $\mathrm{f}_2^{\min}$ and $\mathrm{f}_2^{\max}$ constrain the lower and upper limits of $f_2(x)$, respectively. Both the method that weights the importance of objectives and the method that sets constraints to objectives convert multiple objectives to a single objective, and the optimization problem with a single objective can be solved efficiently. However, the method that weights the importance of each objective in the final objective function makes the physical meaning of the final objective unclear, and its solution largely depends on the predefined weights of multiple objectives [33, 47]. The method that sets constraints to objectives does not optimize the objectives in the constraints and it only requires them within certain ranges, and the solution of this method depends on the predefined ranges in the constraints [46, 51].

An alternative method to those methods that tackle multiple objectives through the conversion and then the optimization of the final objective function, is to optimize multiple objectives simultaneously and directly through finding the Pareto-optimal front. The Pareto-optimal front consists of a set of optimal solutions of the multi-objective optimization problem and these solutions are nondominated by other solutions in the feasible domain, which is demonstrated via the optimization problem with the consideration of the minimizations of two objectives. Let Ω denote the set of feasible solutions of the optimization problem. For $x_i, x_j \in \Omega$, if

$$\begin{cases} f_1(x_i) < f_1(x_j) \\ f_2(x_i) < f_2(x_j) \end{cases} \tag{2.4.3}$$

it can be defined that x_i dominates x_j [52]. That x_i dominates x_j shows both the objectives of solution x_i are better than those of x_j. For the solutions of the Pareto-optimal front, they are not dominated by other solutions in Ω, i.e. no solutions can

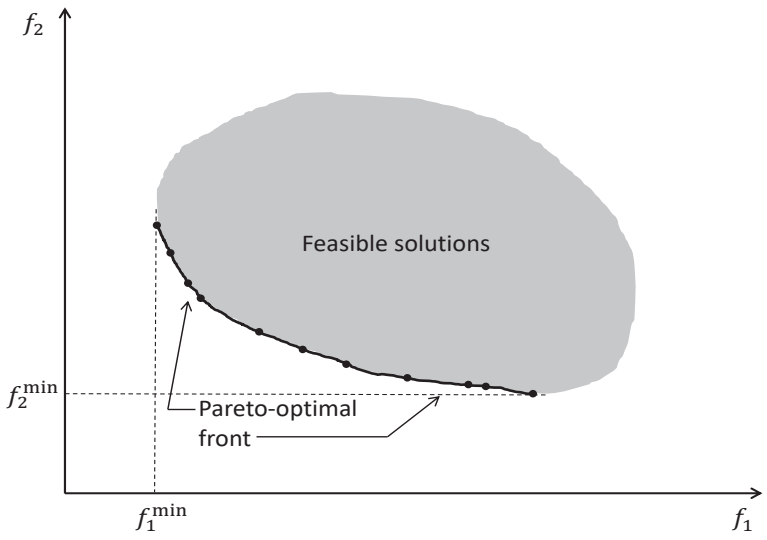

Figure 2.6: The Pareto-optimal front

be found in Ω with both the objectives better than the solutions of the Pareto-optimal front. Besides, the solutions of the Pareto-optimal front are not dominated by each other. The illustration of the Pareto-optimal front is presented in Fig. 2.6 with the consideration of two objectives [96]. It can be seen from Fig. 2.6 that there are no solutions among feasible solutions with both f_1 and f_2 smaller than the solutions of the Pareto-optimal front. The method of finding the Pareto-optimal front does not depend on the predefined weights or ranges. It simultaneously optimizes multiple objectives with clear physical meanings and directly presents relationships among multiple objectives. For example, the Pareto-optimal front in Fig. 2.6 shows that f_2 is reduced with the increase of f_1. However, the Pareto method is more complex in finding solutions than the methods that convert multiple objectives to a single objective. The method of finding the Pareto-optimal front is adopted to optimize the electricity cost and users' comfort in [52].

2.4.2 Methods of tackling uncertainties

Many methods have been proposed to tackle uncertainties in optimization problems including stochastic optimization approach (SOA), robust optimization approach (ROA), and distributionally robust optimization approach (DROA).

The SOA requires the exact probability distribution of the uncertain variable [97–102] and it considers the expected value of the objective function under the uncertainty, which is usually formulated as

$$\min_{x} \ \mathbb{E}_{P_\xi}\{f(x,\xi)\} \tag{2.4.4}$$

where x indicates the decision variable, ξ indicates the uncertain variable and its probability distribution is denoted by P_ξ, and $f(x,\xi)$ indicates the objective function. The uncertainty of the outdoor temperature is considered through the SOA with the normal distribution in [45] when the energy consumption of the air conditioning is scheduled. The normal distribution is used to simulate the uncertainty of the electricity price and the RDSS with the consideration of the uncertainty of the electricity price is solved through the SOA in [53].

The ROA does not require the exact probability distribution of the uncertain variable and only the maximum interval of the uncertain variable is needed [103–107], and the ROA takes into account the worst case of the uncertain variable, which is usually formulated as

$$\min_{x} \ \max_{\xi\in\Xi} \ f(x,\xi) \tag{2.4.5}$$

where Ξ denotes the maximum interval of the uncertain variable ξ. The uncertainty of the electricity price is taken into account through the ROA with only the knowledge of the interval of the price [53]. [59] considers the interval of the outdoor temperature to schedule the energy consumption of HVAC.

The expected value of the SOA under uncertainties is a good measure of the performance of the solution of the optimization problem. However, the deviation between the actual probability distribution of the uncertain variable and the adopted distribution by the SOA may result in suboptimal solutions [108]. Though the ROA does not require the probability distribution of the uncertain variable [109], it may be overly conservative as it only considers the worst case of the uncertainty [110–114]. The DROA combines the advantages of both the SOA and the ROA [115–117]. It does not require the exact probability distribution of the uncertain variable and its conservativeness is reduced with the consideration of the probabilistic information

observed from historical data [60], which is formulated as

$$\min_{x} \quad \mathbb{E}_{P_\xi \in \Gamma}\{f(x,\xi)\} \tag{2.4.6}$$

where Γ denotes a set of probability distributions of the uncertain variable ξ and it can be extracted from historical data. [60] addresses the reserve scheduling problem in the power system through the DROA assuming that the probability distribution of the renewable generation is not fixed but within a set of distributions. The uncertainty of wind power is taken into account in the same way through the DROA in the reserve scheduling problem in [118]. [60, 118] construct the set of the probability distributions of the uncertain variable based on the mean and the variance of the uncertain variable extracted from historical data.

Many studies have been carried out to deal with the uncertainty of the outdoor temperature when the energy consumption of HVAC is scheduled [45, 58, 59]. The uncertainty of the outdoor temperature is considered through the SOA with a certain probability distribution in [45] and through the ROA with a temperature interval in [59]. The DROA has not been used to schedule the energy consumption of HVAC with the consideration of the uncertainty of the outdoor temperature. Considering that the probability distribution of the outdoor temperature can only be estimated from the historical data and that the probability distribution is itself uncertain, the DROA has advantage in dealing with the uncertainty of the outdoor temperature since it does not require the exact probability distribution of the outdoor temperature. Compared with the ROA, the conservativeness of the DROA is reduced as the DROA takes into account more information of the outdoor temperature rather than only the maximum temperature interval. The DROA is mostly based on the mean and the variance of historical data and it formulates the optimization problem with the consideration of uncertainties as semidefinite programming (SDP) [60] which is computationally expensive. The DROA can be further improved with more information exacted from historical data.

2.5 Conclusions

As the RDSS plays an important role in smart grid, more efforts can be made to improve the RDSS. More users' concerns, e.g. the appliances' operational safety should be considered, and more uncertain factors which may affect users' concerns should be taken into account, e.g. the uncertainty of MOAs' energy consumption. Besides, new methods can be used to deal with the existing problems in the RDSS to improve the performance of the RDSS, e.g. the DROA can be applied to tackling the uncertainty of the outdoor temperature when the energy consumption of HVAC is scheduled.

Chapter 3

Users' concern on operational safety of appliances

3.1 Introduction

Though several users' concerns have been considered in the residential demand side scheduling (RDSS), e.g. the electricity cost [46], the operational delay of appliances [47], and the users' convenience level [44], the improvement of appliances' operational safety has not been taken into account. There were 1083 fires caused by washing machines and tumble driers, and 475 fires caused by dishwashers in the United Kingdom in $2011/2012$ [48]. There was a 265 million dollar loss in the United States in 2010 caused by 8500 fires of home appliances [49]. Users would worry about these accidents happening when the appliances are automatically scheduled in periods when they are not at home or when they are asleep. Users would prefer the appliances to be operated under their monitoring, i.e. in periods when they are at home and awake, thus they can give quick response in case of appliances' operation faults. For example, when an operation fault of washing machine happens, users can cut off the power immediately to avoid more serious consequence such as fire [50]. The previous work of RDSS does not take into account users' perception of risk and the possible faults of appliances' operations when appliances are scheduled in periods when users are not at home or are asleep. The operational safety of appliances

is taken into account based on whether the appliances are operated in periods when users are at home and awake. The operational safety of appliances is one of users' concerns and it is worth considering in the RDSS.

In this chapter, the multi-objective RDSS (MORDSS) is investigated with the consideration of the appliances' operational safety as a new objective. The approach of finding the Pareto-optimal front is adopted to deal with the MORDSS and to investigate the relationships between the operational safety and other objectives. This approach is compared with the approach that weights the importance of multiple objectives and the approach that sets constraints to the deviations of objectives from their optimal values. For convenience, these three approaches are referred to as the Pareto approach, the Weight approach and the Constraint approach, respectively. The operational safety is taken into account based on whether users are at home and awake to monitor the appliances' operations. Apart from the operational safety, the electricity cost and the operational delay are considered in the MORDSS. Three situations are taken into account in the comparisons between the Pareto approach and the other two approaches including situations where the operational safety together with one or both of the electricity cost and the operational delay are considered in the MORDSS. Furthermore, a method with the consideration of the relationships among the three objectives is proposed to make the final scheduling decision of energy consumption among solutions of the Pareto-optimal front. Simulation results demonstrate that the operational safety is improved with the sacrifice of the electricity cost and the operational delay, and that in the comparison with the Constraint approach and the Weight approach, the Pareto approach obtains solutions that better satisfy users' concerns and presents the relationships among multiple objectives.

3.2 System model

The structure of the home energy management system is shown in Fig. 3.1. Based on the day-ahead real-time electricity price [119,120], users' demands for the appliances' operations and users' at-home and awake status, the energy management controller (EMC) will automatically control the energy consumption of schedulable

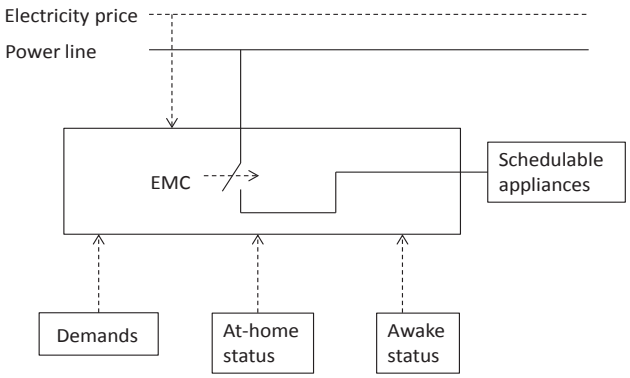

Figure 3.1: Home energy management system

appliances (SAs). The electricity price is announced a day ahead with a various price for each time slot of next day, which is adopted by some utility companies, i.e. the Ameren Illinois Power Company [32]. This day-ahead RTP is different from the RTP that is announced every a certain interval in a day, e.g. every 5 minutes. The EMC is required to be with high computation efficiency for the RTP which is announced every a certain interval as the energy consumption scheduling should be solved and updated in this interval. Meanwhile, the day-ahead RTP leaves the EMC a whole day to solve the problem of energy consumption scheduling, thus the requirement for the computation efficiency of the EMC is much lower than that of the RTP which is announced every a certain interval. Based on the day-ahead real-time pricing scheme, [47, 88, 119, 120] schedule the energy consumption of home appliances.

The EMC is the main part of the home energy management system. The electricity price is transmitted to the EMC a day ahead with the real-time price for next day from the utility company [44, 119, 120]. The users' demands for the appliances' operations and their at-home and awake status are defined and input to the EMC by users as users have different demands for appliances' operations and their at-home status and awake status are different as well. Based on the day-ahead real-time electricity price, users' demands and status, the EMC works out the energy consumption schedules for SAs based on the proposed method that will be introduced in the following sections. Then SAs will be controlled automatically by the EMC according

to the energy consumption schedules through the home area network [47]. The energy consumption of SAs is assumed to be non-interruptible [46]. Manually operated appliances (MOAs) are not included as they are manually controlled when users are at home and awake [121].

Users' demands for appliances' operations include the length of operation time (LOT) and the operation time interval (OTI), which are represented by γ_a and $[\alpha_a, \beta_a]$ for appliance a, respectively [47], where α_a indicates the earliest start time of the operation and β_a indicates the deadline of the operation. Considering the general operation time of appliances, 1 hour is divided into 5 time slots [47] and the LOT is mapped to time slots with one time slot representing 12 minutes. For example, the LOT is 2, i.e. $\gamma = 2$, for an appliance whose operation length is 24 minutes. The LOT is approximated to be the greater and nearest integer when the operation length is not an integer multiple of 12 minutes [47]. One day is mapped to 120 time slots and the OTI is also mapped to the corresponding time slot. For instance, the OTI is from 1 to 60, i.e. $\alpha = 1, \beta = 60$, for an appliance whose operation is predefined between 12 midnight and 12 noon.

3.3 Multi-objective residential demand side scheduling

Multiple objectives including minimizations of the appliances' operational unsafety, the electricity cost and the appliances' operational delay are considered in the MORDSS. Firstly their formulations are respectively presented, and then the problem of the MORDSS is formulated.

3.3.1 Appliances' operational safety

The maximization of appliances' operational safety, i.e. the minimization of appliances' operational unsafety is taken into account in the energy consumption scheduling of home appliances. The operational unsafety of appliances is considered based on whether users are at home and awake to monitor appliances' operations. When users are at home and awake to monitor appliances' operations, their perception of risk would be relieved and they can also give quick response in case

of appliances' operation faults, e.g. they can cut off the power immediately. The situation where the energy consumption of appliances is scheduled in periods when users are not at home or are asleep is to be reduced and this situation is formulated by introducing the unsafety time rate

$$
\begin{aligned}
&UTR_a(x_a) = \tfrac{\gamma_a - s_a(x_a)}{\gamma_a} \\
&s_a(x_a) = \sum_{t=1}^{T} S_a(x_a, t) \cdot M(t) \cdot N(t) \\
&S_a(x_a, t) = \begin{cases} 1, & t \in [x_a, x_a + \gamma_a - 1] \\ 0, & t \in H \backslash [x_a, x_a + \gamma_a - 1] \end{cases} \\
&M(t) = \begin{cases} 1, & \text{users are at home} \\ 0, & \text{users are away} \end{cases} \\
&N(t) = \begin{cases} 1, & \text{users are awake} \\ 0, & \text{users are asleep} \end{cases} \\
&H = \{1, 2, \cdots, T\},\ x_a \in [\alpha_a, \beta_a - \gamma_a + 1]
\end{aligned}
\tag{3.3.1}
$$

where UTR_a denotes the unsafety time rate of appliance a and x_a is the start time slot of the appliance's operation. s_a denotes the number of time slots in which users are at home and awake when appliance a is in operation and it is determined by the appliance's operation status $S_a(x_a, t)$ with the knowledge of users' at-home status $M(t)$ and awake status $N(t)$ in a day. $[x_a, x_a + \gamma_a - 1]$ indicates time slots in which appliance a is in operation. The expression $t \in H \backslash [x_a, x_a + \gamma_a - 1]$ indicates that time slot t belongs to $H = \{1, 2, \cdots, T\}$ excluding the range $[x_a, x_a + \gamma_a - 1]$ and $T = 120$ is the scheduling horizon that indicates the number of time slots ahead which the energy consumption schedule is made for SAs. $x_a \in [\alpha_a, \beta_a - \gamma_a + 1]$ since the operation should start ahead the deadline by at least the length of the operation time. The unsafety time rate (UTR) is the ratio between the time slots of unsafe operation and the operation length, and the time slots of unsafe operation are the

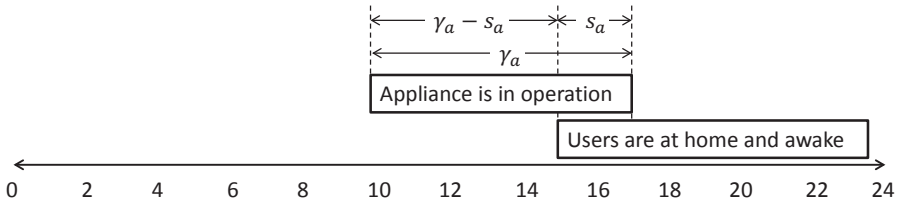

Figure 3.2: The illustration of the concept of unsafety time rate

ones when the appliance is in operation but users are not at home or users are asleep. Fig. 3.2 shows the illustration of the concept of UTR.

For a home with n SAs, the minimization of the appliances' operational unsafety is formulated as

$$
\begin{aligned}
&\min_{X} f_1(X) \\
&f_1(X) = \sum_{a=1}^{n} \rho_a^{UTR_a(x_a)} \\
&UTR_a(x_a) = \tfrac{\gamma_a - s_a(x_a)}{\gamma_a} \\
&s_a(x_a) = \sum_{t=1}^{T} S_a(x_a, t) \cdot M(t) \cdot N(t) \\
&S_a(x_a, t) = \begin{cases} 1, & t \in [x_a, x_a + \gamma_a - 1] \\ 0, & t \in H \backslash [x_a, x_a + \gamma_a - 1] \end{cases} \\
&M(t) = \begin{cases} 1, & \text{users are at home} \\ 0, & \text{users are away} \end{cases} \\
&N(t) = \begin{cases} 1, & \text{users are awake} \\ 0, & \text{users are asleep} \end{cases} \\
&H = \{1, 2, \cdots, T\} \\
&X = \{x_1, x_2, \cdots, x_a, \cdots, x_n\} \\
&\text{subject to} \\
&x_a \in [\alpha_a, \beta_a - \gamma_a + 1], \;\; a = \{1, 2, \cdots, n\}
\end{aligned}
\tag{3.3.2}
$$

where $X = \{x_1, x_2, \cdots, x_a, \cdots, x_n\}$ denotes the set of appliances' start time slots. $\rho_a > 1$ denotes the unsafety parameter of appliance a and it is determined by the probability of appliance a's operation fault and the impact of the operation fault [48]. If the probability of the operation fault of appliance a is higher and the impact of the

fault is more serious, ρ_a can be assumed with a larger value. The higher the value of ρ_a, the higher will be the cost of the operational unsafety. Note that different appliances may have the same UTR and ρ_a is introduced to differentiate the operational unsafety of appliances, and that the UTR and ρ_a jointly determine the appliance's operational unsafety with $\rho_a^{UTR_a}$ which indicates that the appliances' operational unsafety geometrically increases with the increase of the UTR. The appliances' operational unsafety is exponentially increased considering that users' perception of risk is much more intensified when the appliances are more scheduled in periods when users are not at home or users are asleep, i.e. when the UTR increases.

It is noted that users' at-home status $M(t)$ and awake status $N(t)$ are individually defined by users as different users have different at-home status and awake status. Based on the users' predefined at-home status and awake status, the appliances' operational unsafety is obtained by Eqn. (3.3.2). For the same energy consumption schedule, the operational unsafety is different under different users' statuses. For example, when the washing machine is scheduled to operate through 49 time slot to 53 time slot, for one user who is at home all day long except the period from 51 time slot to 60 time slot, and awake from 41 time slot to 115 time slot and asleep for other time slots, the UTR of the washing machine is 3/5 while the UTR is 0 for another user who is with the same awake status and at-home all day long. The corresponding operational unsafety of the washing machine is 1.52 and 1 for the two users with different at-home statuses, respectively, when the unsafety parameter of the washing machine is assumed to be 2.

3.3.2 Electricity cost

The minimization of the electricity cost is taken into account in the energy consumption scheduling of home appliances. Let p_a denote the power of appliance a. Since 1 hour is divided into 5 time slots and it is assumed that the energy consumption is the same in all the time slots during the operation periods of an appliance [47], the energy consumption of appliance a in a time slot is $\frac{p_a}{5}$ when it is in operation.

The energy consumption schedule of appliance a is

$$\begin{aligned} E_a \quad = \Big\{ & e_a^t \,|e_a^t = \tfrac{p_a}{5}, && t \in [x_a, x_a + \gamma_a - 1], \\ & e_a^t = 0, && t \in H \backslash [x_a, x_a + \gamma_a - 1], \\ & H = \{1, 2, \cdots, T\}, && x_a \in [\alpha_a, \beta_a - \gamma_a + 1] \Big\} \end{aligned} \tag{3.3.3}$$

where e_a^t is the energy consumption of appliance a during time slot t. Based on the energy consumption of appliances and the day-ahead real-time electricity price, the minimization of electricity cost is formulated as

$$\begin{aligned} & \min_X f_2(X) \\ & f_2(X) = \sum_{t=1}^{T} prc_t \cdot l_t(X) \\ & l_t(X) = \sum_{a=1}^{n} e_a^t \\ & X = \{x_1, x_2, \cdots, x_a, \cdots, x_n\} \\ & \text{subject to} \\ & x_a \in [\alpha_a, \beta_a - \gamma_a + 1], \;\; a = \{1, 2, \cdots, n\} \end{aligned} \tag{3.3.4}$$

where prc_t is the real-time electricity price at time slot t, and l_t is the total energy consumption of all the SAs during time slot t, and it can be obtained after the energy consumption of each appliance is scheduled by Eqn. (3.3.3).

3.3.3 Appliances' operational delay

The minimization of appliances' operational delay is taken into account in the energy consumption scheduling of home appliances. As shown in Fig. 3.3, the appliance's operational delay is the delay time from α_a, the earliest start time of the operation, and the longest delay occurs when the appliance just meets the deadline to finish its operation, i.e. the appliance starts at the time slot $\beta_a - \gamma_a + 1$ [47]. The delay time rate is introduced to illustrate the appliance's operational delay

$$DTR_a(x_a) = \frac{x_a - \alpha_a}{\beta_a - \gamma_a + 1 - \alpha_a} \tag{3.3.5}$$

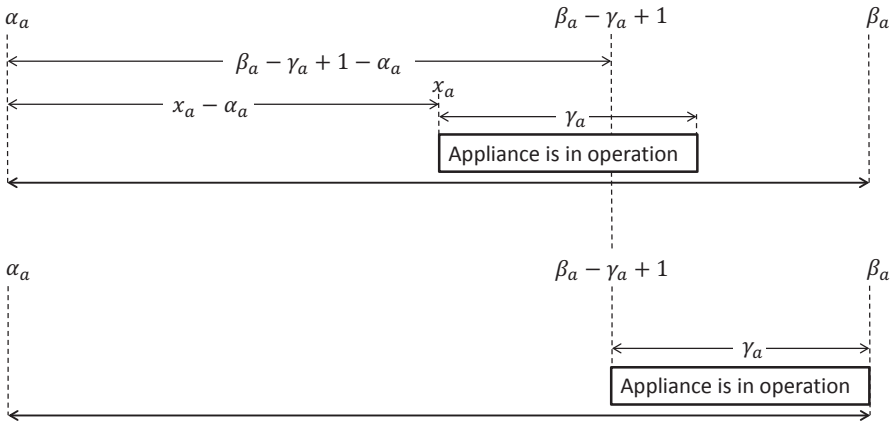

Figure 3.3: The illustration of the concept of delay time rate

where DTR_a is the delay time rate of appliance a. For a home with n SAs, the minimization of operational delay is formulated as

$$\begin{aligned}
&\min_X f_3(X) \\
&f_3(X) = \sum_{a=1}^{n} \sigma_a^{DTR_a(x_a)} \\
&DTR_a(x_a) = \tfrac{x_a - \alpha_a}{\beta_a - \gamma_a + 1 - \alpha_a} \\
&X = \{x_1, x_2, \cdots, x_a, \cdots, x_n\} \\
&\text{subject to} \\
&x_a \in [\alpha_a, \beta_a - \gamma_a + 1], \;\; a = \{1, 2, \cdots, n\}
\end{aligned} \tag{3.3.6}$$

where $\sigma_a > 1$ denotes the delay parameter of appliance a, the higher the value of σ_a, the higher will be the cost of the operational delay [47].

3.3.4 Problem formulation

Considering minimizations of the appliances' operational unsafety, the electricity cost and the appliances' operational delay, the MORDSS is formulated as

$$\begin{aligned}
&\min_X F(X)\\
&F(X) = (f_1(X), f_2(X), f_3(X))\\
&f_1(X) = \sum_{a=1}^{n} \rho_a^{UTR_a(x_a)},\ \ UTR_a(x_a) = \tfrac{\gamma_a - s_a(x_a)}{\gamma_a}\\
&f_2(X) = \sum_{t=1}^{T} prc_t \cdot l_t(X),\ \ l_t(X) = \sum_{a=1}^{n} e_a^t\\
&f_3(X) = \sum_{a=1}^{n} \sigma_a^{DTR_a(x_a)},\ \ DTR_a(x_a) = \tfrac{x_a - \alpha_a}{\beta_a - \gamma_a + 1 - \alpha_a}\\
&X = \{x_1, x_2, \cdots, x_a, \cdots, x_n\}\\
&\text{subject to}\\
&x_a \in [\alpha_a, \beta_a - \gamma_a + 1],\ \ a = \{1, 2, \cdots, n\}
\end{aligned} \tag{3.3.7}$$

where $F(X)$ is the vector of multiple objectives.

3.4 Three approaches to tackling multiple objectives

To solve the problem of the RDSS with the consideration of the multiple objectives presented in the previous section, three approaches including the Pareto approach, the Weight approach and the Constraint approach are presented in this section.

3.4.1 Pareto approach

The Pareto approach aims to find a set of optimal solutions of the multi-objective optimization problem and these solutions are nondominated by other solutions in the feasible domain, which is defined as follows. Let $\mathbf{\Omega}$ denote the set of feasible solutions of Eqn. (3.3.7)

$$\begin{aligned}
\mathbf{\Omega} = \ &\big\{X | X = \{x_1, x_2, \cdots, x_a, \cdots, x_n\},\\
&x_a \in [\alpha_a, \beta_a - \gamma_a + 1],\ \ a = \{1, 2, \cdots, n\}\big\}.
\end{aligned} \tag{3.4.1}$$

For the set of appliances' start time slots $X_i, X_j \in \mathbf{\Omega}$, if

$$\begin{cases} f_1(X_i) < f_1(X_j) \\ f_2(X_i) < f_2(X_j) \\ f_3(X_i) < f_3(X_j) \end{cases} \tag{3.4.2}$$

it can be defined that $F(X_i) < F(X_j)$ and X_i dominates X_j [52]. That X_i dominates X_j shows all the objectives of solution X_i are better than that of X_j. If some objectives of X_i are better and some are worse than the corresponding objectives of X_j, it cannot be concluded that X_i dominates X_j. Let $\mathbf{X} = \{X_1, X_2, \cdots, X_k\}$ denote the set of nondominated solutions. For each $X_j \in \mathbf{X}$, it is not possible to find a $X_i \in \mathbf{\Omega}$ that satisfies $F(X_i) < F(X_j)$, i.e. there is no solution among the feasible solutions that satisfies all the objectives are better than the solutions in $\mathbf{X}$. The solutions in $\mathbf{X}$ cannot be dominated by each other as well. The objective values of the solutions of the nondominated set constitute a front known as the Pareto-optimal front, i.e. the nondominated solutions are the ones that correspond to the Pareto-optimal front. To obtain the solutions of the Pareto-optimal front, the nondominated sorting genetic algorithm-II (NSGA-II) is usually adopted, and more details of this algorithm can be found in [96].

3.4.2 Weight approach

The Weight approach attaches importance factors to the three objectives in Eqn. (3.3.7). To make the three objectives commensurable, the problem of demand side

scheduling considering multiple objectives is formulated as

$$
\begin{aligned}
&\min_{X} \ \ w_1\tfrac{f_1(X)}{\underline{f_1}} + w_2\tfrac{f_2(X)}{\underline{f_2}} + w_3\tfrac{f_3(X)}{\underline{f_3}} \\
&w_1 + w_2 + w_3 = 1 \\
&f_1(X) = \sum_{a=1}^{n} \rho_a^{UTR_a(x_a)}, \ \ UTR_a(x_a) = \tfrac{\gamma_a - s_a(x_a)}{\gamma_a} \\
&f_2(X) = \sum_{t=1}^{T} prc_t \cdot l_t(X), \ \ l_t(X) = \sum_{a=1}^{n} e_a^t \\
&f_3(X) = \sum_{a=1}^{n} \sigma_a^{DTR_a(x_a)}, \ \ DTR_a(x_a) = \tfrac{x_a - \alpha_a}{\beta_a - \gamma_a + 1 - \alpha_a} \\
&\underline{f_1} = \min_{X \in \mathbf{\Omega}} f_1(X) \\
&\underline{f_2} = \min_{X \in \mathbf{\Omega}} f_2(X) \\
&\underline{f_3} = \min_{X \in \mathbf{\Omega}} f_3(X) \\
&X = \{x_1, x_2, \cdots, x_a, \cdots, x_n\} \\
&\text{subject to} \\
&x_a \in [\alpha_a, \beta_a - \gamma_a + 1], \ \ a = \{1, 2, \cdots, n\}
\end{aligned}
\tag{3.4.3}
$$

where $0 \leq w_1, w_2, w_3 \leq 1$ are the importance factors of the operational unsafety, the electricity cost and the operational delay, respectively, and $\underline{f_1}$, $\underline{f_2}$ and $\underline{f_3}$ are the minimum values of $f_1(X)$, $f_2(X)$ and $f_3(X)$. Using the Weight approach, the multi-objective optimization problem is converted to a problem with a single objective, which can be solved by genetic algorithm (GA), and only one optimal solution will be obtained [33, 47].

3.4.3 Constraint approach

The Constraint approach optimizes one objective in Eqn. (3.3.7) subject to the constraint that the deviations of the other two objectives from their corresponding optimal values are within certain ranges. Taking it as an example that $f_1(X)$ is minimized with the constraints of $f_2(X)$ and $f_3(X)$, the problem of MORDSS based

on the Constraint approach is formulated as

$$
\begin{aligned}
&\min_{X} f_1(X) \\
&f_1(X) = \sum_{a=1}^{n} \rho_a^{UTR_a(x_a)}, \;\; UTR_a(x_a) = \tfrac{\gamma_a - s_a(x_a)}{\gamma_a} \\
&X = \{x_1, x_2, \cdots, x_a, \cdots, x_n\} \\
&\text{subject to} \\
&f_2(X) \leq (1+\eta_2)\underline{f_2} \\
&f_3(X) \leq (1+\eta_3)\underline{f_3} \\
&f_2(X) = \sum_{t=1}^{T} prc_t \cdot l_t(X), \;\; l_t(X) = \sum_{a=1}^{n} e_a^t \\
&f_3(X) = \sum_{a=1}^{n} \sigma_a^{DTR_a(x_a)}, \;\; DTR_a(x_a) = \tfrac{x_a - \alpha_a}{\beta_a - \gamma_a + 1 - \alpha_a} \\
&\underline{f_2} = \min_{X \in \mathbf{\Omega}} f_2(X) \\
&\underline{f_3} = \min_{X \in \mathbf{\Omega}} f_3(X) \\
&x_a \in [\alpha_a, \beta_a - \gamma_a + 1], \;\; a = \{1, 2, \cdots, n\}
\end{aligned}
\tag{3.4.4}
$$

where $\eta_2, \eta_3 \geq 0$ are the constraint factors of the electricity cost and the operational delay, respectively [46]. The problem Eqn. (3.4.4) can also be solved through GA and only one optimal solution will be obtained [46, 51].

It can be seen from the formulations of approaches that the Weight approach and the Constraint approach depend on the importance factors and the constraint factors, respectively. The physical meaning of the objective function of the Weight approach is unclear and the objectives in the constraints are not optimized for the Constraint approach. By comparison, the Pareto approach does not depend on the predefined factors and it simultaneously optimizes multiple objectives with a clear physical meaning. Therefore, the Pareto approach is adopted to solve the problem of MORDSS.

3.5 Decision making of Pareto approach

As the Pareto approach provides a set of optimal solutions, this thesis proposes a method to make the final scheduling decision taking into account the importance

factors w_1, w_2, w_3 of the three objectives. The important factors can be defined by users, or users can just decide the importance rank of multiple objectives as input and the important factors are determined by the EMC based on the following method [122–125]. Considering that the sum of the importance factors is 1 and that the more important objective has a higher factor, the importance factors are

$$w_m = (1/N) \sum_{j=\delta_m}^{N} (1/j), m = 1, 2, \cdots, N \tag{3.5.1}$$

where N denotes the number of objectives and δ_m denotes the importance rank of objective m. Users decide the importance rank based on their concerns. If they care more about the operational safety than the electricity cost and the operational delay, they will assume the operational safety with the highest importance. For the case where the importance rank of the three objectives is the operational safety, the electricity cost, the operational delay, i.e. the operational safety is the most important, following the electricity cost and the operational delay, the importance factors are $w_1 = 1/3 \times (1 + 1/2 + 1/3) = 11/18, w_2 = 1/3 \times (1/2 + 1/3) = 5/18$ and $w_3 = 1/3 \times 1/3 = 1/9$. This method of determining the importance factors which is based on the importance rank is adopted in [122–125] and it is taken into account that the more important objective has a higher factor.

Let $F^i = (f_1^i, f_2^i, f_3^i)$ denote the ith solution of the Pareto-optimal front, where f_1^i, f_2^i and f_3^i represent the values of the operation unsafety, the electricity cost and the operational delay, respectively, $i \in I = \{1, 2, \cdots, k\}$ and k is the number of solutions of the Pareto-optimal front. Firstly, the Pareto-optimal solutions are sorted based on the order that the value of the most important objective is increasing. If the values of the most important objective are equal, the solutions are sorted according to the order that the value of the sub-important objective is increasing, etc.. For example, if $w_1 \geq w_2 \geq w_3$, the final rank of Pareto-optimal solutions satisfies

$$\begin{cases} f_1^j \leq f_1^{j+1} \\ f_2^j \leq f_2^{j+1} \quad \text{if } f_1^j = f_1^{j+1} \\ f_3^j \leq f_3^{j+1} \quad \text{if } f_1^j = f_1^{j+1} \text{ and } f_2^j = f_2^{j+1} \end{cases} \tag{3.5.2}$$

for any $j \in \{1, 2, \cdots, k-1\}$. Then, the final decision $F^* = (f_1^*, f_2^*, f_3^*)$ is made taking into account the rank of the Pareto-optimal solutions and the following rule. The solution with a smaller rank number, i.e. with a smaller value of the more important objective, is chosen to be the final optimal solution unless the sacrifice of this objective can bring a sufficient improvement to the sub-important objective. For example, if the operational safety and the electricity cost are considered with $w_1 = 0.8$ and $w_2 = 0.2$, i.e. the operational safety is four times more important than the cost, the solution with a smaller value of the operational unsafety is preferred. However, if 1% of the sacrifice of the safety can bring greater than 4% of the reduction of the electricity cost, the sacrifice of the operational safety brings a sufficient reduction of the cost and the solution with a bigger operational unsafety and a smaller cost is chosen.

The procedure of the final decision making based on the obtained rank of the Pareto-optimal solutions is

Step 1 $F^* = F^1, i = 2$

Step 2 if $f_1^i > f_1^*$ and Eqn. (3.5.3)

$$\begin{cases} \frac{(f_2^* - f_2^i)/(f_2^{\max} - f_2^{\min})}{(f_1^i - f_1^*)/(f_1^{\max} - f_1^{\min})} > \frac{w_1}{w_2} \\ f_3^* \geq f_3^i \end{cases} \tag{3.5.3}$$

then $F^* = F^i$

Step 3 if $f_1^i = f_1^*$ and Eqn. (3.5.4)

$$\frac{(f_3^* - f_3^i)/(f_3^{\max} - f_3^{\min})}{(f_2^i - f_2^*)/(f_2^{\max} - f_2^{\min})} > \frac{w_2}{w_3} \tag{3.5.4}$$

then $F^* = F^i$

Step 4 $i = i + 1$ and go to **Step 2**

where $f_1^{\min} = \min_{i \in I} f_1^i$, $f_2^{\min} = \min_{i \in I} f_2^i$, $f_3^{\min} = \min_{i \in I} f_3^i$, $f_1^{\max} = \max_{i \in I} f_1^i$, $f_2^{\max} = \max_{i \in I} f_2^i$ and $f_3^{\max} = \max_{i \in I} f_3^i$. Step 2 shows that when three objectives are considered, in addition to the requirement that the sacrifice of the operational

safety brings a sufficient reduction of the electricity cost, it is essential that the operational delay does not get worse, then the solution with a bigger value of the operational unsafety is preferred. The start time slots of appliances corresponding to F^* will be adopted and the EMC will automatically control home appliances according to the obtained start time slots.

It is noted that the Pareto approach does not depend on the importance factors and the importance factors are taken into account for the final decision making among the Pareto-optimal solutions. This is different from the Weight approach which relates the importance factors to the values of the objectives, whilst the proposed method of decision making connects the importance factors with the variations of the objectives.

3.6 Simulation results

In this section, the Pareto approach is compared with the Weight approach and the Constraint approach in the performance of solving the MORDSS and the relationships between the operational safety and other objectives are investigated. Eight typical appliances are considered and some appliances are used more than once in a day, and the parameters of the appliances are shown in Table 3.1 [47, 48]. It is assumed that the users' at-home status and awake status are as shown in Fig. 3.4. The day-ahead real-time pricing data on August 3rd 2012 is adopted from the Ameren Illinois Power Company [32]. Both the parameters ρ_a and σ_a, $a = \{1, 2, \cdots, n\}$, are assumed to be 2 [33, 47]. It is noted that users' at-home status and awake status in Fig. 3.4 are illustrated to show how users' statuses are taken into account in the appliances' operational safety, and the at-home status and the awake status are individually defined by users.

3.6.1 Comparison of Pareto approach and Weight approach

The Pareto approach is compared with the Weight approach under three situations: minimizations of the operational unsafety and the electricity cost, minimizations of the operational unsafety and the operational delay, and minimizations of

Table 3.1: Parameters of appliances

Appliance	OTI	LOT	Power (kW)
Rice cooker[1]	1-40	2	0.5
Rice cooker[2]	56-65	2	0.5
Rice cooker[3]	71-90	2	0.5
Water heater	86-105	3	1.5
Dishwasher	101-120	2	0.6
Washing machine	1-60	5	0.38
Electric kettle[1]	1-40	1	1.5
Electric kettle[2]	81-90	1	1.5
Clothes dryer	71-90	5	0.8
Oven	71-90	3	1.9
Electric radiator[1]	56-65	5	1.8
Electric radiator[2]	81-110	20	1.8

$*^1$, $*^2$ and $*^3$ denote that appliance $*$ is used three times within different OTIs in one day.

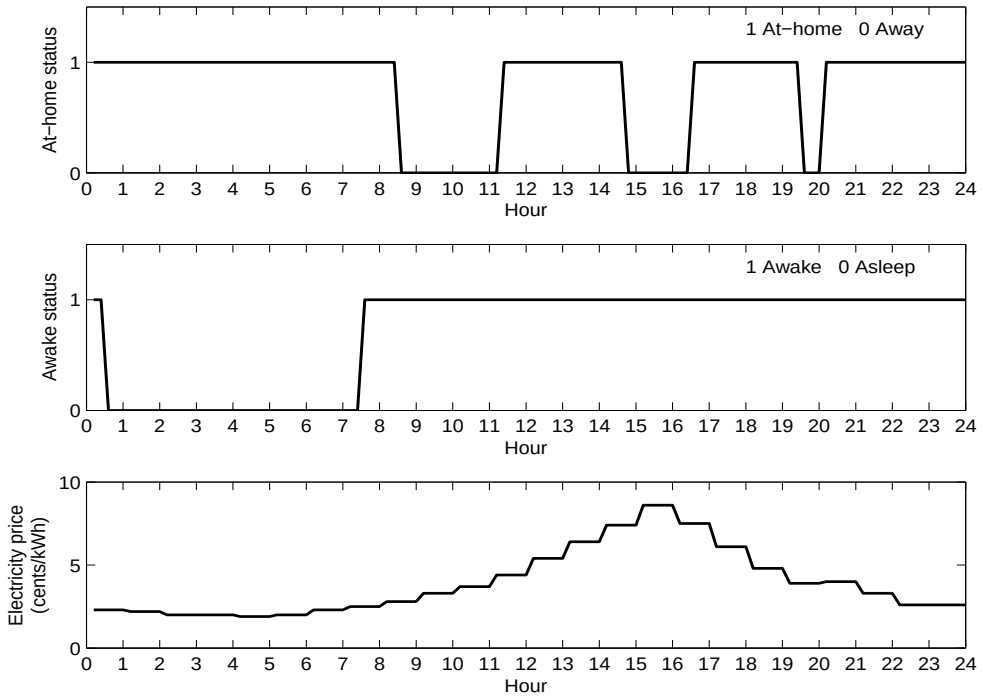

Figure 3.4: Users' at-home status, awake status and electricity price during the day

all the three objectives. The maximum generation number is set to be 200 for the NSGA-II of the Pareto approach under the three situations, and the population sizes are set to be 100 and 1000 for the situation considering two objectives and the situation considering three objectives, respectively [123]. For the GA of the Weight approach, the maximum generation number is 200 and the population size is set to be 2000 for all the situations [126].

Considering operational unsafety and electricity cost

In this case, $F(X) = (f_1(X), f_2(X))$ for the Pareto approach, and $w_3 = 0$, $w_1 + w_2 = 1$ for the Weight approach. Fig. 3.5 shows the objective values of optimal solutions obtained through the Pareto approach and the Weight approach taking into account the operational unsafety and the electricity cost. The Pareto-optimal front shows that the operational unsafety is reduced with the sacrifice of the electricity cost. The Weight approach proposes only an optimal solution based on a certain set of importance factors of multiple objectives provided by users while the Pareto approach provides a set of optimal solutions. The multiple solutions of the Weight approach in Fig. 3.5 are obtained with different sets of importance factors, and the operational unsafety and the electricity cost of these solutions with respect to the importance factor w_1 are shown in Fig. 3.6. The Pareto approach clearly shows the relationship between the sacrifice of one objective and the improvement of the other objective through the Pareto-optimal front, which is not presented by the Weight approach with a single solution. For example, when the electricity cost increases from 58.29 cents to 58.37 cents, the operational unsafety drops from 15.52 to 14.85, and a 0.14% in the increase of the electricity cost results in a 4.32% reduction in the operational unsafety. The relationship between the sacrifice of one objective and the improvement of the other objective is clearly shown through the Pareto-optimal front, which provides more information to make the decision of the MORDSS.

It is noted that though the Weight approach can provide a set of optimal solutions through multiple runs with different sets of importance factors, the Pareto approach provides the Pareto-optimal front with a single run. Moreover, the Pareto approach deals with noncommensurable objectives directly, and these objectives

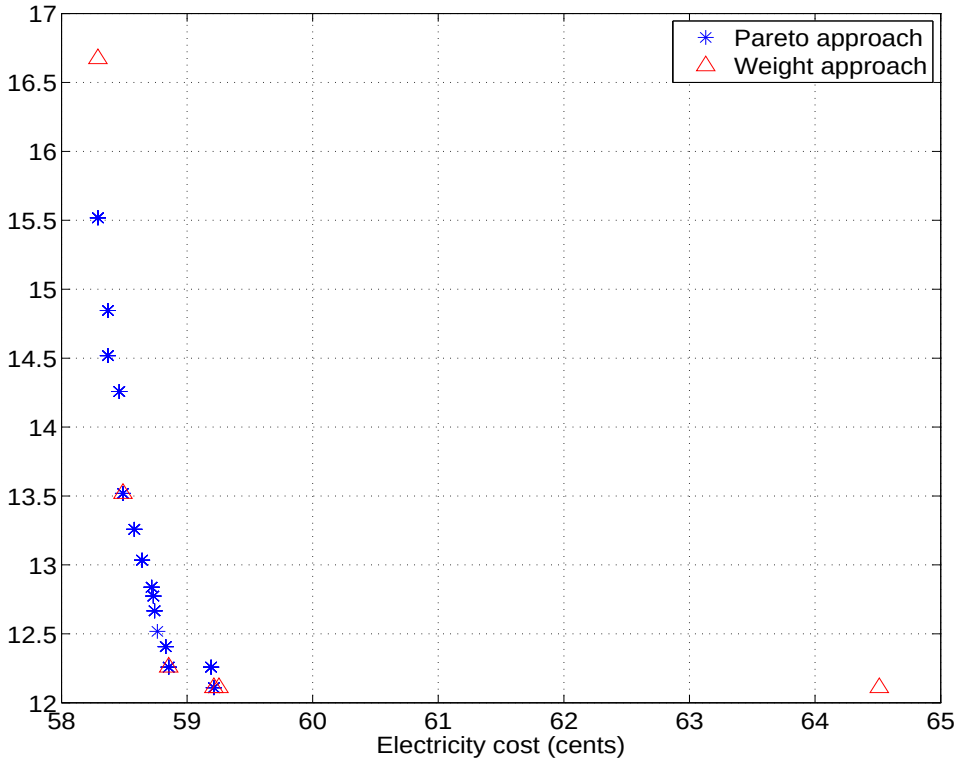

Figure 3.5: Comparison between the Pareto approach and the Weight approach considering the operational unsafety and the electricity cost

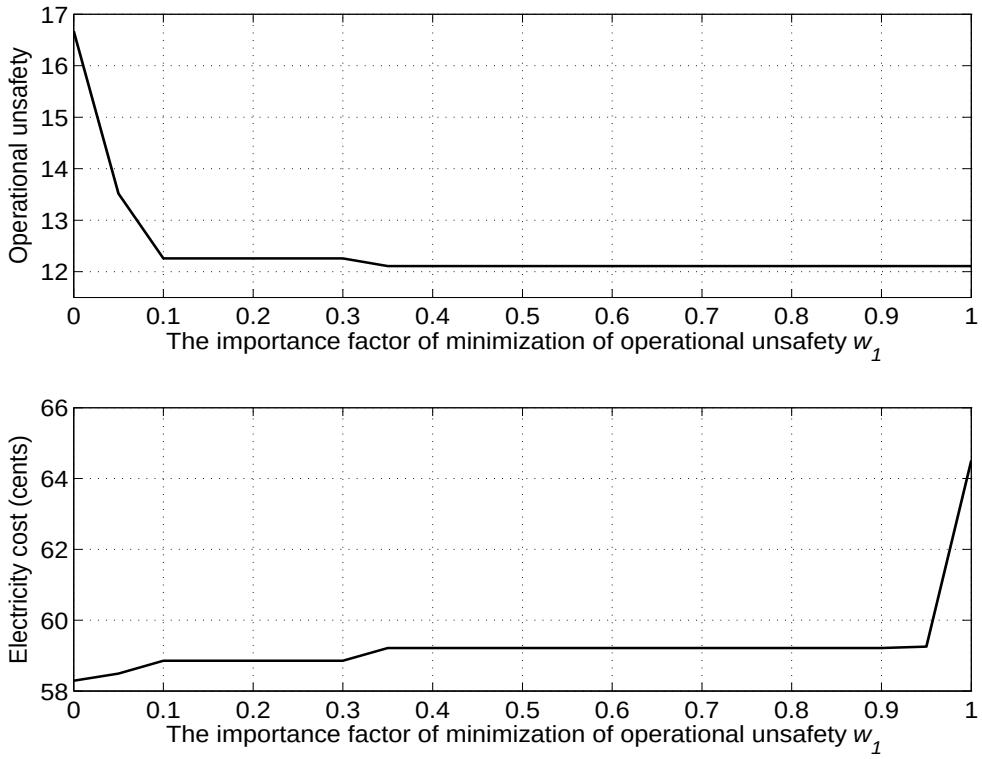

Figure 3.6: Operational unsafety and electricity cost with respect to w_1

need transforming to be commensurable through the Weight approach.

Considering operational unsafety and operational delay

In this case, $F(X) = (f_1(X), f_3(X))$ for the Pareto approach, and $w_2 = 0$, $w_1 + w_3 = 1$ for the Weight approach. Fig. 3.7 shows the objective values of optimal solutions obtained through the Pareto approach and the Weight approach taking into account the operational unsafety and the operational delay. The Pareto-optimal front shows that the operational unsafety is reduced with the sacrifice of the operational delay, which is not presented by the Weight approach with a single solution. The multiple solutions of the Weight approach in Fig. 3.7 are obtained with different sets of importance factors, and the operational unsafety and the operational delay of these solutions with respect to the importance factor w_1 are shown in Fig. 3.8.

Considering operational unsafety, electricity cost and operational delay

In this case, $F(X) = (f_1(X), f_2(X), f_3(X))$ for the Pareto approach, and $w_1 + w_2 + w_3 = 1$ for the Weight approach. Fig. 3.9 and Fig. 3.10 show the objective values of solutions obtained through the Pareto approach and the Weight approach taking into account the operational unsafety, the electricity cost and the operational delay. 100 cases of the Weight approach are illustrated with the importance factors w_1, w_2, w_3 randomly chosen satisfying $w_1 + w_2 + w_3 = 1$. Fig. 3.10 is the top view of Fig. 3.9, and the color gradients indicate different values of the electricity cost. The Pareto approach provides a set of optimal solutions with the relationships among the three objectives presented while the Weight approach only obtains one solution. The multiple solutions of the Weight approach in Fig. 3.9 and Fig. 3.10 are obtained with different sets of importance factors. It can be seen from Fig. 3.9 and Fig. 3.10 that the operational unsafety and the operational delay are reduced with the sacrifice of the electricity cost as the electricity cost increases in the decreasing directions of the operational unsafety and the operational delay. The relationship between the operational unsafety and the operational delay is shown in Fig. 3.9 and Fig. 3.10. With the electricity cost fixed, the operational unsafety decreases in the increasing direction of the operational delay, which indicates that the operational

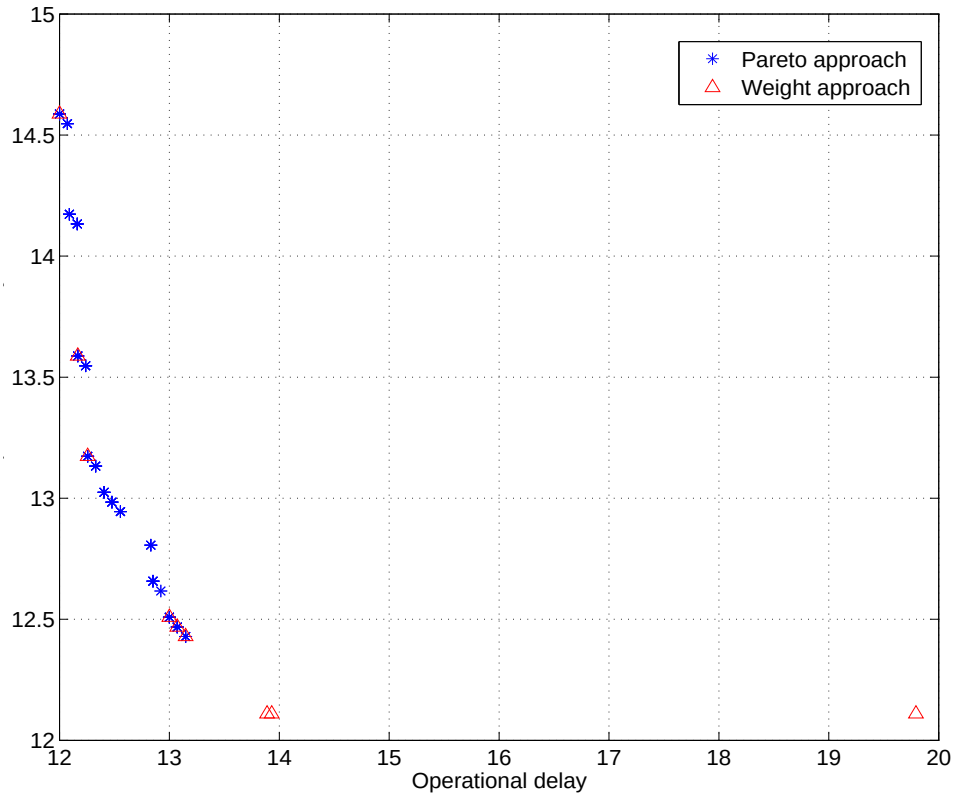

Figure 3.7: Comparison between the Pareto approach and the Weight approach considering the operational unsafety and the operational delay

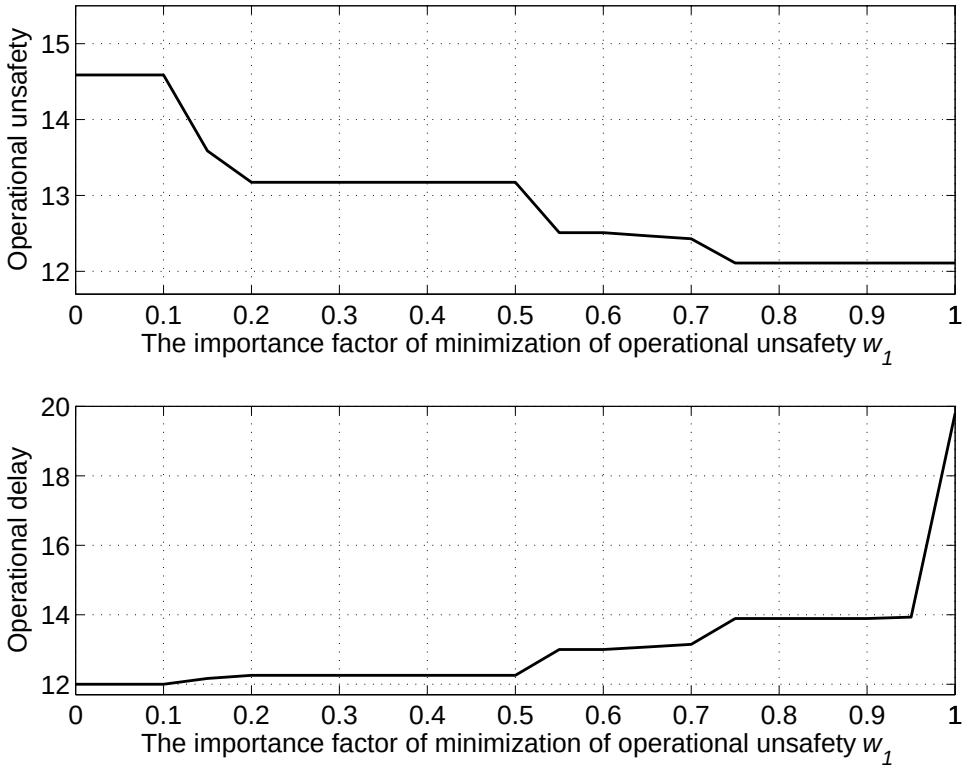

Figure 3.8: Operational unsafety and operational delay with respect to w_1

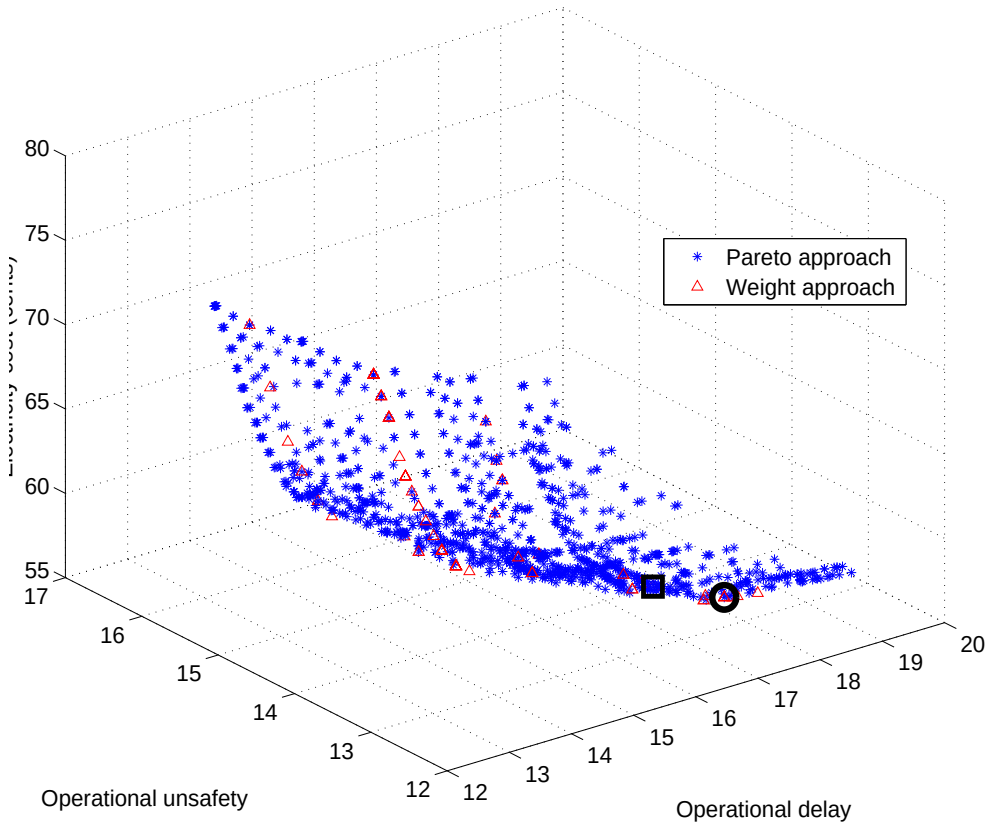

Figure 3.9: Comparison between the Pareto approach and the Weight approach considering the operational unsafety, the electricity cost and the operational delay

safety is improved with the sacrifice of the operational delay.

3.6.2 Comparison of Pareto approach and Constraint approach

In this section, the Pareto approach is compared with the Constraint approach with the consideration of the operational safety, together with one or both of the electricity cost and the operational delay. The maximum generation number and the population size of the NSGA-II for the Pareto approach and those of the GA for the Constraint approach are set as the same as parameters in the comparison between the Pareto approach and the Weight approach.

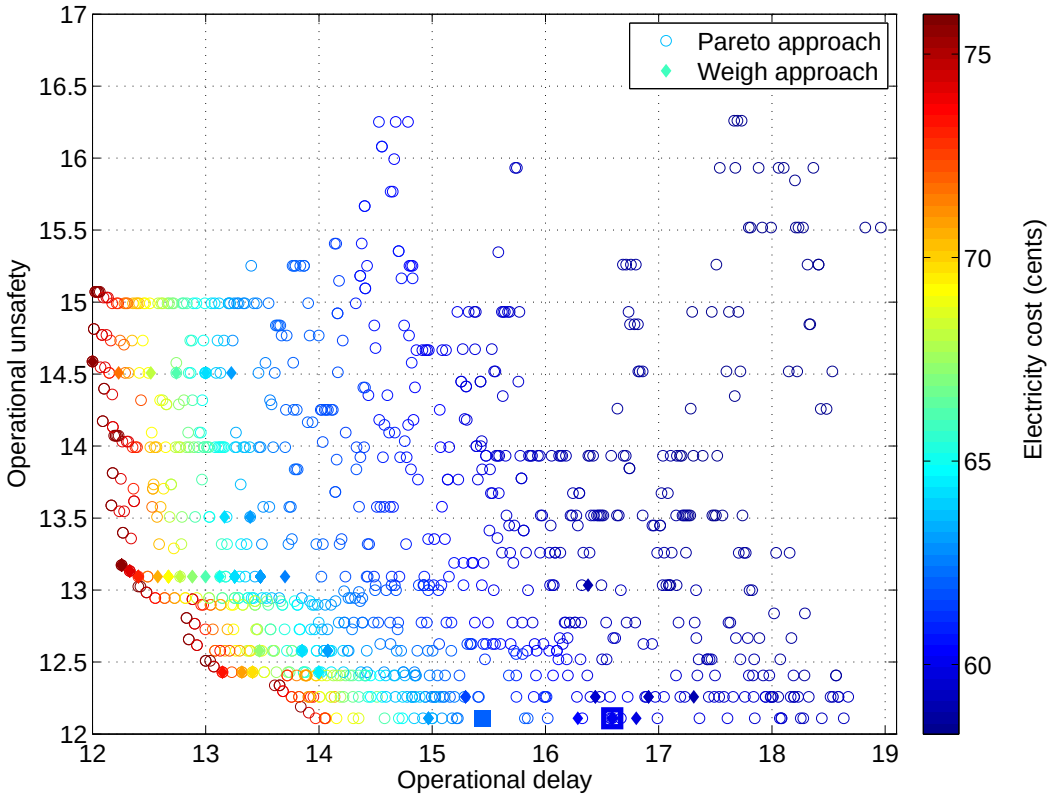

Figure 3.10: Top view of comparison between the Pareto approach and the Weight approach considering the operational unsafety, the electricity cost and the operational delay

Considering operational unsafety and electricity cost

In this case, $F(X) = (f_1(X), f_2(X))$ for the Pareto approach, and the two situations, the minimization of the operational unsafety with the constraint of the electricity cost and the minimization of the electricity cost with the constraint of the operational unsafety are considered for the Constraint approach. Fig. 3.11 shows the comparison between the Pareto approach and the Constraint approach taking into account the operational unsafety and the electricity cost. Blue stars denote the Pareto approach in Fig. 3.11, red squares represent the results of the Constraint approach where the operational unsafety is minimized under the condition that the deviation of the electricity cost from its optimal value is within a certain range, and red triangles denote the results of the Constraint approach where the electricity cost is minimized with the constraint of the operational unsafety. The operational unsafety and the electricity cost with respect to the constraint factor η_2 in the first situation of the Constraint approach are shown in Fig. 3.12. The situation where the operational unsafety is minimized with the constraint of the electricity cost is similar to the situation where the electricity cost is minimized with the constraint of the operational unsafety, and the simulation results of the first situation are presented as an example.

The Pareto approach provides a set of optimal solutions while the Constraint approach proposes only an optimal solution and the relationship between the operational safety and the electricity cost is presented through the Pareto approach. The operational safety is improved with the sacrifice of the electricity cost. It is noted that multiple solutions of the Constraint approach shown in Fig. 3.11 are obtained with different constraints and constraint factors. Moreover, it can be seen from Fig. 3.11 that some solutions proposed via the Constraint approach are in the upper right of the Pareto-optimal front, i.e. these solutions can be dominated by solutions proposed via the Pareto approach since the Constraint approach does not optimize the objectives in the constraints as long as the deviations of these objectives from their corresponding optimal values are within certain ranges. Taking the following situation as an example, the operational unsafety is minimized with the constraint of the electricity cost, i.e. $\min_X f_1(X)$ subject to $f_2(X) \leq (1 + \eta_2)\underline{f_2}$. For two set-

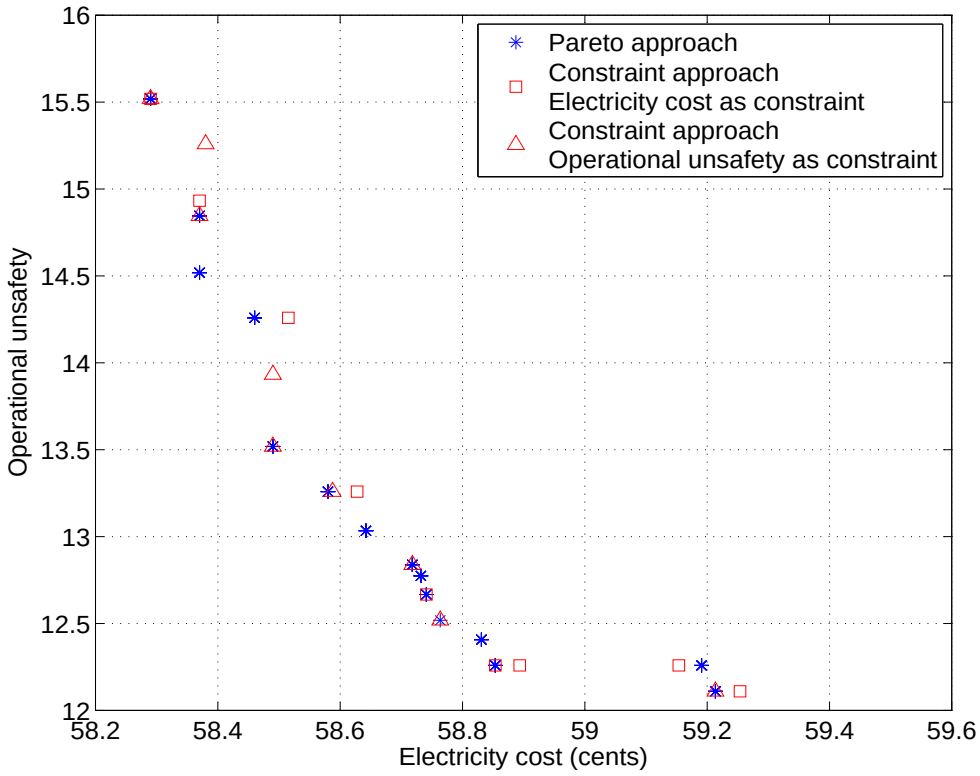

Figure 3.11: Comparison between the Pareto approach and the Constraint approach considering the operational unsafety and the electricity cost

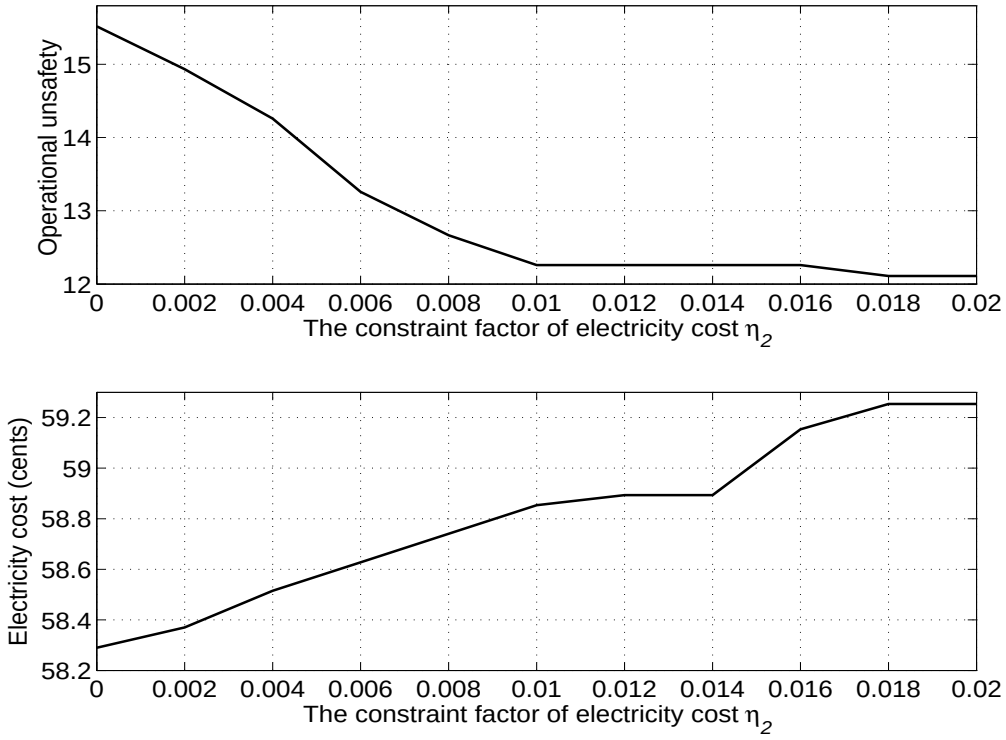

Figure 3.12: Operational unsafety and electricity cost with respect to η_2

s of appliances' start time slots X_1 and X_2, it is assumed that $f_1(X_1) = f_1(X_2)$, $f_2(X_1) \leq (1+\eta_2)\underline{f_2}$, $f_2(X_2) \leq (1+\eta_2)\underline{f_2}$, and $f_2(X_1) < f_2(X_2)$. The Constraint approach does not guarantee X_1 is selected with priority though $f_1(X_1) = f_1(X_2)$ and $f_2(X_1) < f_2(X_2)$.

Considering operational unsafety and operational delay

In this case, $F(X) = (f_1(X), f_3(X))$ for the Pareto approach, and the two situations, the minimization of the operational unsafety with the constraint of the operational delay and the minimization of the operational delay with the constraint of the operational unsafety are considered for the Constraint approach. Fig. 3.13 shows the comparison between the Pareto approach and the Constraint approach taking into account the operational unsafety and the operational delay. Blue stars denote the Pareto approach in Fig. 3.13, red squares represent the results of the Constraint approach where the operational unsafety is minimized under the condition that the deviation of the operational delay from its optimal value is within a certain range, and red triangles denote the results of the Constraint approach where the operational delay is minimized with the constraint of the operational unsafety. The operational unsafety and the operational delay with respect to the constraint factor η_3 in the first situation of the Constraint approach are shown in Fig. 3.14. The situation where the operational unsafety is minimized with the constraint of the operational delay is similar to the situation where the operational delay is minimized with the constraint of the operational unsafety, and the simulation results of the first situation are presented as an example. It can be seen from Fig. 3.13 that the operational safety is improved with the sacrifice of the operational delay and that some solutions of the Constraint approach are dominated by solutions proposed via the Pareto approach.

Considering operational unsafety, electricity cost and operational delay

In this case, $F(X) = (f_1(X), f_2(X), f_3(X))$ for the Pareto approach, and three situations, where one of the three objectives is minimized with the constraints of the other two objectives, are taken into account for the Constraint approach. Fig. 3.15 and Fig. 3.16 show the objective values of optimal solutions obtained by the Pareto

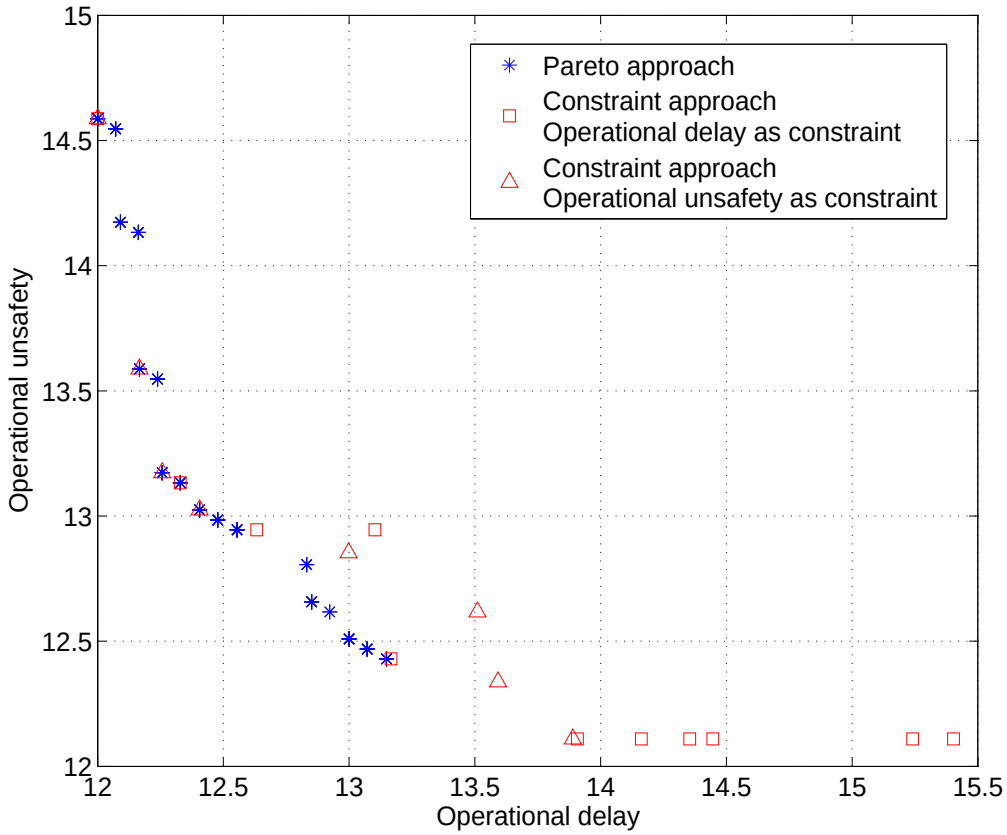

Figure 3.13: Comparison between the Pareto approach and the Constraint approach considering the operational unsafety and the operational delay

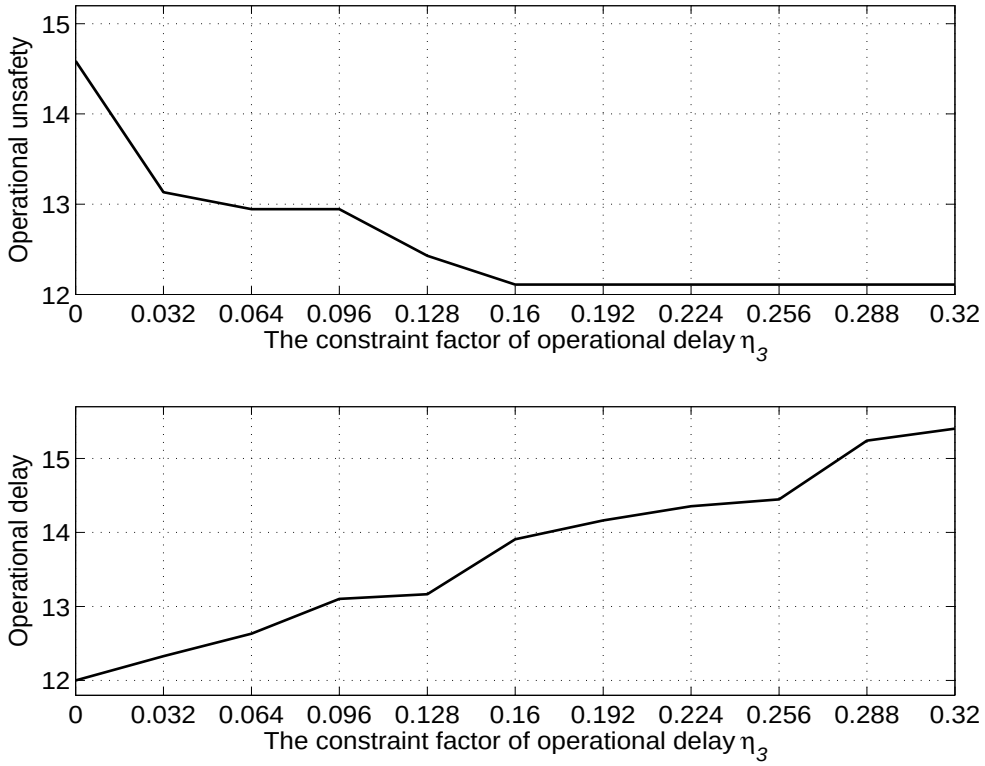

Figure 3.14: Operational unsafety and operational delay with respect to η_3

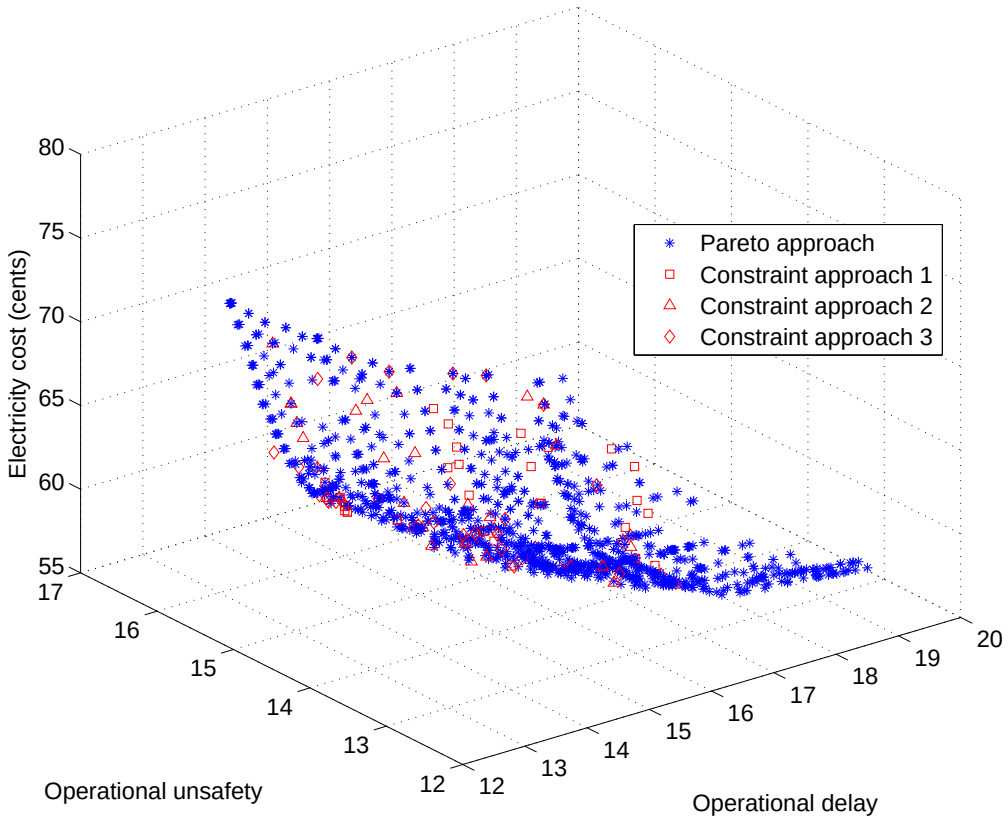

Figure 3.15: Comparison between the Pareto approach and the Constraint approach considering the operational unsafety, the electricity cost and the operational delay

approach and the Constraint approach taking into account the operational unsafety, the electricity cost and the operational delay. Squares, triangles and diamonds denote the results of the Constraint approach where the operational unsafety, the operational delay and the electricity cost are minimized with the constraints of the other two objectives, which are indicated as Constraint approach 1, 2 and 3 in Fig. 3.15 and Fig. 3.16, respectively. For each situation of the Constraint approach, 33 cases are illustrated where the constraint factors are randomly chosen within [0, 0.3]. Fig. 3.16 is the top view of Fig. 3.15, where the color gradients indicate different electricity costs.

The Pareto approach provides a set of optimal solutions while the Constraint

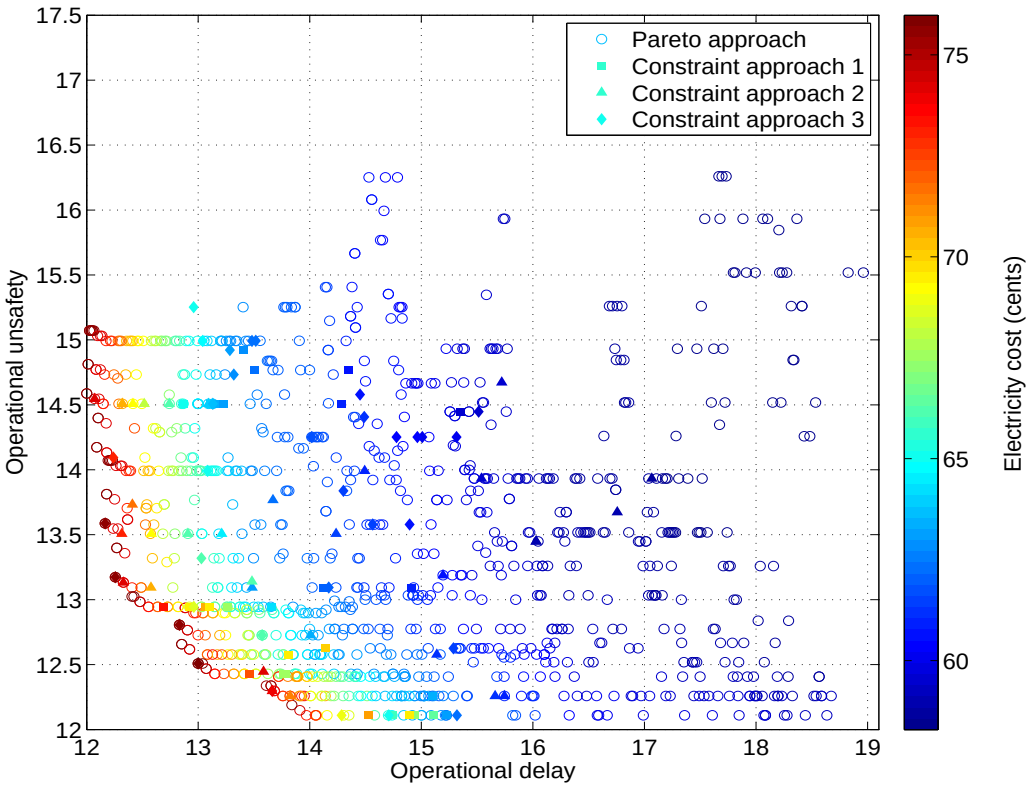

Figure 3.16: Top view of comparison between the Pareto approach and the Constraint approach considering the operational unsafety, the electricity cost and the operational delay

approach proposes only an optimal solution, and the multiple solutions of the Constraint approach in Fig. 3.15 and Fig. 3.16 are obtained with different constraints and constraint factors. It can be seen from Fig. 3.15 and Fig. 3.16 that the operational unsafety and the operational delay are reduced with the sacrifice of the electricity cost and that the operational safety is improved with the sacrifice of the operational delay. Moreover, Fig. 3.16 shows that some solutions of the Constraint approach can be dominated by solutions proposed by the Pareto approach as the electricity cost of the Constraint approach is larger than that of the Pareto approach.

3.6.3 Final decision making of Pareto approach

Through the proposed method of decision making of the Pareto approach, the final solution obtained is illustrated under the situation that the operational safety is considered as the most important objective, the electricity cost as the second important and the operational delay the last, i.e. $w_1 = 11/18, w_2 = 5/18$ and $w_3 = 1/9$ according to Eqn. (3.5.1), and this solution is compared with the solution proposed by the Weight approach with the same importance factors. The adopted situation with the operational safety as the most important objective is illustrated to show the comparison between the proposed method of decision making of the Pareto approach and the Weight approach, and other situations with different importance ranks can be adopted based on users' concerns and importance preference of the three objectives. As shown in Table 3.2, the operational unsafety, the electricity cost and the operational delay of the Pareto approach are 12.11, 59.99 cents and 16.59, respectively, and this solution is the one highlighted with a black circle shown in Fig. 3.9, corresponding to the solution in the blue hollow square in Fig. 3.10, while the solution proposed by the Weight approach is the one in the black square in Fig. 3.9 with the operational unsafety 12.11, the electricity cost 61.89 cents and the operational delay 15.44, corresponding to the solution in the solid light blue square in Fig. 3.10. Compared with the solution based on the Pareto approach, the operational unsafety is the same, the electricity cost is greater and the operational delay is less for the solution of the Weight approach. The relationship between the sacrifice of the electricity cost and the improvement of the operational delay is presented

Table 3.2: Comparison of final solution between the Pareto approach and the Weight approach

Approach	Operational unsafety	Electricity cost (cents)	Operational delay
Pareto approach	12.11	59.99	16.59
Weight approach	12.11	61.89	15.44

according to Eqn. (3.5.4)

$$\begin{aligned} & \frac{(f_3^{\mathrm{P}}-f_3^{\mathrm{W}})/(f_3^{\max}-f_3^{\min})}{(f_2^{\mathrm{W}}-f_2^{\mathrm{P}})/(f_2^{\max}-f_2^{\min})} \\ = \; & \frac{(16.59-15.44)/(18.96-12.00)}{(61.89-59.99)/(75.98-58.29)} \\ = \; & 1.54 \end{aligned} \tag{3.6.1}$$

where f_2^{P} and f_3^{P} are the electricity cost and the operational delay of the Pareto approach, respectively, f_2^{W} and f_3^{W} are the cost and the operational delay of the Weight approach, respectively, and $f_2^{\max} = 75.98$, $f_2^{\min} = 58.29$, $f_3^{\max} = 18.96$, $f_3^{\min} = 12.00$ are the bounds of the electricity cost and the operational delay. The electricity cost is 2.50 times more important than the operational delay and $1.54 < 2.50$ shows that the sacrifice of the electricity cost does not bring a sufficient improvement of the operational delay comparing the solution of the Weight approach with that of the Pareto approach. Therefore, the solution based on the Pareto approach with the same operational unsafety and less electricity cost is preferred according to the proposed method of final decision making. The start time slots of the appliances in Table 3.1 are $1, 57, 71, 95, 101, 38, 1, 86, 86, 86, 57$ and 91, respectively, corresponding to the solution based on the Pareto approach.

3.7 Conclusions

In this chapter, the operational safety of appliances is considered in the RDSS along with the electricity cost and the operational delay. The Pareto approach is adopted to solve the MORDSS and to present the relationships between the operational safety and the other two objectives, and it is compared with the Weight approach and the Constraint approach in the performance of multi-objective optimiza-

tion. Simulation results have demonstrated that the operational safety is improved with the sacrifice of the electricity cost and the operational delay. Compared with the Weight approach, the Pareto approach clearly presents the relationships between the operational safety and the other two objectives. In the comparison with the Constraint approach, the solutions proposed by the Pareto approach better satisfy users' concerns.

Chapter 4

Uncertainty of manually operated appliances

4.1 Introduction

Home appliances are categorized into schedulable appliances (SAs), e.g. washing machine and dishwasher, and manually operated appliances (MOAs), e.g. lights and TV. When the energy consumption of SAs is scheduled ahead, the energy consumption of MOAs is uncertain since MOAs are manually controlled by users based on their real-time demands. However, the uncertainty of MOAs' energy consumption is not considered in [33, 47, 54], and this simplification will cause the degradation of the energy consumption schedules for SAs. When the electricity pricing scheme with the combination of real-time pricing (RTP) and inclining block rate (IBR) is adopted, the simplification will make users confront the risk of a high electricity cost as the total energy consumption of home appliances may exceed the energy consumption threshold set by the IBR when the energy consumption of MOAs is accidentally involved. The energy consumption of MOAs usually accounts for 30% to 40% of the energy consumption of home appliances [33, 54, 55], and it is necessary and worth to consider the uncertainty of MOAs so as to further improve the performance of the optimal scheduling scheme of home appliances.

Users' real-time demands and behaviors are usually affected by many random

factors and external disturbances, and the probabilistic information of MOAs' energy consumption is not easily obtained. Since the robust optimization approach (ROA) does not require the probabilistic information of the uncertain variable, it is adopted to solve the residential demand side scheduling (RDSS) problem with the consideration of the uncertainty of MOAs' energy consumption. Based on the electricity pricing scheme that combines RTP and IBR, the maximal disturbance of MOAs, i.e. the energy consumption case of MOAs that causes the maximum electricity cost of all home appliances, is taken into account, and the ROA is used to minimize this maximum electricity cost. The problem of energy scheduling is formulated as a min-max, two-level optimization problem and the intergeneration projection evolutionary algorithm (IP-EA) is adopted to solve the proposed robust optimization problem [127]. The IP-EA, which is a two-level evolutionary algorithm with the inner genetic algorithm (GA) and the outer particle swarm optimization (PSO) algorithm, is effective in solving the proposed nonlinear problem with the two-level framework [127]. The ROA is compared with other two approaches, one without considering the impact of MOAs and one considering MOAs with the fixed energy comsumption. Simulation results illustrate the effectiveness of the proposed approach in reducing the electricity cost compared with the other two approaches.

4.2 Home energy management system

The model of the home energy management system is introduced at first and then the model formulation is presented.

4.2.1 System model

As shown in Fig. 4.1, the energy management controller (EMC) schedules energy consumption of home appliances a day ahead based on the electricity price and users' demands. The electricity pricing scheme with the combination of RTP and IBR is adopted. Home appliances are categorized into MOAs and SAs. MOAs are manually operated based on users' real-time demands and users must be available to operate them. SAs are appliances whose energy consumption can be scheduled

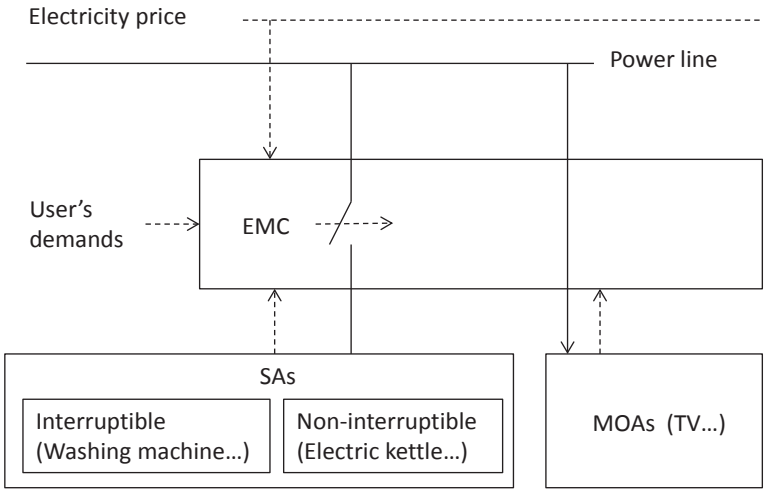

Figure 4.1: Home energy management system

ahead and automatically controlled by the EMC and does not require the users' participation during their operations, though users are required to prepare for the operations and preset the operation time interval and the operation length. For example, after users put food in the oven and set the operation interval and the operation length, the EMC will start the oven at the optimal time slot automatically, so is the case for the washing machine. Based on the above characteristics, oven and washing machine are classified as SAs, and they are scheduled automatically no matter whether users are at home or not. SAs include interruptible and non-interruptible appliances [33]. Interruptible appliances can suspend their operations during the operation processes, and then restart again to continue their operations. For example, the washing machine is interruptible as it can be paused during the process of washing. Once non-interruptible appliances are started, they cannot be stopped until they finish their tasks, such as the electric kettle. The common MOAs include hair drier, lights, laptop and TV. For SAs, clothes dryer, oven, water heater and electric kettle are non-interruptible, washing machine and humidifier are interruptible.

The EMC only schedules energy consumption for the SAs, not for the MOAs since the operations of MOAs are manually controlled based on the real-time demands of users. However, it does not mean that the MOAs can be ignored when

the energy consumption of the SAs is scheduled. The EMC schedules energy consumption for the SAs taking into account the uncertainty and the impact of MOAs' energy consumption. The possible operation time intervals and operation lengths of MOAs can be pre-specified by users. For example, the watching time of TV is pre-specified between 6 pm and 12 am and the watching length is pre-specified between 3 hours and 4 hours while when and how long users watch TV are still dependent upon users' real-time demand. Though users predefine the possible operation time intervals and operation lengths, it is noted that users are still in control of the operations of MOAs with their convenience fully maintained since these intervals and lengths which are predefined by users themselves can guarantee the flexibility of operations of MOAs. Taking into account the possible operation intervals and operation lengths of MOAs, the EMC will only schedule the energy consumption of SAs, i.e. control SAs' energy consumption and the energy consumption of MOAs is still totally controlled by users themselves. In the home energy management system, the operation time intervals and the operation lengths of appliances are input by users and they can also be learned by monitoring users' behaviours, e.g. the interval and the length of watching TV [128].

4.2.2 Model formulation

Firstly, the model formulation of the electricity pricing scheme that combines RTP and IBR is presented. In this pricing scheme, users are charged at a higher electricity price than RTP when the total energy consumption within a certain period exceeds a threshold, which is formulated as

$$prc_t(l_t) = \begin{cases} e_t, & \text{if } 0 \leq l_t < c \\ \varepsilon \cdot e_t, & \text{if } l_t \geq c \end{cases} \tag{4.2.1}$$

where l_t denotes the total energy consumption at time slot t, e_t denotes RTP at time slot t, c denotes the threshold and ε is a coefficient greater than 1 [33, 47].

Then the model of users' demands is formulated. Users' demands include the length of operation time (LOT) and the operation time interval (OTI) for home appli-

ances [47]. Let γ denote the LOT and $[\alpha, \beta]$ denote the OTI of an appliance, where α is the earliest start time of the operation and β is the deadline that the operation must be finished. Taking into account the general operation time of appliances, 1 hour is divided into 5 time slots and the energy consumption is scheduled with 12-minute time resolution. One day is mapped to 120 time slots and the LOT and the OTI are represented via time slots with one time slot representing 12 minutes. It is noted that though the energy consumption of MOAs cannot be scheduled in advance, users' demands for MOAs are also modelled via the possible OTIs and the ranges of LOTs which are pre-specified by users.

4.3 Impact of the uncertainty of MOAs' energy consumption

Based on the pricing scheme with the combination of RTP and IBR, the electricity cost is

$$f(\mathbf{X}, \mathbf{U}) = \sum_{t=1}^{T} prc_t(l_t(\mathbf{X}, \mathbf{U})) \cdot l_t(\mathbf{X}, \mathbf{U}) \tag{4.3.1}$$

where $\mathbf{X}$ denotes the energy consumption schedule of SAs, $\mathbf{U}$ denotes the energy consumption case of MOAs, $\mathbf{X}$ and $\mathbf{U}$ are matrixes in which each row stands for the energy consumption schedule of a certain appliance, T is the scheduling horizon that indicates the number of time slots ahead which the energy consumption schedule is made for SAs, and $T = 120$ since the energy consumption of appliances is scheduled a day ahead with one hour divided into 5 time slots, and prc_t is the electricity price at time slot t as shown in Eqn. (4.2.1).

Let $\mathbf{\Omega}$ represent all the possible energy consumption schedules of SAs and $\mathbf{\Gamma}$ represent all the possible energy consumption cases of MOAs. For a certain $\mathbf{X}$, $f(\mathbf{X}, \mathbf{U})$ is uncertain due to the uncertainty of $\mathbf{U}$. Among all the possible energy consumption cases of MOAs, there exists an energy consumption case of MOAs that makes the smallest impact to the electricity cost, i.e. with this energy consumption case of MOAs, the electricity cost is smallest. The electricity cost with the smallest

impact of MOAs is formulated as

$$f^{\mathrm{L}}(\mathbf{X}) = \min_{\mathbf{U}\in\mathbf{\Gamma}} f(\mathbf{X}, \mathbf{U}). \tag{4.3.2}$$

Similarly, there exists an energy consumption case of MOAs that makes the worst impact to the electricity cost, corresponding to the highest electricity cost

$$f^{\mathrm{R}}(\mathbf{X}) = \max_{\mathbf{U}\in\mathbf{\Gamma}} f(\mathbf{X}, \mathbf{U}). \tag{4.3.3}$$

Therefore, for a certain energy consumption schedule of SAs $\mathbf{X}$, the electricity cost $f(\mathbf{X}, \mathbf{U}) \in [f^{\mathrm{L}}(\mathbf{X}), f^{\mathrm{R}}(\mathbf{X})]$.

For any two different energy consumption schedules of SAs $\mathbf{A}$ and $\mathbf{B}$, the electricity costs are within $[f^{\mathrm{L}}(\mathbf{A}), f^{\mathrm{R}}(\mathbf{A})]$ and $[f^{\mathrm{L}}(\mathbf{B}), f^{\mathrm{R}}(\mathbf{B})]$, respectively. Fig. 4.2 shows all the possible relationships between these two electricity cost intervals [127]. For relationships shown in Fig. 4.2-(1) and Fig. 4.2-(6), the performance comparison between schedules $\mathbf{A}$ and $\mathbf{B}$ is deterministic, since the electricity cost intervals of the two schedules are not overlapped and the electricity cost with one energy consumption schedule is always less than the cost with the another schedule regardless of the uncertainty of the MOAs. However, the uncertainty of MOAs' energy consumption should be taken into account for relationships shown in Fig. 4.2-(2) - Fig. 4.2-(5) when schedules $\mathbf{A}$ and $\mathbf{B}$ are compared, since the electricity cost intervals of two schedules are overlapped and the comparison of the electricity cost is uncertain due to the uncertainty of MOAs' energy consumption.

4.4 Robust optimization approach

As shown in Fig. 4.2, the uncertainty of MOAs' energy consumption has impact on the electricity cost whose interval is between Eqn. (4.3.2) and Eqn. (4.3.3), it is necessary to take into account the uncertainty of MOAs' energy consumption in the RDSS. In this section, a robust approach is proposed to deal with the uncertainty of MOAs' energy consumption. A complete optimization model is given at first, then the IP-EA which is adopted to solve the robust optimization problem is

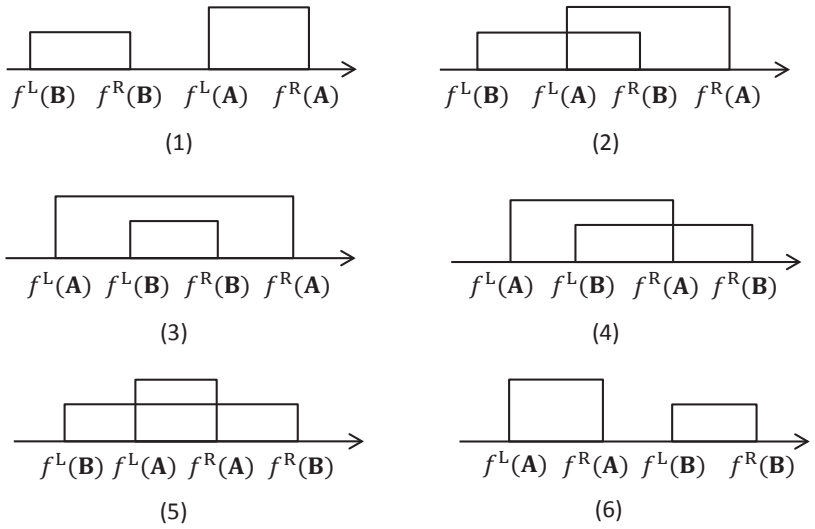

Figure 4.2: Six possible relationships between electricity cost intervals

demonstrated.

4.4.1 Complete optimization model

Among all the possible cases of MOAs' energy consumption, the ROA takes into account the case that causes $f^{\mathrm{R}}(\mathbf{X})$, i.e. with the worst impact on the electricity cost of home appliances, and the problem of scheduling the energy consumption of SAs with the consideration of the worst impact of MOAs is formulated as

$$\begin{aligned} &\min_{\mathbf{X}\in\mathbf{\Omega}} f^{\mathrm{R}}(\mathbf{X}) \\ &f^{\mathrm{R}}(\mathbf{X}) = \max_{\mathbf{U}\in\mathbf{\Gamma}} f(\mathbf{X},\mathbf{U}) \\ &f(\mathbf{X},\mathbf{U}) = \sum_{t=1}^{T} prc_t(l_t(\mathbf{X},\mathbf{U}))\cdot l_t(\mathbf{X},\mathbf{U}) \end{aligned} \tag{4.4.1}$$

which is equivalent to

$$\begin{aligned} &\min_{\mathbf{X}\in\mathbf{\Omega}} \max_{\mathbf{U}\in\mathbf{\Gamma}} f(\mathbf{X},\mathbf{U}) \\ &f(\mathbf{X},\mathbf{U}) = \sum_{t=1}^{T} prc_t(l_t(\mathbf{X},\mathbf{U}))\cdot l_t(\mathbf{X},\mathbf{U}) \end{aligned} \tag{4.4.2}$$

with the electricity price prc_t presented in Eqn. (4.2.1). For a home with n SAs and m MOAs, the energy consumption schedule of SAs is

$$\mathbf{X} = \begin{bmatrix} X_1 \\ X_2 \\ \vdots \\ X_n \end{bmatrix} = \begin{bmatrix} x_1^1 & x_1^2 & \dots & x_1^t & \dots & x_1^T \\ x_2^1 & x_2^2 & \dots & x_2^t & \dots & x_2^T \\ \vdots & \vdots & & \ddots & & \vdots \\ x_n^1 & x_n^2 & \dots & x_n^t & \dots & x_n^T \end{bmatrix} \tag{4.4.3}$$

where each row of the matrix $\mathbf{X}$ represents the energy consumption schedule of a SA within T time slots. The energy consumption case of MOAs is

$$\mathbf{U} = \begin{bmatrix} U_1 \\ U_2 \\ \vdots \\ U_m \end{bmatrix} = \begin{bmatrix} u_1^1 & u_1^2 & \dots & u_1^t & \dots & u_1^T \\ u_2^1 & u_2^2 & \dots & u_2^t & \dots & u_2^T \\ \vdots & \vdots & & \ddots & & \vdots \\ u_m^1 & u_m^2 & \dots & u_m^t & \dots & u_m^T \end{bmatrix} \tag{4.4.4}$$

where each row of the matrix $\mathbf{U}$ represents the energy consumption case of a MOA. Therefore, the total energy consumption at time slot t is

$$l_t(\mathbf{X}, \mathbf{U}) = \sum_{i=1}^{n} x_i^t + \sum_{j=1}^{m} u_j^t, t \in \{1, 2, \cdots, T\}. \tag{4.4.5}$$

The energy consumption of appliances is constrained with users' demands. Based on the classifications of appliances, the constraints of the energy consumption of appliances are presented and the illustrative examples of the constraints of appliances are shown in Fig. 4.3. Let $P = [p_1, p_2, \cdots, p_\gamma]$ denote the power vector of an appliance, which represents the appliance's power consumption during the whole operation process. For example, the power vector of the clothes dryer is [1.2 1.2 1] kW, which shows that the power consumption of the clothes dryer in the first, second and third time slot are 1.2, 1.2 and 1 kW, respectively.

When the appliance b belongs to the non-interruptible SAs, the energy consump-

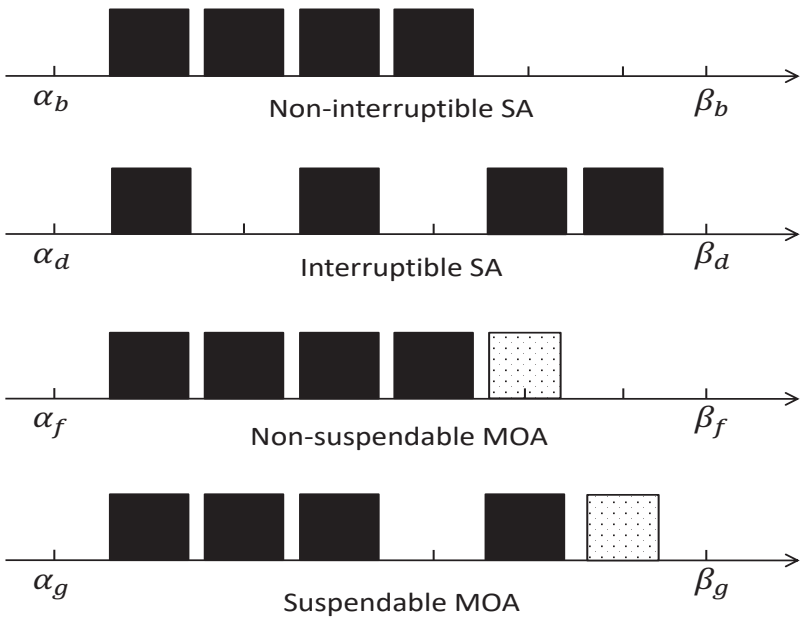

Figure 4.3: Illustrative examples of the constraints of appliances

tion schedule X_b is

$$\begin{aligned} X_b = \Big\{ x_b^t | \quad & x_b^{t_b+\theta} = \tfrac{p_{\theta+1}}{5}, \text{for all } \theta = 0, 1, \cdots, \gamma_b - 1 \\ & t_b \in [\alpha_b, \beta_b - \gamma_b + 1], \\ & x_b^t = 0,\ t \in H \backslash [t_b, t_b + \gamma_b - 1], \\ & H = \{1, 2, \cdots, T\} \Big\} \end{aligned} \tag{4.4.6}$$

where t_b is the start time slot of the appliance's operation and $t_b \in [\alpha_b, \beta_b - \gamma_b + 1]$ since the operation should start ahead the deadline by at least the length of operation time, the expression $t \in H \backslash [t_b, t_b + \gamma_b - 1]$ indicates that t belongs to H excluding the range $[t_b, t_b + \gamma_b - 1]$, and since one hour is divided into 5 time slots with 12 minutes in each time slot, the energy consumption in each time slot is $1/5$ of the power which is the energy consumption in an hour. Eqn. (4.4.6) shows the constraints of non-interruptible SAs: the operation is within the OTI $[\alpha_b, \beta_b]$, and the energy consumption is continuous and reaches LOT γ_b. When the appliance d belongs to

the interruptible SAs, the energy consumption schedule X_d is

$$\begin{aligned} X_d = \Big\{ x_d^t | \quad & x_d^{t_\theta} = \tfrac{p_\theta}{5}, \text{for all } \theta = 1, \cdots, \gamma_d \\ & \alpha_d \leq t_1 < t_2 < t_3 < \cdots < t_{\gamma_d} \leq \beta_d, \\ & x_d^t = 0,\ t \in H \backslash \{t_1, t_2, t_3, \cdots, t_{\gamma_d}\}, \\ & H = \{1, 2, \cdots, T\} \Big\} \end{aligned} \tag{4.4.7}$$

which shows the constraints of interruptible SAs: the operation is within the OTI $[\alpha_d, \beta_d]$, the energy consumption is interruptible and reaches LOT γ_d. The LOT is 4 for both the interruptible and non-interruptible SAs in Fig. 4.3.

MOAs are categorized into two groups, non-suspendable and suspendable ones. The energy consumption of a non-suspendable MOA f is

$$\begin{aligned} U_f = \Big\{ u_f^t | \quad & u_f^{t_f+\theta} = \tfrac{p_{\theta+1}}{5}, \text{for all } \theta = 0, 1, \cdots, \gamma_f - 1 \\ & t_f \in [\alpha_f, \beta_f - \gamma_f + 1], \gamma_f \in [\gamma_f^{\min}, \gamma_f^{\max}], \\ & u_f^t = 0,\ t \in H \backslash [t_f, t_f + \gamma_f - 1], \\ & H = \{1, 2, \cdots, T\} \Big\} \end{aligned} \tag{4.4.8}$$

where t_f is the start time slot of the appliance's operation, $\gamma_f^{\min}$ and $\gamma_f^{\max}$ denote the minimum and maximum LOTs of MOA f, respectively. Eqn. (4.4.8) shows the constraints of non-suspendable MOAs: the operation is within the OTI $[\alpha_f, \beta_f]$, and the LOT γ_f is within the range $[\gamma_f^{\min}, \gamma_f^{\max}]$ and is flexible based on users' real-time demands. The energy consumption of a suspendable MOA g is

$$\begin{aligned} U_g = \Big\{ u_g^t | \quad & u_g^{t_\theta} = \tfrac{p_\theta}{5}, \text{for all } \theta = 1, \cdots, \gamma_g \\ & \alpha_g \leq t_1 < t_2 < t_3 < \cdots < t_{\gamma_g} \leq \beta_g, \\ & u_g^t = 0,\ t \in H \backslash \{t_1, t_2, t_3, \cdots, t_{\gamma_g}\}, \\ & \gamma_g \in [\gamma_g^{\min}, \gamma_g^{\max}], H = \{1, 2, \cdots, T\} \Big\} \end{aligned} \tag{4.4.9}$$

which shows the constraints of suspendable MOAs: the operation is within the OTI $[\alpha_g, \beta_g]$, and the energy consumption is suspendable and reaches LOT γ_g. The range of LOT is $[4, 5]$ for the illustrative MOAs in Fig. 4.3. Note that the constraints of MOAs are only to define the possible cases of MOAs' energy consumption and the

energy consumption of MOAs is still controlled by users in real time.

With the consideration of the constraints of appliances, the complete optimization model of the energy consumption scheduling based on the ROA is formulated as

$$
\begin{aligned}
&\min_{\mathbf{X}\in\mathbf{\Omega}} \max_{\mathbf{U}\in\mathbf{\Gamma}} f(\mathbf{X},\mathbf{U}) \\
&f(\mathbf{X},\mathbf{U}) = \sum_{t=1}^{T} prc_t(l_t(\mathbf{X},\mathbf{U}))\cdot l_t(\mathbf{X},\mathbf{U}) \\
&\mathbf{X} = \begin{bmatrix} X_1 \\ X_2 \\ \vdots \\ X_n \end{bmatrix} = \begin{bmatrix} x_1^1 & x_1^2 & \dots & x_1^t & \dots & x_1^T \\ x_2^1 & x_2^2 & \dots & x_2^t & \dots & x_2^T \\ \vdots & \vdots & & \ddots & & \vdots \\ x_n^1 & x_n^2 & \dots & x_n^t & \dots & x_n^T \end{bmatrix} \\
&\mathbf{U} = \begin{bmatrix} U_1 \\ U_2 \\ \vdots \\ U_m \end{bmatrix} = \begin{bmatrix} u_1^1 & u_1^2 & \dots & u_1^t & \dots & u_1^T \\ u_2^1 & u_2^2 & \dots & u_2^t & \dots & u_2^T \\ \vdots & \vdots & & \ddots & & \vdots \\ u_m^1 & u_m^2 & \dots & u_m^t & \dots & u_m^T \end{bmatrix} \\
&l_t(\mathbf{X},\mathbf{U}) = \sum_{i=1}^{n} x_i^t + \sum_{j=1}^{m} u_j^t, t\in\{1,2,\cdots,T\} \\
&prc_t(l_t(\mathbf{X},\mathbf{U})) = \begin{cases} e_t, & \text{if } 0 \le l_t(\mathbf{X},\mathbf{U}) < c \\ \varepsilon\cdot e_t, & \text{if } l_t(\mathbf{X},\mathbf{U}) \ge c \end{cases} \\
&\mathbf{\Omega} = \left\{ \mathbf{X} | \mathbf{X} = \begin{bmatrix} X_1 \\ X_2 \\ \vdots \\ X_n \end{bmatrix}, \begin{array}{l} X_i \text{ subject to Eqn. } (4.4.6) \\ \text{if } i \text{ is a non-interruptible SA} \\ X_i \text{ subject to Eqn. } (4.4.7) \\ \text{if } i \text{ is an interruptible SA} \\ i = \{1,2,\cdots,n\} \end{array} \right\} \\
&\mathbf{\Gamma} = \left\{ \mathbf{U} | \mathbf{U} = \begin{bmatrix} U_1 \\ U_2 \\ \vdots \\ U_m \end{bmatrix}, \begin{array}{l} U_j \text{ subject to Eqn. } (4.4.8) \\ \text{if } j \text{ is a non-suspendable MOA} \\ U_j \text{ subject to Eqn. } (4.4.9) \\ \text{if } j \text{ is a suspendable MOA} \\ j = \{1,2,\cdots,m\} \end{array} \right\}
\end{aligned}
\tag{4.4.10}
$$

which is a nonlinear problem with a two-level framework. The elements of $\mathbf{X}$ and $\mathbf{U}$ are discrete since the energy consumption of appliances is determined by the on/off states of appliances. When an appliance is operated (on state), the corresponding element is the energy consumption of the appliance; and when the appliance is not operated (off state), the corresponding element is zero.

4.4.2 Solution algorithm

The intergeneration projection evolutionary algorithm (IP-EA) is adopted to solve the proposed robust optimization problem of the energy consumption scheduling. The IP-EA, which is a two-level evolutionary algorithm with the inner genetic algorithm (GA) and the outer particle swarm optimization (PSO) algorithm, is effective in solving the proposed nonlinear problem with the two-level framework [127]. The GA is a global optimization algorithm while the PSO algorithm makes a trade-off between global search and local search [129], and the PSO algorithm is more computationally efficient [130]. The GA is adopted in the inner level to raise the accuracy of the solution and the PSO algorithm is adopted in the outer level to improve the computation efficiency.

The GA mimics the process of natural selection. The individuals with better fitness are chosen to generate the next generation through the crossover and the mutation, and this process cycles until the individual with a satisfactory fitness is found [47]. The PSO algorithm is based on the behavior of particles of a swarm. Particles in a swarm approach to the optimum by tracking the best location of individual particle ($pbest$) and the best location of particle swarm ($gbest$), which is formulated as

$$\begin{aligned} v_\zeta^{k+1} &= w v_\zeta^k + c_1 r_1 (pbest_\zeta^k - p_\zeta^k) + c_2 r_2 (gbest^k - p_\zeta^k) \\ p_\zeta^{k+1} &= p_\zeta^k + v_\zeta^{k+1} \end{aligned} \tag{4.4.11}$$

where v_ζ and p_ζ are the velocity and the position of the particle ζ, respectively, k is the iteration index, w is the inertia weight factor, c_1 and c_2 are the acceleration constants, and r_1 and r_2 are randomly generated numbers in the range of $[0, 1]$ [131].

The flowchart of the IP-EA for solving the problem of the energy consumption

scheduling is shown in Fig. 4.4. The outer PSO algorithm is for searching the optimal schedule of SAs' energy consumption and the inner GA is for searching the energy consumption case of MOAs with the worst impact on the electricity cost. More specifically, for a trial schedule of SAs' energy consumption, the worst case of MOAs' energy consumption is obtained through the GA. Then we can get the electricity cost with the trial schedule of SAs' energy consumption and the worst case of MOAs' energy consumption, and this electricity cost is used for tracking the optimal energy consumption schedule among the swarm of energy consumption schedules of SAs. The optimal schedule of SAs' energy consumption is obtained after the convergency of the electricity cost with the worst impact of MOAs. Within the itermax iterations in Fig. 4.4, the electricity cost converges and does not change at the end.

4.5 Simulation results

In this section, simulation studies are carried out to verify the effectiveness of the proposed approach. Eight typical SAs and six typical MOAs are considered and the parameters of SAs and MOAs are given in Table 4.1 and Table 4.2 based on their operation characteristics. The first six SAs are non-interruptible and the last two SAs are interruptible, and the first three MOAs are suspendable and the last three MOAs are non-suspendable. For appliances whose powers are not represented as vectors in Table 4.1 and Table 4.2, their powers are constant during the operation processes. The RTP data in August 2012 is adopted from the Ameren Illinois Power Company [32], and it is the electricity price used for the energy scheduling. We assume that the coefficient $\varepsilon = 1.4423$ and the energy consumption threshold $c = 0.45$ kWh [33, 47]. Note that the threshold is for the energy consumption within 12 minutes. For the inner GA of the solution algorithm IP-EA, the population size of each generation is 200, the probability of crossover is 0.8 and the max generation number is 100 [47, 132]. For the outer PSO of the IP-EA, the number of particles is 20, the inertial weight factor w decreases linearly from 0.9 to 0.4 with the increase of the iteration index, both the acceleration constants c_1 and c_2 are 2, and the maximum

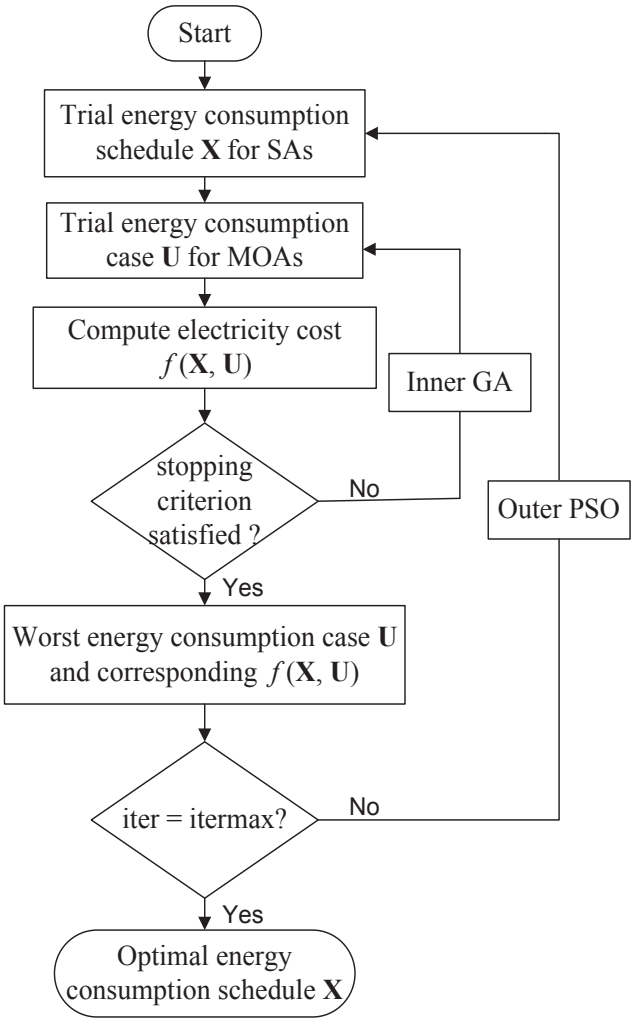

Figure 4.4: The flowchart of the intergeneration projection evolutionary algorithm (IP-EA)

Table 4.1: Parameters of SAs

SA	OTI	LOT	Power (kW)
Electric kettle [47]	1-25	1	1.5
Clothes dryer [47, 135]	61-90	3	[1.2 1.2 1]
Oven [136, 137]	71-85	3	[2.1 1.9 1.9]
Water heater [47, 138]	86-105	3	[1.7 1.7 1.4]
Electric radiator [47, 139]	96-110	5	[2.2 1.8 1.8 1.8 1.8]
Dishwasher [47]	101-120	2	0.6
Washing machine [47]	1-60	5	0.38
Humidifier [47]	1-30	8	0.05

Table 4.2: Parameters of MOAs

MOA	OTI	LOT	Power (kW)
Electric iron [136, 137]	61-70	3	[1.7 1.5 1.5]
Vacuum cleaner [47]	71-80	3	1.5
Hair drier [47]	101-110	1	1
Lights [47]	81-120	30-35	0.2
Laptop [136]	86-115	15-20	0.1
TV [47]	91-120	15-20	0.1

iteration number is 300 [133, 134]. Two cases, one day operation of all SAs and MOAs on August 3rd 2012, and one month operation of different combinations of home appliances in August 2012, are presented. All simulations are implemented in MATLAB on an Intel Core-i3 3.3-GHz personal computer with 8 GB RAM.

The ROA is compared with other two approaches without considering the uncertainty of MOAs' energy consumption, including the approach without considering MOAs which minimizes the electricity cost of SAs and the approach considering the fixed energy consumption of MOAs which minimizes the electricity cost of all home appliances with an assumed energy consumption of MOAs. For convenience, these three approaches are referred to as A1-A3 as follows,

- A1: The approach without considering MOAs
- A2: The approach considering the fixed energy consumption of MOAs
- A3: The proposed robust approach considering the worst impact of MOAs

All the three approaches are implemented through the IP-EA.

Table 4.3: Assumed energy consumption periods of MOAs

MOA	Energy consumption period
Electric iron	61-63
Vacuum cleaner	73-75
Hair drier	110
Lights	85-117
Laptop	101-115
TV	94-113

4.5.1 One day case

The energy consumption periods of MOAs are assumed as shown in Table 4.3 within the OTIs and ranges of LOTs of MOAs in Table 4.2 for A2. It is noted that the fixed energy consumption of MOAs is assumed for A2 in the decision making process of SAs' energy consumption, the energy consumption of MOAs is still controlled by users in real time and can be consumed at anytime in OTIs with any possible LOTs. The proposed A3 is compared with A1 and A2 on August 3rd 2012 from the following three aspects.

Energy consumption schedule

Fig. 4.5 and Fig. 4.6 show comparisons of the energy consumption schedule of SAs between A1 and A3, and A1 and A2, respectively. The gray area is the possible energy consumption period of the electric iron and the vacuum cleaner in Fig. 4.5 and it is the assumed energy consumption of the electric iron and the vacuum cleaner in Fig. 4.6. We can see from Fig. 4.5 and Fig. 4.6 that, compared with A1, some SAs are shifted from low electricity price periods to periods with a little higher electricity price to avoid the risk of much higher electricity price charged in low price periods, which is caused by the excess of the threshold set by the IBR when operations of MOAs happen to be in these low price periods. More specifically, the energy consumption of the cloth dryer and the oven is shifted from 61-63, 72-74 time slots to 88-90, 83-85 time slots, respectively, to avoid all the possible consumption periods of the electric iron and the vacuum cleaner for A3. By comparison, only the energy consumption of the oven is shifted and the energy consumption of the cloth dryer still remains in low price periods for A2. That is to say, A3 considers all

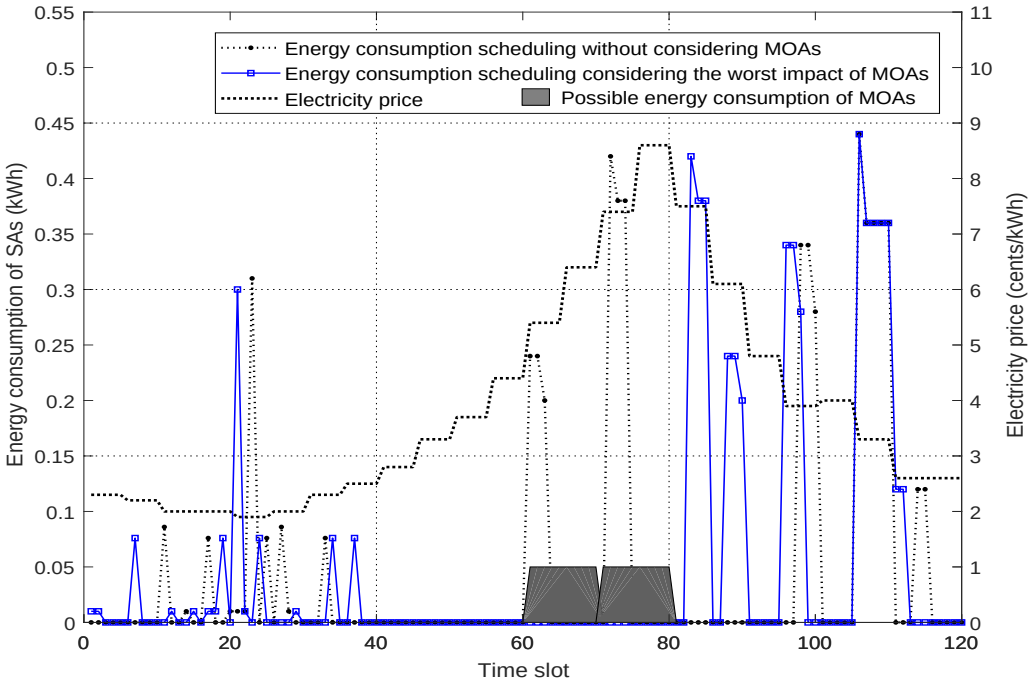

Figure 4.5: Energy consumption comparison between the approach considering the worst impact of MOAs and the approach without considering MOAs

the possible cases of energy consumption of MOAs and A2 only considers a certain case of MOAs' energy consumotion.

Electricity cost with the worst impact of MOAs

The effectiveness of A3 is tested with the consideration of the worst impact of MOAs. Based on the energy consumption schedules of SAs and the electricity price shown in Fig. 4.5 and Fig. 4.6, the electricity costs of A1-A3 with the worst impact of MOAs' energy consumption are 59.06 cents, 56.21 cents and 52.29 cents, respectively. The worst electricity cost of A3 drops by 11.46% and 6.97% compared with A1 and A2, respectively.

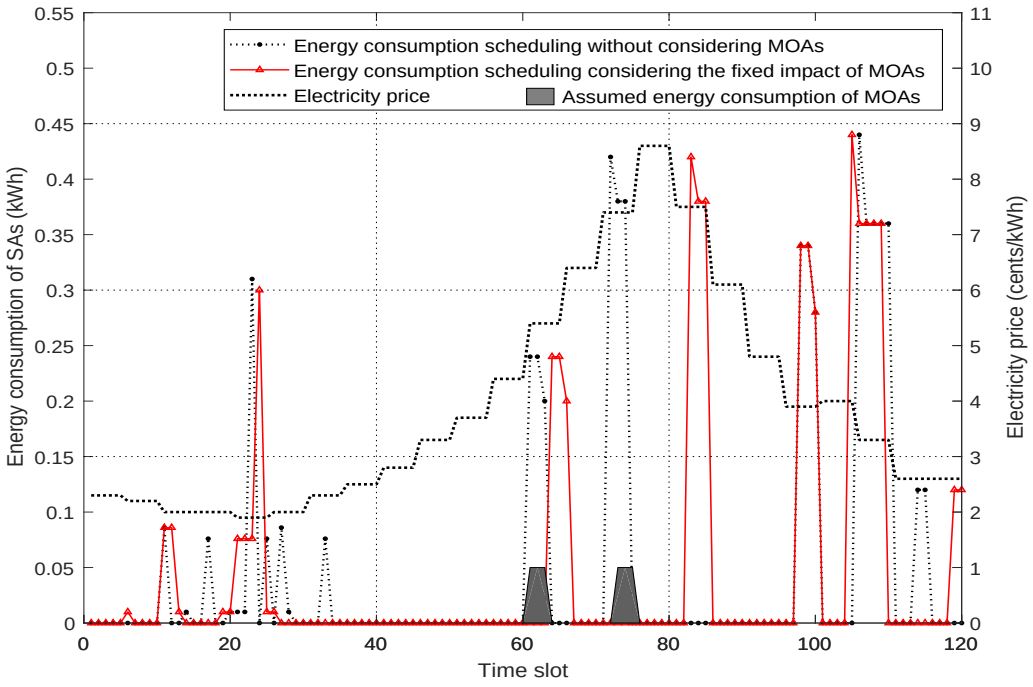

Figure 4.6: Energy consumption comparison between the approach considering the fixed energy consumption of MOAs and the approach without considering MOAs

Electricity cost with random impact of MOAs

The effectiveness of A3 is tested under 1000 random cases where the MOAs' energy consumption is evenly distributed among all the possible cases. Two situations of the RTP including the RTP as the same as the predicted one and the RTP considering $\pm 10\%$ random noises, i.e. the electricity price varying between 90% and 110% of the predicted RTP [33], are taken into account.

- The RTP as the same as the predicted one

  The effectiveness of A3 is tested under 1000 random cases where the RTP is the same as the predicted one and the MOAs' energy consumption is evenly distributed among all the possible cases. Fig. 4.7-Fig. 4.9 show the comparisons of the electricity cost under random MOAs between the situation without energy consumption scheduling of SAs in which the energy consumption of SAs is randomly distributed, and the situations with the scheduling schemes obtained by A1, A2 and A3, respectively. The scheduling schemes obtained by A1, A2 and A3 are shown in Fig. 4.5 and Fig. 4.6. The average electricity cost of 1000 random cases is 48.43 cents for A3, 50.50 cents for A1, 49.79 cents for A2, and 58.12 cents for the situation without the energy consumption scheduling. Through A3, the average electricity cost decreases by 16.77%, 4.10% and 2.73% compared with the situation without the energy consumption scheduling, A1 and A2, respectively.

- The RTP with random noises

  The effectiveness of A3 is tested under 1000 random cases where the MOAs' energy consumption is evenly distributed among all the possible cases and $\pm 10\%$ random noises are added into the RTP. Fig. 4.10-Fig. 4.12 show the comparisons of the electricity cost under random MOAs and uncertain RTP between the situation without the energy consumption scheduling of SAs in which the energy consumption of SAs is randomly distributed, and the situations with the scheduling schemes obtained by A1, A2 and A3, respectively. The scheduling schemes obtained by A1, A2 and A3 are shown in Fig. 4.5 and Fig. 4.6. The average electricity cost of 1000 random cases is 48.42 cents

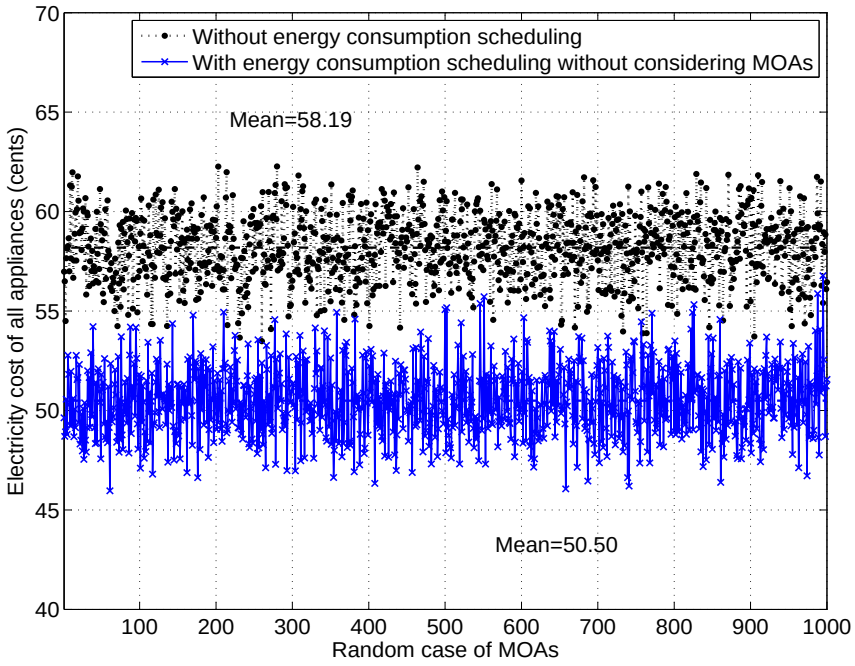

Figure 4.7: Comparison of electricity cost with the predicted RTP between no scheduling and the approach without considering MOAs

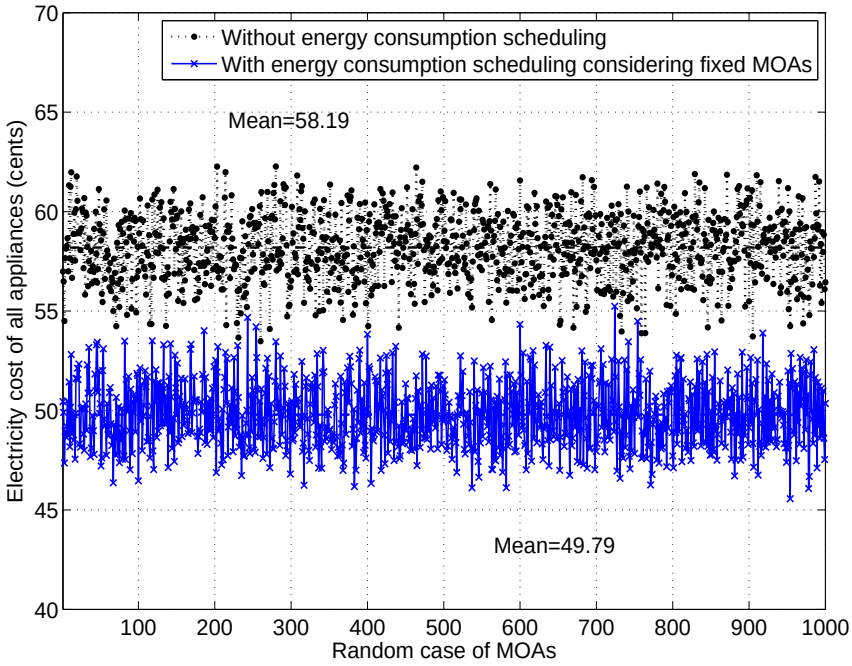

Figure 4.8: Comparison of electricity cost with the predicted RTP between no scheduling and the approach considering the fixed energy consumption of MOAs

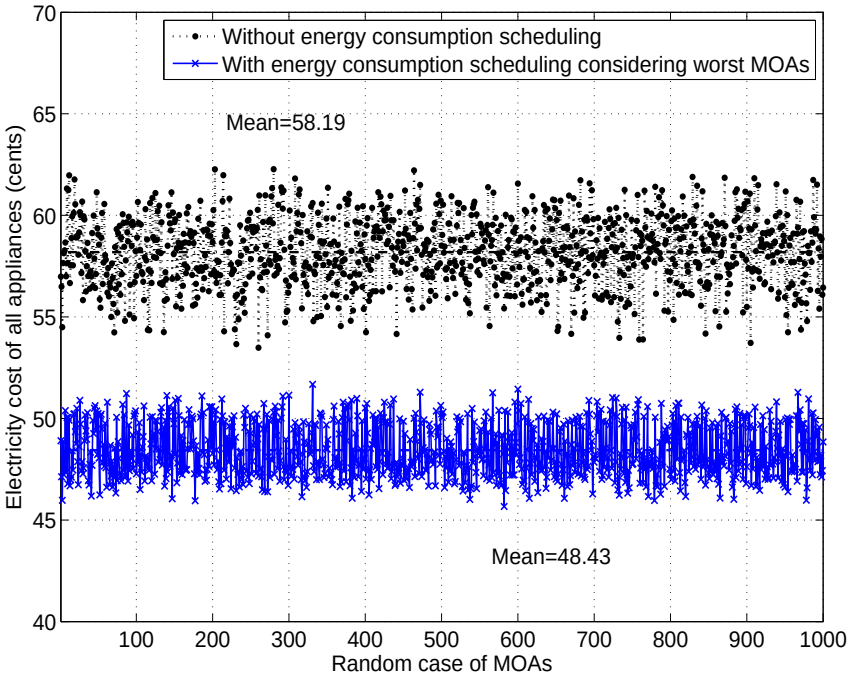

Figure 4.9: Comparison of electricity cost with the predicted RTP between no scheduling and the approach considering the worst impact of MOAs

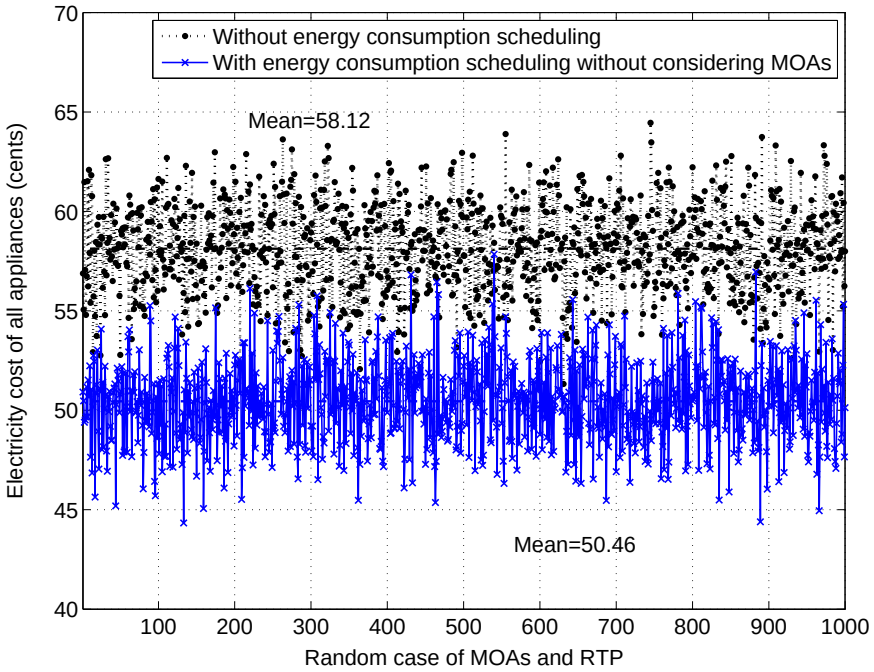

Figure 4.10: Comparison of electricity cost with random RTP between no scheduling and the approach without considering MOAs

for A3, 50.46 cents for A1, 49.76 cents for A2, and 58.12 cents for the situation without the energy consumption scheduling. Through A3, the average electricity cost decreases by 16.69%, 4.04% and 2.69% compared with the situation without the energy consumption scheduling, A1 and A2, respectively.

4.5.2 One month case

To further verify the effectiveness of the proposed A3, it is tested in one month period of August 2012 with different combinations of home appliances, and $7-8$ SAs in Table 4.1 and $5-6$ MOAs in Table 4.2 are randomly chosen each day. The electricity cost with the worst impact of MOAs and the cost with random impact of MOAs are compared between A3 and A1, A3 and A2, respectively.

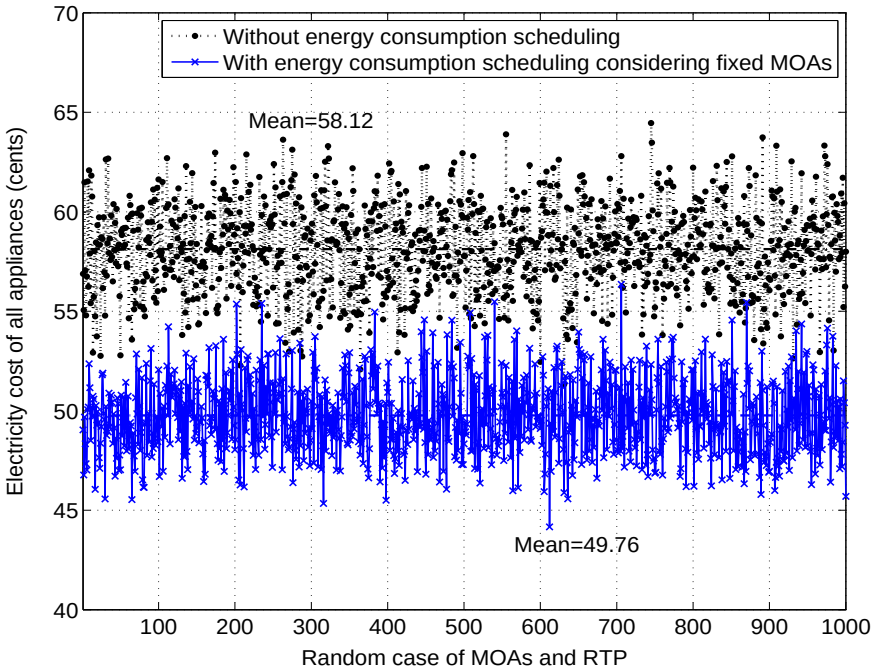

Figure 4.11: Comparison of electricity cost with random RTP between no scheduling and the approach considering the fixed energy consumption of MOAs

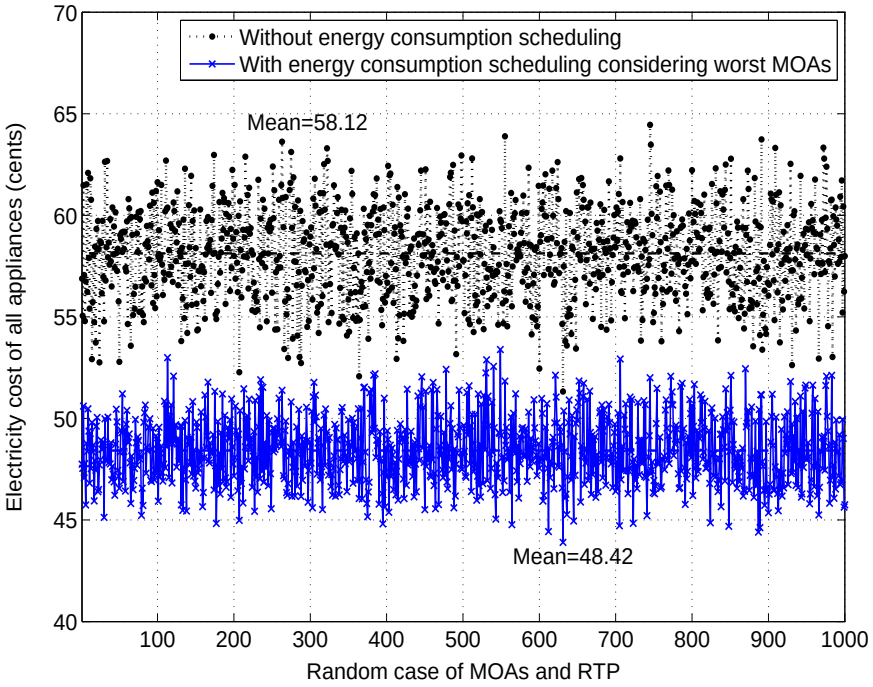

Figure 4.12: Comparison of electricity cost with random RTP between no scheduling and the approach considering the worst impact of MOAs

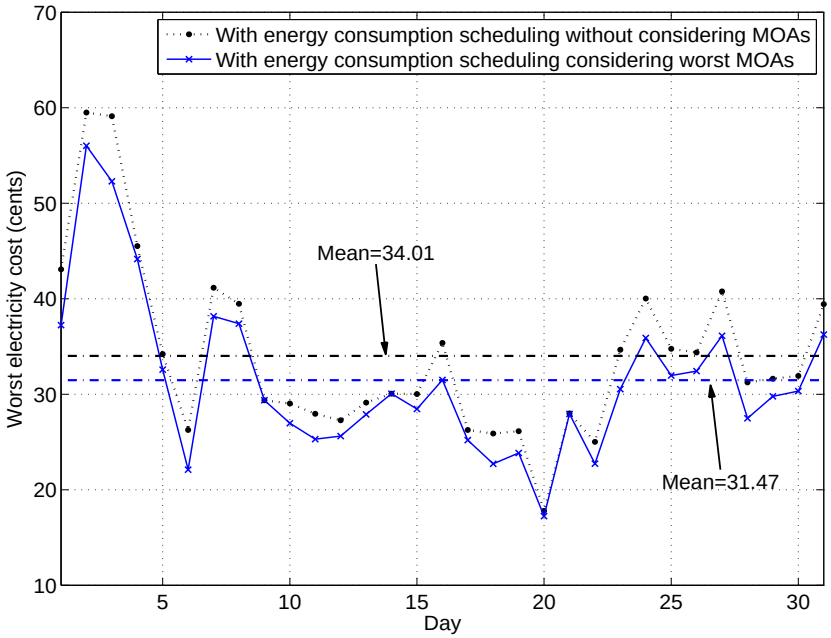

Figure 4.13: Comparison of electricity cost with the worst impact of MOAs between the proposed approach and the approach without considering MOAs

Electricity cost with the worst impact of MOAs

Fig. 4.13 and Fig. 4.14 show the comparisons of the electricity cost with the worst impact of MOAs' energy consumption between A1 and A3, A2 and A3, respectively. As shown in Fig. 4.13 and Fig. 4.14, the average value of the worst electricity cost of A3 in 31 days is 31.47 cents, reduced by 7.47% from A1 with 34.01 cents and by 5.38% from A2 with 33.26 cents.

Electricity cost with random impact of MOAs

The effectiveness of A3 is tested under 1000 random cases where the MOAs' energy consumption is evenly distributed among all the possible cases. Two situations of the RTP including the RTP as the same as the predicted one and the RTP considering $\pm 10\%$ random noises are taken into account.

- The RTP as the same as the predicted one

  With the RTP remaining as the same as the predicted one, Fig. 4.15 and

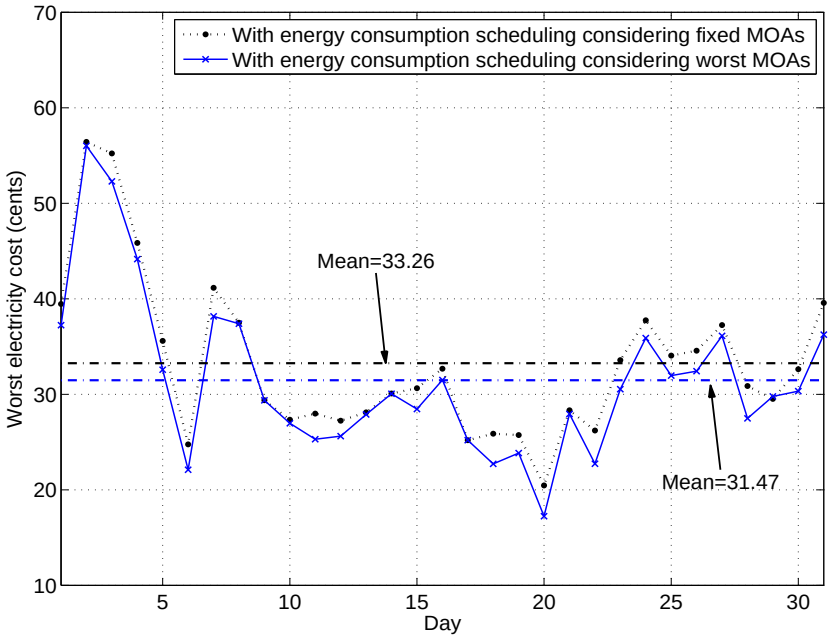

Figure 4.14: Comparison of electricity cost with the worst impact of MOAs between the proposed approach and the approach considering the fixed energy consumption of MOAs

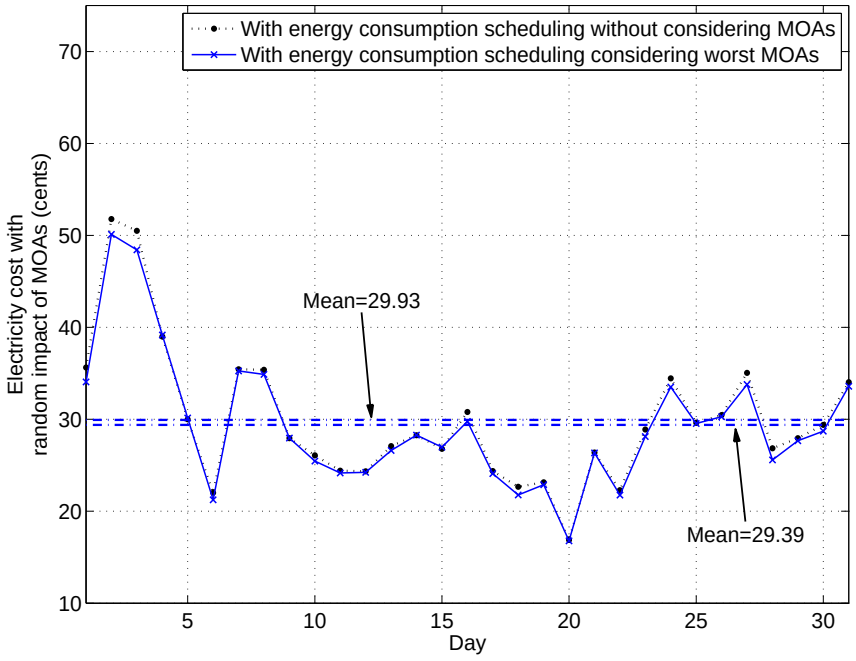

Figure 4.15: Comparison of electricity cost with the predicted RTP between the proposed approach and the approach without considering MOAs

Fig. 4.16 show the comparisons of the electricity cost with random impact of MOAs. The average value of the cost with random impact of MOAs in 31 days is 29.39 cents for A3, 29.93 cents for A1 and 29.85 cents for A2. Through A3, the electricity cost with random impact of MOAs deceases by 1.80% and 1.54% compared with A1 and A2, respectively.

- The RTP with random noises

  Fig. 4.17 and Fig. 4.18 show the comparisons of the electricity cost with random impact of MOAs and RTP. The average value of the cost with random impact of MOAs and RTP in 31 days is 29.39 cents for A3, 29.93 cents for A1 and 29.85 cents for A2. Through A3, the electricity cost with random impact of MOAs and RTP deceases by 1.80% and 1.54% compared with A1 and A2, respectively.

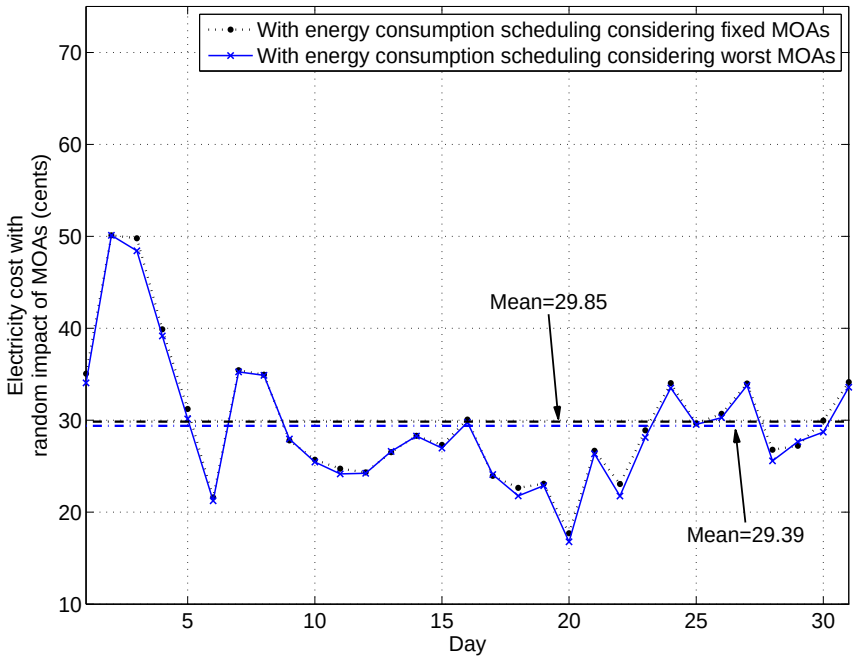

Figure 4.16: Comparison of electricity cost with the predicted RTP between the proposed approach and the approach considering the fixed energy consumption of MOAs

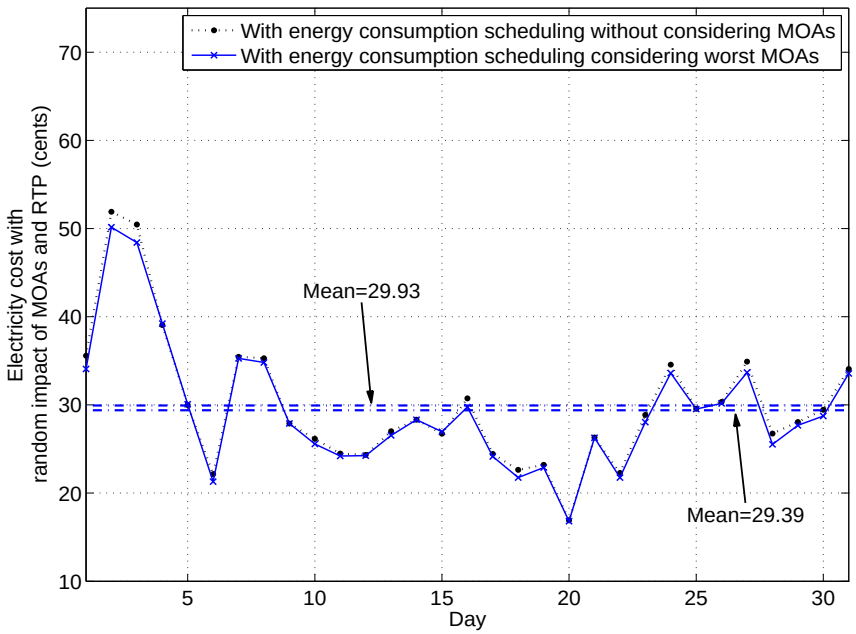

Figure 4.17: Comparison of electricity cost with random RTP between the proposed approach and the approach without considering MOAs

Figs. 4.15-4.18 show that the electricity cost of the proposed A3 is reduced compared with A1 and A2. Though the proposed A3 takes into account the worst impact of MOAs when it schedules the energy consumption of SAs, it can be seen from Figs. 4.15-4.18 that the electricity cost with the random impact of MOAs is also reduced. Since users will pay a much higher electricity cost when the total energy consumption exceeds the threshold, which probably happens even with random impact of MOAs, the proposed A3 which takes into account the worst impact of MOAs effectively reduces the situations of exceeding the threshold of total energy consumption and reduces the electricity cost under random impact of MOAs.

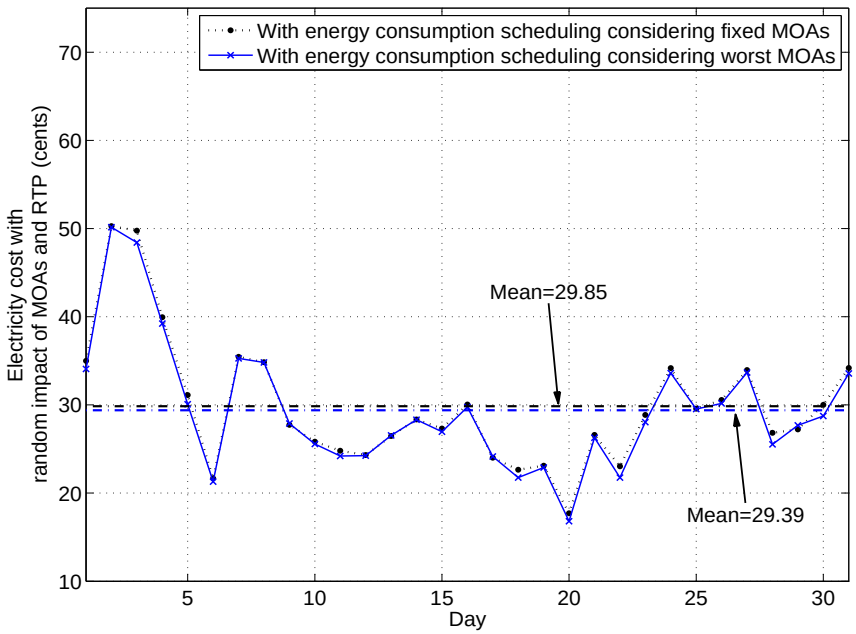

Figure 4.18: Comparison of electricity cost with random RTP between the proposed approach and the approach considering the fixed energy consumption of MOAs

4.5.3 Case of MOAs' usage probability

The proposed approach assumes all MOAs are used and it is now extended to take into account the probability of MOAs' usage, which is formulated as

$$\min_{\mathbf{X}\in\mathbf{\Omega}} \sum_{s=1}^{NS} \rho_s \cdot \max_{\mathbf{U}_s\in\mathbf{\Gamma}_s} f(\mathbf{X}, \mathbf{U}_s) \tag{4.5.1}$$

where s is the index of scenario and each scenario represents one combination of MOAs. Considering each MOA may be used or not, the total number of scenarios NS is 2^m for total m MOAs. ρ_s is the probability of scenario s and $\sum_{s=1}^{NS} \rho_s = 1$. $\mathbf{U}_s$ is the energy consumption case of MOAs in scenario s and $\mathbf{\Gamma}_s$ is the set of energy consumption cases of MOAs in scenario s. It is noted that the uncertainty of MOAs' energy consumption in the proposed approach indicates when users start MOAs and how long users operate them are uncertain, and the proposed approach is now extended to consider the probability of MOAs' usage.

To test the extension of the proposed approach, the electric iron and the vacuum cleaner are assumed to be used with the probability of 0.5 and other MOAs in Table 4.2 are assumed to be certainly used. Table 4.4 presents the energy consumption schedule of SAs on August 3rd 2012 based on the extension of the proposed approach. The electricity cost with the worst impact of MOAs under the predicted RTP is 52.59 cents for the extended approach and it is 59.06 cents for A1, 56.21 cents for A2 and 52.29 cents for the proposed A3. The worst electricity costs of A1-A3 are the same as in one day case of simulation results. The worst electricity cost of the extended approach is reduced compared with A1 and A2, and it is lager than that of A3 since A3 schedules the energy consumption directly considering the worst impact of MOAs, and the extended approach takes into account the cases where some MOAs are not used and these cases are not with the worst impact. The electricity cost with random impact of MOAs is tested under two situations of the electricity price including the situation where the RTP is the same as the predicted one and the situation where $\pm 10\%$ random noises are taken into account in the predicted RTP. The electricity cost with the random impact of MOAs and the predicted RTP is 41.32 cents for the extended approach, and it is 42.02 cents for A1, 42.45 cents for A2, and 41.71 cents for A3. The electricity costs with the random impact of MOAs under the random RTP are 41.65 cents, 42.50 cents, 42.79 cents and 42.08 cents for the extended approach and A1-A3, respectively. With MOAs' usage probability taken into account in the scheduling process, the electricity cost of the extended approach with the random impact of MOAs is reduced compared with A1-A3. Note that the probability of MOAs' usage is now considered in the testing process of the obtained scheduling schemes and the electricity costs of A1-A3 with the random impact of MOAs are different from the corresponding costs in one day case of simulation results where the probability of MOAs' usage is not considered.

4.6 Conclusions

This chapter proposes a ROA for the energy scheduling of home appliances, taking into account the worst impact of the uncertainty of MOAs' energy consumption.

Table 4.4: Energy consumption schedule of SAs

SA	Energy consumption period
Electric kettle	12
Clothes dryer	88-90
Oven	81-83
Water heater	96-98
Electric radiator	106-110
Dishwasher	118-119
Washing machine	17,21,22,24,32
Humidifier	1,13,15,17,21,26,27,28

The effectiveness of the ROA has been verified by case studies based on one day and one month periods. Compared with the scheduling approach without considering MOAs' uncertainty, and the scheduling approach considering MOAs' uncertainty with a fixed energy consumption, the ROA effectively avoids the risk of a high electricity cost caused by the MOAs' uncertainty and reduces the electricity cost with the worst impact of MOAs' energy consumption. The electricity cost with the random impact of MOAs' energy consumption is also reduced through the ROA.

Chapter 5

Uncertainty of outdoor temperature

5.1 Introduction

Among the main potential residential demand side scheduling (RDSS) resources are heating, ventilation and air conditioning (HVAC) systems because of their relatively large energy consumption. The energy consumption of HVAC accounts for about 40% of the energy consumption in a building [140] and can be up to 60% [141]. The energy consumption of HVAC is usually scheduled based on the forecast outdoor temperature to minimize the electricity cost with the indoor temperature maintained in a comfortable zone [142]. The forecast error is one of the main factors which affect the indoor temperature and may cause a violation of the comfortable temperature zone [57]. Many studies have been carried out to deal with the forecast error, i.e. the uncertainty of the outdoor temperature, in the energy consumption scheduling of HVAC, e.g. through the stochastic optimization approach (SOA) [45] and the robust optimization approach (ROA) [59]. The SOA requires the exact probability distribution of the uncertain variable [97] and the ROA is overly conservative [110]. The distributionally robust optimization approach (DROA), which combines the advantages of both the SOA and the ROA, has been applied in the reserve scheduling problem in the power system with the uncertainty of renewable energy taken into account [60]. The DROA does not require the exact probability distribution of the uncertain variable and its conservativeness is reduced with

the probabilistic information observed from historical data [60]. The uncertainty of renewable energy is considered with the mean and the variance extracted from historical data and the reserve scheduling problem is solved based on the semidefinite programming (SDP) [60].

In this chapter, a newly proposed DROA based on the probabilistic information of subintervals of the outdoor temperature is adopted to schedule the energy consumption of HVAC. This DROA is different from the DROA based on the mean and the variance as more information is extracted from historical weather data. The proposed DROA partitions the maximum interval of the outdoor temperature into subintervals, and it constructs the ambiguity set of the probability distribution of the outdoor temperature taking into account the probabilistic information of historical data within these subintervals. To compensate the effect of the deviation between the actual outdoor temperature and the forecast one, the actual energy consumption of HVAC is proposed to be adjusted in real time based on the scheduled consumption and the forecast error. With the consideration of the ambiguity set of the outdoor temperature, the energy consumption scheduling of HVAC is formulated as a nonlinear problem with distributionally robust chance constraints. These constraints are reformulated to be linear and the energy consumption scheduling of HVAC is obtained through linear programming (LP). The proposed DROA based on the probabilities of subintervals is compared with the DROA based on the mean and the variance and the ROA. Simulation results demonstrate that the proposed DROA helps reduce the electricity cost with approximate 10% of computation time of the DROA based on the mean and the variance of the outdoor temperature. The electricity cost is also reduced compared with the traditional ROA.

5.2 Problem formulation

In this section, the energy consumption scheduling of HVAC based on the proposed DROA is formulated. Firstly, the uncertainty of the outdoor temperature is modeled, and the distributionally robust chance constraints of the energy consumption of HVAC are introduced. Then the complete optimization model of the energy

consumption scheduling of HVAC with the consideration of the uncertainty of the outdoor temperature is presented.

5.2.1 Model of the uncertainty of outdoor temperature

The weather forecast predicts an outdoor temperature but the actual temperature may be different from that forecast. The proposed DROA partitions the maximum interval of the outdoor temperature into nested subintervals as follows

$$\begin{aligned} &U_t^i = \{\xi_t \in \mathcal{R} \mid l_t^i \leq \xi_t \leq u_t^i\}, i = 1, \cdots, m \\ &U_t^1 \subseteq \cdots \subseteq U_t^m \end{aligned} \tag{5.2.1}$$

where ξ_t denotes the outdoor temperature at time slot t, U_t^m denotes its maximum interval, and m denotes the number of temperature intervals. The lower and upper bounds of subintervals are represented as

$$\begin{aligned} &l_t^{m-i} = l_t^m + i \cdot \tfrac{u_t^m - l_t^m}{2m-1} \\ &u_t^{m-i} = u_t^m - i \cdot \tfrac{u_t^m - l_t^m}{2m-1}, i = 0, 1, 2, \cdots, m-1. \end{aligned} \tag{5.2.2}$$

The example of temperature intervals with $m = 3$ is shown in Fig. 5.1. For $m = 3$, the maximum interval is partitioned into 5 segments as shown in Fig. 5.1 and the length of each segment is $\frac{u_t^m - l_t^m}{5}$. The lower and upper bounds of U_t^2 are the bounds of the maximal interval with a segment added and deducted, respectively, and the bounds of U_t^1 are obtained as the same way. Based on the historical weather data, the ambiguity set of the probability distribution of the outdoor temperature is constructed with the consideration of the maximum interval of the outdoor temperature and the probabilistic information of subintervals

$$\mathcal{P}_t^1 = \left\{ \mathbb{P}_t \in \mathcal{P}_t^0(U_t^m) \;\middle|\; \begin{aligned} &\mathbb{E}_{\mathbb{P}_t}\{\xi_t\} = \mu_t \\ &\mathbb{P}_t\{\xi_t \in U_t^i\} = p_t^i,\ i = 1, \cdots, m \\ &U_t^1 \subseteq \cdots \subseteq U_t^m, p_t^m = 1 \end{aligned} \right\} \tag{5.2.3}$$

where μ_t denotes the forecast temperature, and p_t^i denotes the probability of $\xi_t \in U_t^i$ where its value is obtained from historical weather data. $\mathbb{P}_t$ denotes the probability

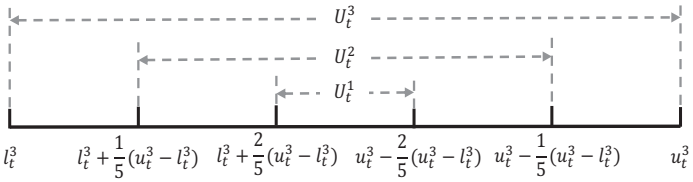

Figure 5.1: Nested temperature intervals with $m = 3$

Table 5.1: Parameters of HVAC system

Parameter	Units	Description
C	kWh/°F	Thermal capacity of HVAC
R	°F/kW	Thermal resistance
η	none	Coefficient of performance of HVAC. This value is positive for cooling and negative for heating.

distribution of ξ_t and $\mathcal{P}_t^0(U_t^m)$ denotes the set of all the probability distributions supported on U_t^m. $p_t^m = 1$ can be achieved by adopting a large enough interval to guarantee the outdoor temperature will be definitely located in this interval.

5.2.2 Distributionally robust chance constraints

To compensate the effect of the weather forecast error, the energy consumption of HVAC is proposed to be adjusted in real time according to the deviation of the actual outdoor temperature from the forecast one, and the energy consumption is scheduled with the consideration of this adjustment through distributionally robust chance constraints. Based on the model of HVAC system [45, 142], the indoor temperature is

$$\theta_t = \theta_{t-1} - \frac{\Delta t}{C \cdot R} \cdot (\theta_{t-1} - \xi_{t-1} + \eta \cdot R \cdot q_{t-1}) \tag{5.2.4}$$

where θ_t denotes the indoor temperature at time slot t, q_{t-1} denotes the power of the energy consumption of HVAC at time slot $t-1$ and Δt denotes the time period. Note that q_{t-1} is with unit kW and it is the power of HVAC at time slot $t-1$ rather than the energy consumption of HVAC. The energy consumption of HVAC is with unit kWh and it is calculated as $q_{t-1}\Delta t$. The parameters C, R and η of HVAC system are summarized in Table 5.1 [142]. The indoor temperature will remain the same when

the energy consumption of HVAC is adjusted in real time according to the forecast error of the outdoor temperature

$$q_t = q_t^{\text{ref}} + \frac{1}{\eta \cdot R} \cdot (\xi_t - \mu_t) \tag{5.2.5a}$$

$$\mathbb{P}_t\{q_t \geq 0\} \geq 1 - \varepsilon, \forall \mathbb{P}_t \in \mathcal{P}_t^1 \tag{5.2.5b}$$

$$\mathbb{P}_t\{q_t \leq q^{\max}\} \geq 1 - \varepsilon, \forall \mathbb{P}_t \in \mathcal{P}_t^1 \tag{5.2.5c}$$

where q_t^{ref} denotes the reference power of energy consumption, i.e. the energy consumption schedule, which is proposed in advance. How the reference energy consumption of HVAC is determined will be introduced in the next section. $q^{\max}$ denotes the maximum power of HVAC. ε denotes the probability of exceeding the limits of power consumption of HVAC and the distributionally robust chance constraints Eqn. (5.2.5b) and Eqn. (5.2.5c) show that both probabilities of the power consumption satisfying the upper limit and the lower limit should be no smaller than $1 - \varepsilon$ for all the probability distributions of the outdoor temperature in the ambiguity set $\mathcal{P}_t^1$.

5.2.3 Complete optimization model

Based on the electricity price and the users' predefined comfort zone for the indoor temperature, the energy consumption of HVAC is scheduled aiming to minimize the electricity cost with users' satisfaction of the indoor temperature, which is formulated as

$$\min_{q_t^{\text{ref}}} \mathbb{E}\{\sum_{t=1}^{T}(e_t \cdot q_t \cdot \Delta t)\} \tag{5.2.6a}$$

$$q_t = q_t^{\text{ref}} + \frac{1}{\eta \cdot R} \cdot (\xi_t - \mu_t) \tag{5.2.6b}$$

$$\theta_t = \theta_{t-1} - \frac{\Delta t}{C \cdot R} \cdot (\theta_{t-1} - \xi_{t-1} + \eta \cdot R \cdot q_{t-1}) \tag{5.2.6c}$$

$$\theta^{\min} \leq \theta_t \leq \theta^{\max} \tag{5.2.6d}$$

$$\mathbb{P}_t\{q_t \geq 0\} \geq 1 - \varepsilon, \forall \mathbb{P}_t \in \mathcal{P}_t^1 \tag{5.2.6e}$$

$$\mathbb{P}_t\{q_t \leq q^{\max}\} \geq 1 - \varepsilon, \forall \mathbb{P}_t \in \mathcal{P}_t^1 \tag{5.2.6f}$$

where e_t denotes the electricity price at time slot t and T denotes the scheduling horizon. $\theta^{\min}$ and $\theta^{\max}$ denote the lower bound and the upper bound of the comfortable temperature zone, respectively. The energy consumption is scheduled taking into account the weather forecast error based on the nested intervals of the outdoor temperature, and the effect of the weather forecast error is compensated through the real-time adjustment of the energy consumption with the consideration of the distributionally robust chance constraints. For example, if the outdoor temperature is higher than the forecast and the HVAC is working in the cooling mode, the HVAC will consume more energy than the reference consumption and thus the room temperature will not be affected by the forecast error and the effect of the forecast error is compensated.

This energy consumption model can be applied in the HVAC system with only on-off control action, i.e. the power of HVAC can be either $q^{\max}$ or 0. Firstly, the power of HVAC's energy consumption is obtained based on the proposed system model and this power will last for Δt. Note that the effect of the energy consumption on the indoor temperature is the same when the energy consumption of HVAC in Δt is the same. When the HVAC system with only on-off control action is adopted, the time when HVAC is on can be adjusted to satisfy the same energy consumption in Δt, i.e. the time when HVAC is on is $\frac{q_t \cdot \Delta t}{q^{\max}}$.

5.3 Solution approach

In this section, the distributionally robust chance constraints Eqn. (5.2.6e) and Eqn. (5.2.6f) are reformulated to be tractable and linear based on the theorem proposed below, and then the energy consumption scheduling of HVAC based on the proposed DROA can be solved through LP. In brief, the constraints Eqn. (5.2.6e) and Eqn. (5.2.6f) are firstly replaced by two more strict constraints and these more strict constraints are converted to linear constraints based on duality theory. The more detailed reformulation of Eqn. (5.2.6e) and Eqn. (5.2.6f) is introduced as

follows. For convenience, these two constraints are presented in a uniform form

$$\mathbb{P}_t\{a_t \cdot \xi_t \leq b_t\} \geq 1-\varepsilon, \forall \mathbb{P}_t \in \mathcal{P}_t^1 \tag{5.3.1}$$

where a_t and b_t for Eqn. (5.2.6e) and Eqn. (5.2.6f) are specified in Table 5.2. It has been proved in [143] that

$$\begin{aligned} &\mathbb{P}_t\text{-CVaR}_\varepsilon(a_t \cdot \xi_t - b_t) \leq 0 \Rightarrow \mathbb{P}_t\{a_t \cdot \xi_t \leq b_t\} \geq 1-\varepsilon \\ &\qquad \mathbb{P}_t\text{-CVaR}_\varepsilon(a_t \cdot \xi_t - b_t) \\ &\qquad\quad = \inf_{\beta \in \mathcal{R}} \left\{ \beta + \frac{1}{\varepsilon}\mathbb{E}_{\mathbb{P}_t}\{(a_t \cdot \xi_t - b_t - \beta)^+\} \right\} \end{aligned} \tag{5.3.2}$$

where $(x)^+ = \max(x, 0)$, and CVaR denotes conditional value at risk and it is introduced based on the value at risk (VaR). VaR is a very popular risk measure in finance and portfolio optimization, and it is defined as follows. Let $f(x, \xi)$ be the loss associated with the decision variable x and the random variable ξ. For a given ε, VaR is defined as the smallest loss such that the probability of loss above that level is at most ε [144], which is formulated as

$$VaR_\varepsilon \triangleq \min\{\ell \in \mathcal{R} : P\{f(x, \xi) \leq \ell\} \geq 1-\varepsilon\} \quad \text{for } 0 < \varepsilon \leq 1 \tag{5.3.3}$$

CVaR is defined as the mean of $f(x, \xi)$ on the tail distribution exceeding VaR [144], which is formulated as

$$CVaR_\varepsilon \triangleq \mathbb{E}_\xi(f(x, \xi) | f(x, \xi) \geq VaR_\varepsilon) \tag{5.3.4}$$

The illustration of VaR and CVaR is shown in Fig. 5.2 and ε is the cumulative probability of the dash line area. According to Eqn. (5.3.2), constraint Eqn. (5.3.1) is satisfied if

$$\mathbb{P}_t\text{-CVaR}_\varepsilon(a_t \cdot \xi_t - b_t) \leq 0, \ \forall \mathbb{P}_t \in \mathcal{P}_t^1. \tag{5.3.5}$$

Theorem 1: When the ambiguity set $\mathcal{P}_t^1$ is constructed, the distributionally robust constraint Eqn. (5.3.5) is satisfied if and only if there exist y, β and $\lambda_i, i =$

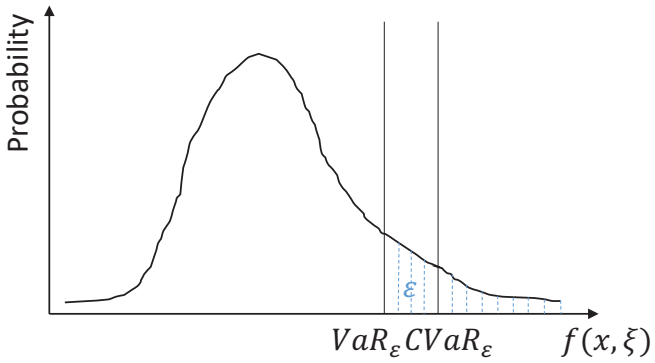

Figure 5.2: Illustration of VaR and CVaR

Table 5.2: Expressions of a_t and b_t

Constraint	a_t	b_t
Eqn. (5.2.6e)	$-\frac{1}{\eta \cdot R}$	$q_t^{\text{ref}} - \frac{1}{\eta \cdot R} \cdot \mu_t$
Eqn. (5.2.6f)	$\frac{1}{\eta \cdot R}$	$q_t^{\max} - q_t^{\text{ref}} + \frac{1}{\eta \cdot R} \cdot \mu_t$

$1, \cdots, m$, such that

$$\beta + \frac{1}{\varepsilon} \cdot (\mu_t \cdot y + \sum_{i=1}^{m} \lambda_i \cdot p_t^i) \leq 0 \tag{5.3.6a}$$

$\forall i = 1, \cdots, m:$

$$y \cdot l_t^i + \sum_{j=i}^{m} \lambda_j \geq 0 \tag{5.3.6b}$$

$$y \cdot u_t^i + \sum_{j=i}^{m} \lambda_j \geq 0 \tag{5.3.6c}$$

$$y \cdot l_t^i + \sum_{j=i}^{m} \lambda_j - (a_t \cdot l_t^i - b_t - \beta) \geq 0 \tag{5.3.6d}$$

$$y \cdot u_t^i + \sum_{j=i}^{m} \lambda_j - (a_t \cdot u_t^i - b_t - \beta) \geq 0 \tag{5.3.6e}$$

Proof: First note that constraint Eqn. (5.3.5) is equivalent to

$$\begin{aligned}&\sup_{\mathbb{P}_t\in\mathcal{P}_t^1}\inf_{\beta\in\mathcal{R}}\left\{\beta+\frac{1}{\varepsilon}\mathbb{E}_{\mathbb{P}_t}\{(a_t\cdot\xi_t-b_t-\beta)^+\}\right\}\\=&\inf_{\beta\in\mathcal{R}}\left\{\beta+\frac{1}{\varepsilon}\sup_{\mathbb{P}_t\in\mathcal{P}_t^1}\mathbb{E}_{\mathbb{P}_t}\{(a_t\cdot\xi_t-b_t-\beta)^+\}\right\}\leq 0\end{aligned}\tag{5.3.7}$$

where the interchangeability of sup and inf is guaranteed by a stochastic saddle point theorem [145]. To reformulate constraint Eqn. (5.3.7), the following worst-case expectation needs to be evaluated

$$\sup_{\mathbb{P}_t\in\mathcal{P}_t^1}\mathbb{E}_{\mathbb{P}_t}\{(a_t\cdot\xi_t-b_t-\beta)^+\}.\tag{5.3.8}$$

Note that the probability distribution of the outdoor temperature is not known and there are infinitely many possible distributions which form an ambiguity set. The infinite dimensional linear optimization problem Eqn. (5.3.8) is equivalent to

$$\sup_{\mathbb{P}_t\in\mathcal{P}_t^0(U_t^m)}\int_{U_t^m}(a_t\cdot\xi_t-b_t-\beta)^+\mathbb{P}_t(d\xi_t)\tag{5.3.9a}$$

$$\text{s.t.}\int_{U_t^m}\xi_t\mathbb{P}_t(d\xi_t)=\mu_t\tag{5.3.9b}$$

$$\int_{U_t^m}I_{U_t^i}\mathbb{P}_t(d\xi_t)=p_t^i,\ i=1,\cdots,m\tag{5.3.9c}$$

where $I_{U_t^i}=1$ when $\xi_t\in U_t^i$, otherwise $I_{U_t^i}=0$. By introducing dual variables y and λ_i, Eqn. (5.3.9) is reformulated as

$$\inf_{y,\boldsymbol{\lambda}}\ \mu_t\cdot y+\sum_{i=1}^m\lambda_i\cdot p_t^i\tag{5.3.10a}$$

$$\text{s.t. } y\in\mathcal{R},\lambda_i\in\mathcal{R},\ i=1,\cdots,m\tag{5.3.10b}$$

$$\inf_{\xi_t\in U_t^m}\left\{y\cdot\xi_t+\sum_{i=1}^m\lambda_i\cdot I_{U_t^i}-(a_t\cdot\xi_t-b_t-\beta)^+\right\}\geq 0.\tag{5.3.10c}$$

Now the problem has been reformulated to a finite dimensional optimization problem. Since U_t^m can be partitioned into m mutually disjoint sets $\mathcal{R}_t^1=U_t^1$, $\mathcal{R}_t^i=$

$U_t^i \setminus U_t^{i-1}$, $i = 2, \cdots, m$, Eqn. (5.3.10c) is equivalent to

$$\inf_{\xi_t \in \mathcal{R}_t^i} \left\{ y \cdot \xi_t + \sum_{j=i}^{m} \lambda_j - (a_t \cdot \xi_t - b_t - \beta)^+ \right\} \geq 0, \quad \forall i = 1, \cdots, m \tag{5.3.11}$$

which can be further equivalently converted to

$$\inf_{\xi_t \in U_t^i} \left\{ y \cdot \xi_t + \sum_{j=i}^{m} \lambda_j - (a_t \cdot \xi_t - b_t - \beta)^+ \right\} \geq 0, \quad \forall i = 1, \cdots, m \tag{5.3.12}$$

considering that $U_t^i \supseteq \mathcal{R}_t^i$, and that the infimum of Eqn. (5.3.12) is attained on the boundary of U_t^i and $\mathcal{R}_t^i$ contains the boundary of U_t^i. Constraint Eqn. (5.3.12) is satisfied if and only if $\forall i = 1, \cdots, m$,

$$y \cdot l_t^i + \sum_{j=i}^{m} \lambda_j \geq 0 \tag{5.3.13a}$$

$$y \cdot u_t^i + \sum_{j=i}^{m} \lambda_j \geq 0 \tag{5.3.13b}$$

$$y \cdot l_t^i + \sum_{j=i}^{m} \lambda_j - (a_t \cdot l_t^i - b_t - \beta) \geq 0 \tag{5.3.13c}$$

$$y \cdot u_t^i + \sum_{j=i}^{m} \lambda_j - (a_t \cdot u_t^i - b_t - \beta) \geq 0 \tag{5.3.13d}$$

By substituting Eqn. (5.3.10) into Eqn. (5.3.7) together with Eqn. (5.3.13), the proposed theorem is proved.

The CVaR approximation is the first step of our method and our main contribution focuses on the reformulation of the constraint after the CVaR approximation. In this reformulation, it is noted that the probability distribution of the outdoor temperature is unknown and there are infinitely many possible distributions which form an ambiguity set, and we propose a method which immunizes the solution of the problem against all possible distributions after the CVaR approximation. Since

the constraint Eqn. (5.3.5) is more conservative than the distributionally chance constraint Eqn. (5.3.1), the electricity cost will be higher after the CVaR approximation. Although the CVaR constraint brings conservatism when approximating Eqn. (5.3.1), it is superior to the original constraint from other aspects. Firstly, as shown in ***Theorem 1***, the distributionally robust CVaR constraint admits a tractable linear reformulation. Secondly, the CVaR constraint imposes higher penalties on larger constraint violations [146]. Therefore, the CVaR constraint confines both the probability and the severity of constraint violations.

5.4 Simulation results

This section presents the simulation results to verify the effectiveness of the proposed DROA in the scheduling of HVAC's energy consumption. The parameters of HVAC system C, R and η are assumed to be 0.33 kWh/°F, 13.5 °F/kW and 2.2, respectively [59, 142]. The maximum power of HVAC is assumed to be 1.75 kW [142] and the scheduling interval Δt is 30 minutes [45]. The energy consumption is scheduled 12 hours ahead with $T = 24$. The electricity price based on the time of use, as shown in Table 5.3, is adopted from the Austin Energy Company [147]. The outdoor temperature in Austin from 12 pm August 6th 2013 to 12pm August 9th 2013 is assumed to be the forecast outdoor temperature [148]. Based on the normal distribution with the forecast temperature as the mean and 2.5° F as the standard deviation [59], 10,000 samples are taken to simulate the historical data and to construct the ambiguity set $\mathcal{P}_t^1$. It is noted that the DROA does not require the probability distribution of the outdoor temperature and the normal distribution is used to generate historical data. In practice, the forecast and the actual temperature values are both recorded as the historical data and $\mathcal{P}_t^1$ is constructed based on these historical weather data. All the simulations are implemented in MATLAB with YALMIP [149] as the modelling tool and SeDuMi [150] as the solver running on an Intel Core-i3 3.3-GHz personal computer with 8 GB RAM. YALMIP provides a simple language to build the model of optimization problems and effectively interfaces external solvers to solve these optimization problems [149]. SeDuMi is a comprehensive solver to

Table 5.3: Time of use electricity prices

Time	12am-2am	2am-6am	6am-10am	10am-12pm
Price($/kWh)	0.00493	0.00493	0.05040	0.05040
Time	12pm-2pm	2pm-8pm	8pm-10pm	10pm-12am
Price($/kWh)	0.05040	0.09761	0.05040	0.00493

tackle linear programming, semidefinite programming and quadratic programming problems [150].

For convenience, the proposed DROA together with other two methods are listed and referred to as M1-M3 as shown below. Firstly, the proposed DROA is compared with the other two methods in the electricity cost, the users' comfort and the computation time. Then the impacts of m, ε and the comfortable temperature zone on the performance of the proposed DROA are investigated, respectively. Furthermore, the proposed DROA is extended to take into account the uncertainty of the electricity price, the effect of users' activities on the indoor temperature and the deviation of users' preferred temperature.

- M1: Based on the proposed DROA considering the probabilistic information of subintervals of the outdoor temperature, the problem of energy consumption scheduling is reformulated to be LP through the proposed ***Theorem 1***.

- M2: The energy consumption is scheduled based on the DROA considering the mean and the variance of historical data, which is formulated as the same as Eqn. (5.2.6) except that the ambiguity set $\mathcal{P}_t^1$ is replaced by

$$\mathcal{P}_t^2 = \left\{ \mathbb{P}_t \in \mathcal{P}_t^0(U_t^m) \;\middle|\; \begin{array}{l} \mathbb{E}_{\mathbb{P}_t}\{\xi_t\} = \mu_t \\ \mathbb{P}_t\{\xi_t \in U_t^m\} = 1, \\ \mathbb{E}_{\mathbb{P}_t}\{(\xi_t - \mu_t)^2\} = \sigma_t^2 \end{array} \right\} \tag{5.4.1}$$

  where σ_t^2 denotes the variance of the outdoor temperature obtained from historical weather data. Then the problem of energy consumption scheduling is reformulated to be SDP based on the theorem below.

  Theorem 2 [151]: When the ambiguity set $\mathcal{P}_t^2$ is constructed, the distributionally robust constraint Eqn. (5.3.5) is satisfied if and only if there exist

$y, \beta, h, \lambda, \tau_0$ and τ_1, such that

$$\beta + \frac{1}{\varepsilon} \cdot (h + \mu_t \cdot y + \lambda \cdot \sigma_t^2 + \lambda \cdot \mu_t^2) \leq 0 \tag{5.4.2a}$$

$$\tau_0 \geq 0, \tau_1 \geq 0 \tag{5.4.2b}$$

$$\mathbf{M} + \tau_0 \cdot \mathbf{W} \succeq 0 \tag{5.4.2c}$$

$$\mathbf{M} + \tau_1 \cdot \mathbf{W} - \mathbf{H} \succeq 0 \tag{5.4.2d}$$

$$\mathbf{M} = \begin{bmatrix} \lambda & \frac{y}{2} \\ \frac{y}{2} & h \end{bmatrix}, \mathbf{W} = \begin{bmatrix} 1 & -\frac{l_t^m + u_t^m}{2} \\ -\frac{l_t^m + u_t^m}{2} & l_t^m \cdot u_t^m \end{bmatrix} \tag{5.4.2e}$$

$$\mathbf{H} = \begin{bmatrix} 0 & \frac{a_t}{2} \\ \frac{a_t}{2} & -b_t - \beta \end{bmatrix} \tag{5.4.2f}$$

Proof: The first two steps of the reformulation are the same as Eqn. (5.3.7) and Eqn. (5.3.8) except that $\mathcal{P}_t^1$ is replaced by $\mathcal{P}_t^2$. Eqn. (5.3.8) with $\mathbb{P}_t \in \mathcal{P}_t^2$ is equivalent to

$$\sup_{\mathbb{P}_t \in \mathcal{P}_t^0(U_t^m)} \int_{U_t^m} (a_t \cdot \xi_t - b_t - \beta)^+ \mathbb{P}_t(d\xi_t) \tag{5.4.3a}$$

$$\text{s.t.} \int_{U_t^m} \xi_t \mathbb{P}_t(d\xi_t) = \mu_t \tag{5.4.3b}$$

$$\int_{U_t^m} \mathbb{P}_t(d\xi_t) = 1 \tag{5.4.3c}$$

$$\int_{U_t^m} (\xi_t - \mu_t)^2 \mathbb{P}_t(d\xi_t) = \sigma_t^2 \tag{5.4.3d}$$

Through ***Theorem 3.7*** in [151] with dual variables y, h and λ introduced, ***Theorem 2*** is proved.

Note that M2 based on the mean and the variance of the outdoor temperature reformulates the problem to be SDP, which is more computationally expensive than LP based on the proposed M1.

- M3: The energy consumption is scheduled based on the ROA, which is formulated as the same as Eqn. (5.2.6) except that constraints Eqn. (5.2.6e) and

Eqn. (5.2.6f) are replaced by conventional robust constraints

$$q_t \geq 0, \forall \xi_t \in U_t^m \tag{5.4.4a}$$

$$q_t \leq q^{\max}, \forall \xi_t \in U_t^m. \tag{5.4.4b}$$

Compared with M1 and M2, M3 is most conservative as it requires the constraints be certainly satisfied within the maximum interval of the outdoor temperature. The computation burden of M3 is the smallest as the constraints (5.4.4a) and (5.4.4b) are linear and they are equivalent to 4 constraints which require that the energy consumption is within the lower and upper limits at the bounds of U_t^m.

Note that the reference energy consumption is proposed taking into account the weather forecast error and that the actual energy consumption will be adjusted in real time based on the reference energy consumption and the weather forecast error as shown in Eqn. (5.2.5a). The actual energy consumption is set to be $q^{\max}$ and 0 under the circumstances where the adjusted energy consumption exceeds these two values, respectively. Eqn. (5.2.5a) shows that the actual energy consumption of HVAC is obtained with a certain value added or reduced on the basis of the reference energy consumption. The added value or reduced value is proportional to the forecast error of the outdoor temperature. When the forecast error is big, the adjusted energy consumption may exceed the energy consumption limits. If the adjusted energy consumption exceeds the upper limit $q^{\max}$, the actual energy consumption is set to be $q^{\max}$. If the adjusted energy consumption is less than 0, the actual energy consumption is set to be 0.

5.4.1 Performance of the solution approach

In this section, the proposed DROA is compared with the other two methods with $m = 15, \varepsilon = 0.005$, [60° F, 70° F] as the comfortable temperature zone [57, 58] and 70 °F as the starting indoor temperature. Firstly, the simulation results in a scheduling cycle from 12 pm to 12 am on August 6th 2013 are demonstrated, then

the simulation results in consecutive cycles from 12 pm August 6th 2013 to 12pm August 9th 2013 are presented.

In a scheduling cycle

The energy consumption schedule and the performances of this energy consumption schedule under one test sample of the outdoor temperature and 10,000 test samples are presented.

- Energy consumption schedule:

  Figs. 5.3-5.5 show the energy consumption schedule and the indoor temperature based on M1, M2 and M3, respectively. From 1pm to 3pm, it can be seen from Figs. 5.3-5.5 that the energy consumption of HVAC is largely scheduled in periods with low electricity price to pre-cool the indoor temperature. Then the energy consumption can be saved in periods with high electricity price. Fig. 5.6 compares the energy consumption schedules of the three methods and the dash line presents the maximum power consumption of HVAC $q^{\max}$. Fig. 5.6 shows that M3 considers the maximum error of the weather forecast and its maximum and minimum energy consumptions are far from $q^{\max}$ and 0, respectively. It can be seen from Fig. 5.6 that M3 is the most conservative and M1 is less conservative than M2.

- Test with a sample of the outdoor temperature:

  Based on the normal distribution with the forecast temperature as the mean and 2.5° F as the standard deviation, a sample of the outdoor temperature, as shown in Fig. 5.7, is taken to test the energy consumption schedules in Fig. 5.6. Fig. 5.8 and Fig. 5.9 show the adjusted energy consumption and the indoor temperature under this test outdoor temperature based on the three methods, respectively. The adjusted energy consumption is obtained based on Eqn. (5.2.5a). The actual energy consumption is set to be $q^{\max}$ and 0 under the circumstances where the adjusted energy consumption exceeds these two values, respectively. As shown in Fig. 5.8, the adjusted energy consumption is within the limits for all the methods, thus the actual energy consumption

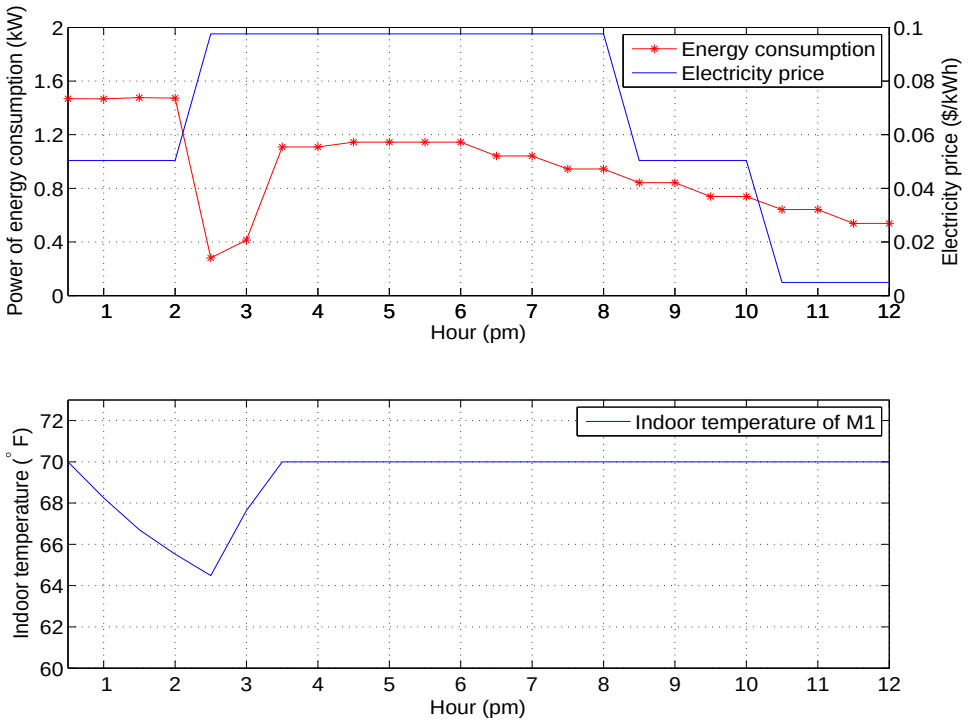

Figure 5.3: Energy consumption schedule and indoor temperature based on M1

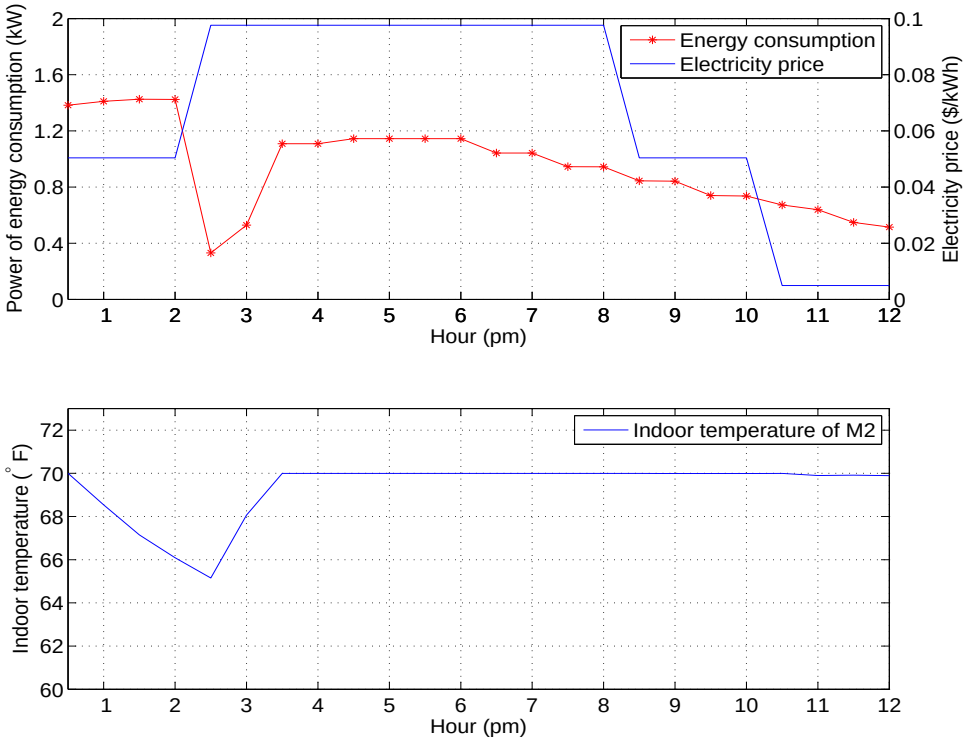

Figure 5.4: Energy consumption schedule and indoor temperature based on M2

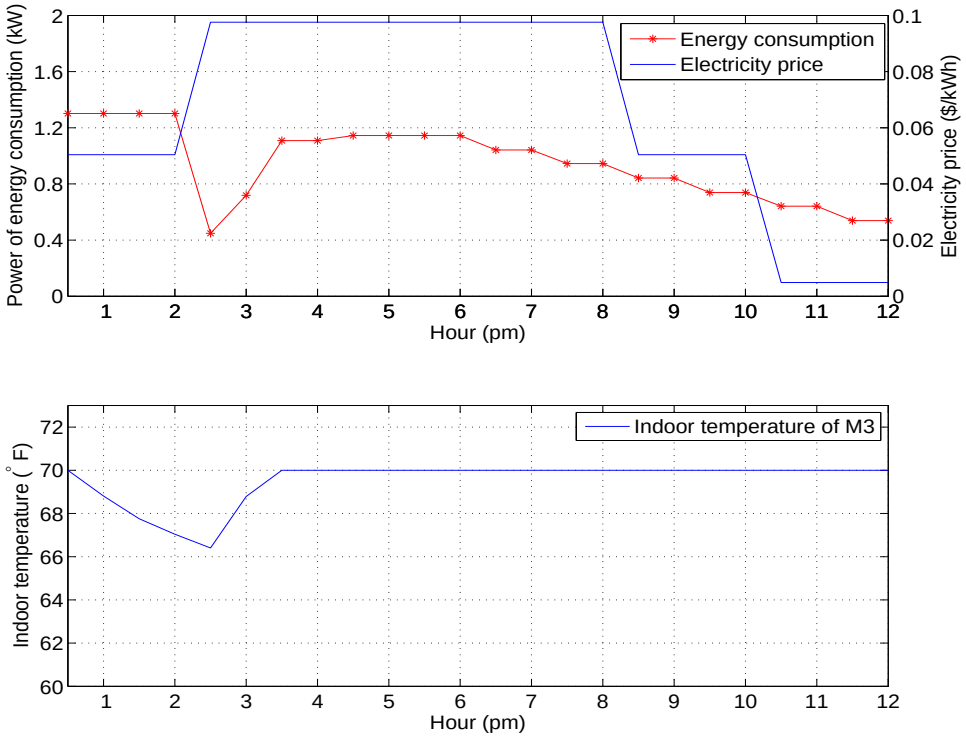

Figure 5.5: Energy consumption schedule and indoor temperature based on M3

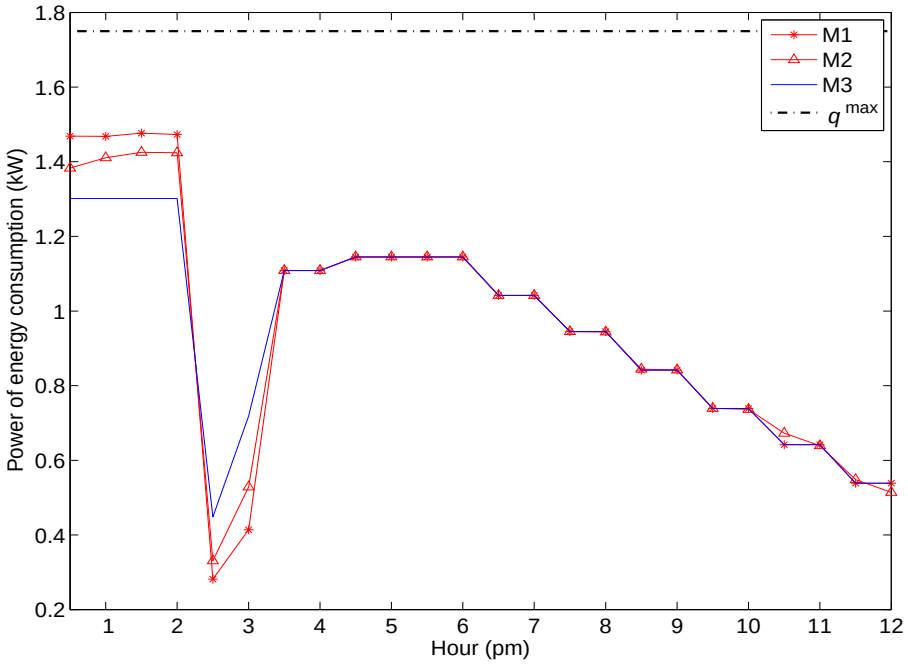

Figure 5.6: Energy consumption schedules based on M1, M2 and M3

equals to the adjusted energy consumption. The electricity costs of the actual energy consumption are \$0.809, \$0.811 and \$0.815 for M1-M3, respectively, and the electricity cost of M1 is reduced compared with M2 and M3. Fig. 5.9 shows that the actual indoor temperature is following the reference indoor temperature based on M1, M2 and M3 and the indoor temperature is within the comfortable temperature zone. The reference indoor temperature is the indoor temperature that is obtained with the reference energy consumption 12 hours ahead. Based on M1, M2 and M3, the weather forecast error is considered in the scheduling process and its effect on the indoor temperature is compensated through the real-time adjustment of the energy consumption, and the electricity cost of the proposed M1 is the smallest.

- Test with 10,000 samples of the outdoor temperature:

  Based on the normal distribution with the forecast temperature as the mean and 2.5° F as the standard deviation, 10,000 samples of the outdoor temper-

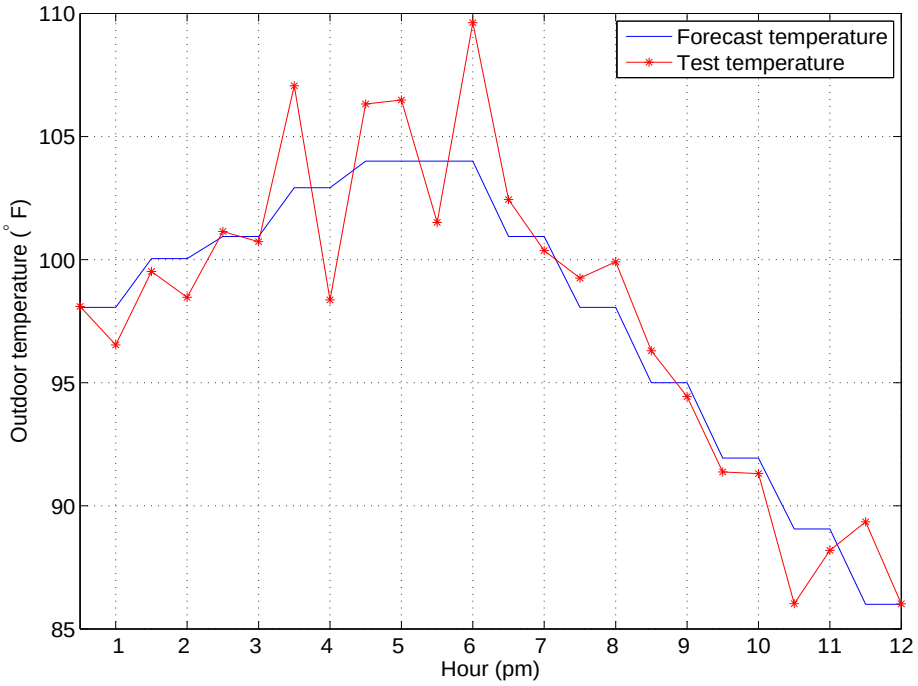

Figure 5.7: The outdoor temperature

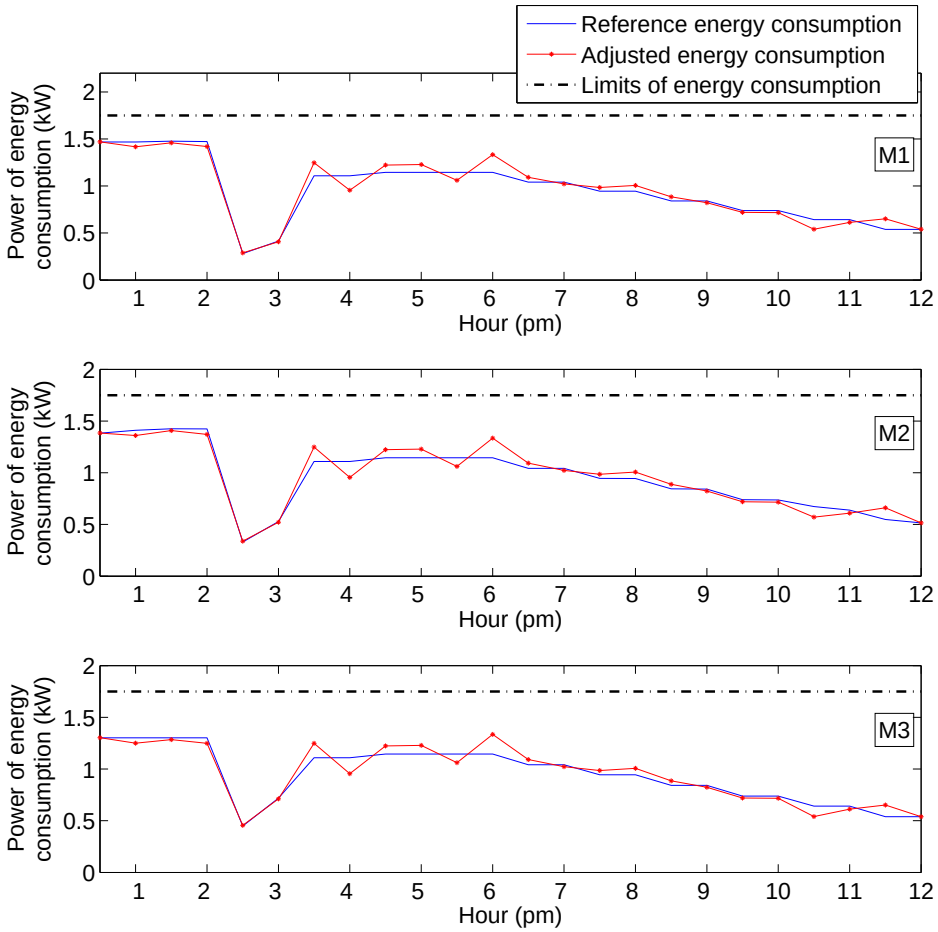

Figure 5.8: The adjusted energy consumption

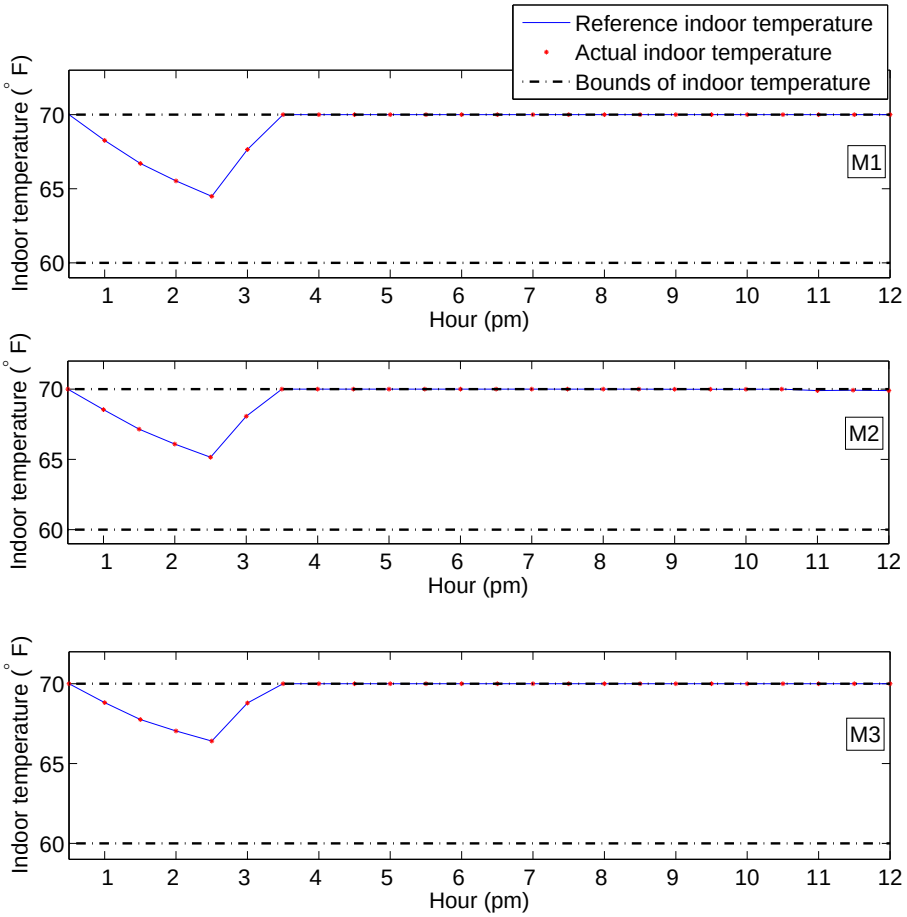

Figure 5.9: The indoor temperature

Table 5.4: Performances of the three methods in a scheduling cycle

Method	Cost ($)	Num_VioTem	VioTem (°F)	Time (s)
M1	0.794	17	0.1405	0.5110
M2	0.796	0	0	5.7651
M3	0.799	0	0	0.1494

ature are taken to test the three methods. Note that 10,000 samples are used as historical data to construct the ambiguity set and the new 10,000 samples are taken for testing. It is remarkable that the DROA does not require the prior knowledge about the distribution of the outdoor temperature, and the probability information in the ambiguity set is extracted from historical data. Any probability distribution can be used to test the DROA only if the data employed in the ambiguity set construction and the performance evaluation is sampled from the same distribution. The average electricity cost of the actual energy consumption (Cost), the number and the maximum of violations from the comfortable temperature zone (Num_VioTem and VioTem), and the computation time (Time) are compared in Table 5.4 for the three methods. It can be seen from Table 5.4 that the indoor temperature is always within the comfortable zone for M3 while M3 pays the highest electricity cost. In the comparison with M2, it is noted that the proposed M1 approximately takes 10% of the computation time to obtain the optimal energy consumption schedule of HVAC and the electricity cost of M1 is also less. The computation time is 0.5110 seconds for M1 and it is 5.7651 seconds for M2. With the probabilistic information of subintervals taken into account and the reformulation of the problem as LP, the proposed M1 helps reduce the electricity cost with less computation time compared with M2 based on the mean and the variance of historical weather data and the reformulation of the problem as SDP.

The energy consumption schedule in each time slot of the scheduling horizon T is tested with 10,000 samples of outdoor temperature, and the numbers of situations where the adjusted energy consumption violates the lower and upper limits of the energy consumption of HVAC can be obtained for each time slot as well as the probabilities of these situations. Table 5.5 shows the maxi-

Table 5.5: Violations of energy consumption limits

Method	M1	M2
Num_VioEneL	5	0
Prob_VioEneL	0.0005	0
Num_VioEneH	6	0
Prob_VioEneH	0.0006	0

mum number of situations (Num_VioEneL and Num_VioEneH) where the adjusted energy consumption violates the lower and upper limits of the energy consumption of HVAC within $T = 24$ for M1 and M2. The probabilities of deviations of the lower and upper limits (Prob_VioEneL and Prob_VioEneH) are calculated by Num_VioEneL/10000 and Num_VioEneH/10000, respectively. The probabilities are all less than $\varepsilon = 0.005$, which shows that the distributionally robust chance constraints Eqn. (5.2.6e) and Eqn. (5.2.6f) are satisfied based on M1 and M2 for all the time slots in the scheduling horizon since the values in Table 5.5 are the maximum probabilities of deviations.

In consecutive scheduling cycles

The performance of the proposed DROA is tested under consecutive cycles from 12 pm August 6th 2013 to 12pm August 9th 2013 (6 scheduling cycles with 12 hours in each cycle) with 70 °F as the starting indoor temperature, and the indoor end temperature of the previous cycle will be the indoor starting temperature of the next cycle. The simulation results are shown in Table 5.6. It can be seen from Table 5.6 that the electricity cost is reduced through the proposed M1 and the computation time of M1 is largely decreased compared with M2.

5.4.2 The solution approach with different parameters

In this section, the impacts of m, ε and the comfortable temperature zone on the performance of the proposed DROA are investigated, respectively, in the scheduling cycle from 12 pm to 12 am on August 6th 2013.

Table 5.6: Performances of the three methods in consecutive scheduling cycles

Cycle	Method	Cost ($)	Num_VioTem	VioTem (°F)
1	M1	0.794	17	0.1405
	M2	0.796	0	0
	M3	0.799	0	0
2	M1	0.140	8	0.0650
	M2	0.153	0	0
	M3	0.159	0	0
3	M1	0.802	9	0.6306
	M2	0.803	4	0.0656
	M3	0.808	0	0
4	M1	0.135	9	0.1631
	M2	0.146	0	0
	M3	0.156	0	0
5	M1	0.806	3	0.5775
	M2	0.812	0	0
	M3	0.812	0	0
6	M1	0.121	17	0.2514
	M2	0.128	0	0
	M3	0.149	0	0
Cycle	Method	Prob_VioEneL	Prob_VioEneH	Time (s)
1	M1	0.0005	0.0006	0.5110
	M2	0	0	5.7651
	M3	0	0	0.1494
2	M1	0.0006	0.0007	0.4586
	M2	0	0	9.8003
	M3	0	0	0.1433
3	M1	0.0004	0.0009	0.3636
	M2	0.0001	0.0004	4.5839
	M3	0	0	0.2590
4	M1	0.0005	0.0007	0.4945
	M2	0	0	7.3025
	M3	0	0	0.0977
5	M1	0.0005	0.0003	0.3278
	M2	0	0	7.5653
	M3	0	0	0.1411
6	M1	0.0007	0.0010	0.4658
	M2	0.0001	0	6.6144
	M3	0	0	0.1499

Table 5.7: Performances of M1 with different m

m	Cost ($)	Num_VioTem	VioTem (°F)
2	0.799	0	0
3	0.795	2	0.0782
4	0.795	6	0.0955
5	0.794	3	0.1433
10	0.794	7	0.3141
15	0.794	17	0.1405
20	0.793	8	0.5678
25	0.793	28	0.1419
m	Prob_VioEneL	Prob_VioEneH	Time (s)
2	0	0	0.1132
3	0.0001	0.0002	0.1860
4	0.0001	0.0004	0.2282
5	0.0002	0.0001	0.2823
10	0.0001	0.0007	0.3141
15	0.0005	0.0006	0.5110
20	0.0010	0.0008	0.5658
25	0.0006	0.0009	0.5897

With different m

M1 with different m is tested with 10,000 samples of the outdoor temperature under the condition of $\varepsilon = 0.005$ and [60° F, 70° F] as the comfortable temperature zone. The performances of M1 with different m are compared in Table 5.7. It can be seen from Table 5.7 that the indoor temperature is mostly within the comfortable zone. With the increase of m, i.e. with more probabilistic information of the outdoor temperature taken into account, the electricity cost is decreasing and the computation time is increasing. Though the difference of the electricity cost is small, the reduce of the electricity cost with the increase of m is in accordance with the analysis that with more information of the uncertainty, a better decision can be made.

With different ε

M1 with different ε is tested with 10,000 samples of the outdoor temperature under the condition of $m = 15$ and [60° F, 70° F] as the comfortable temperature

Table 5.8: Performances of M1 with different ε

ε	Cost ($)	Num_VioTem	VioTem (°F)
0.005	0.794	17	0.1405
0.020	0.792	28	0.5704
0.040	0.792	48	0.9417
0.060	0.792	87	0.9033
0.080	0.790	102	1.0342
ε	Prob_VioEneL	Prob_VioEneH	Time (s)
0.005	0.0005	0.0006	0.5110
0.020	0.0021	0.0028	0.4095
0.040	0.0034	0.0048	0.2490
0.060	0.0073	0.0087	0.2109
0.080	0.0094	0.0102	0.2111

Table 5.9: Performances of M1 with different comfortable temperature zones

Temperature Zone (°F)	Cost ($)	Num_VioTem	VioTem (°F)
[60-70]	0.794	17	0.1405
[62-70]	0.794	13	0.4901
[65-70]	0.794	23	0.1389
[68-70]	0.801	5	0.0457
Temperature Zone (°F)	Prob_VioEneL	Prob_VioEneH	Time (s)
[60-70]	0.0005	0.0006	0.5110
[62-70]	0.0002	0.0009	0.4985
[65-70]	0.0006	0.0011	0.5576
[68-70]	0	0.0005	0.3451

zone. The performances of M1 with different ε are compared in Table 5.8. It can be seen from Table 5.8 that with the increase of ε, the electricity cost is decreasing and the probability of the violation of the comfortable temperature zone is increasing.

With different comfortable temperature zone

M1 with different comfortable temperature zones is tested with 10,000 samples of the outdoor temperature under the condition of $m = 15$ and $\varepsilon = 0.005$. The performances of M1 with different comfortable temperature zones are compared in Table 5.9. It can be seen from Table 5.9 that the electricity cost increases when the comfortable temperature zone is narrowed.

With the consideration of the cost, the number of violations of the comfortable

temperature zone and the computation time, genetic algorithm (GA) can be used to find the optimal combination of m, ε and the comfortable temperature zone. GA mimics the process of natural selection. After evaluating the fitness of each individual in a generation, selecting individuals with high fitness, crossover and mutation, a new generation with better fitness is obtained, and the above process cycles until the individual with a satisfactory fitness is found [47]. To find the optimal combination of parameters, a random combination of m, ε and the comfortable temperature zone indicates an individual of the GA, and the sum of the cost, the number of violations and the computation time with their corresponding importance factors indicates the fitness of the GA, i.e. $w_1 \cdot \text{Cost} + w_2 \cdot \text{Num\_VioTem} + w_3 \cdot \text{Time}$ is the objective function of the GA, where w_1, w_2 and w_3 are the importance factors. With m between 5 and 25, ε between 0.005 and 0.080, the lower limit of the comfortable temperature zone between 60°F and 68°F, and the upper limit of the comfortable temperature zone with the fixed 70°F, $m = 8, \varepsilon = 0.013$ and 67.5°F as the lower limit of the temperature zone is the optimal combination of parameters obtained through the GA for the situation where the cost, the number of violations divided by 100 and the computation time are with the same importance. The number of violations is divided by 100 due to the magnitude difference among the number of violations, the cost and the computation time. The Cost, Num_VioTem, VioTem, Prob_VioEneL, Prob_VioEneH and Time are \$0.799, 9, 0.1554°F, 0, 0.0009 and 0.1336s, respectively, for the optimal combination of parameters.

5.4.3 The extension of the solution approach

In this section, the proposed DROA is extended to take into account the uncertainty of the electricity price, the effect of users' activities on the indoor temperature and the deviation of users' preferred temperature. All the simulations are conducted in the scheduling cycle from 12 pm to 12 am on August 6th 2013.

Considering the uncertainty of the electricity price

The uncertainty of the electricity price is taken into account through the Monte Carlo method with its probability distribution known, which is formulated as the same as Eqn. (5.2.6) except that the objective function is changed to

$$\min_{q_t^{\text{ref}}} \mathbb{E}\{\frac{1}{S_e}\sum_{s_e=1}^{S_e}\sum_{t=1}^{T}(e_t \cdot q_t \cdot \Delta t)\} \tag{5.4.5}$$

where s_e and S_e represent the index of scenario of the electricity price and the total number of scenarios, respectively.

The proposed DROA with $m = 15, \varepsilon = 0.005$ and [60° F, 70° F] as the comfortable temperature zone is tested under 10,000 samples of the outdoor temperature and the electricity price. The uncertainty of the electricity price is considered based on the norm distribution with the TOUP as the mean and 0.0003 $/kWh as the standard deviation. The Cost, Num_VioTem, VioTem, Prob_VioEneL, Prob_VioEneH and Time are $0.793, 22, 0.1873°F, 0.0004, 0.0008 and 0.4064s, respectively.

Considering the effect of users' activities

The effect of users' activities on the indoor temperature as well as the uncertainty of the outdoor temperature is taken into account in the energy consumption

scheduling of HVAC, which is formulated as

$$\min_{q_t^{\text{ref}}} \mathbb{E}\{\sum_{t=1}^{T}(e_t \cdot q_t \cdot \Delta t)\} \tag{5.4.6a}$$

$$q_t = q_t^{\text{ref}} + \frac{1}{\eta \cdot R} \cdot (\xi_t - \mu_t) + \frac{C}{\eta \cdot \Delta t} \cdot (\varphi_t - \phi_t) \tag{5.4.6b}$$

$$\theta_t = \theta_{t-1} - \frac{\Delta t}{C \cdot R} \cdot (\theta_{t-1} - \xi_{t-1} + \eta \cdot R \cdot q_{t-1}) + \varphi_{t-1} \tag{5.4.6c}$$

$$\theta^{\min} \leq \theta_t \leq \theta^{\max} \tag{5.4.6d}$$

$$\mathbb{P}_t\{q_t \geq 0\} \geq 1 - \varepsilon, \forall \mathbb{P}_t \in \mathcal{P}_t^3 \tag{5.4.6e}$$

$$\mathbb{P}_t\{q_t \leq q^{\max}\} \geq 1 - \varepsilon, \forall \mathbb{P}_t \in \mathcal{P}_t^3 \tag{5.4.6f}$$

$$\mathcal{P}_t^3 = \left\{ \mathbb{P}_t \in \mathcal{P}_t^0(B_t^m) \;\middle|\; \begin{array}{l} \mathbb{E}_{\mathbb{P}_t}\{\boldsymbol{\omega}_t\} = \boldsymbol{\rho}_t \\ \boldsymbol{\omega}_t = (\xi_t, \varphi_t)^{\mathrm{T}}, \boldsymbol{\rho}_t = (\mu_t, \phi_t)^{\mathrm{T}} \\ \mathbb{P}_t\{\boldsymbol{\omega}_t \in B_t^i\} = p_t^i,\ i = 1, \cdots, m \\ B_t^i = \{\boldsymbol{\omega}_t \in \mathcal{R}^2 | \\ \qquad l_t^i \leq \xi_t \leq u_t^i \\ \qquad \varphi_t^{\min} \leq \varphi_t \leq \varphi_t^{\max}\} \\ B_t^1 \subseteq \cdots \subseteq B_t^m, p_t^m = 1 \end{array} \right\} \tag{5.4.6g}$$

where φ_{t-1} is the effect of users' activities during $t-1$ time slot on the indoor temperature, and ϕ_t is the forecast effect of users' activities. Eqn. (5.4.6b) is obtained based on $\theta_{t-1} - \frac{\Delta t}{C \cdot R} \cdot (\theta_{t-1} - \mu_{t-1} + \eta \cdot R \cdot q_{t-1}^{\text{ref}}) + \phi_{t-1} = \theta_{t-1} - \frac{\Delta t}{C \cdot R} \cdot (\theta_{t-1} - \xi_{t-1} + \eta \cdot R \cdot q_{t-1}) + \varphi_{t-1}$, therefore the forecast errors of both the outdoor temperature and the effect of users' activities are compensated. Taking into account two uncertainties, the uniform form of distributionally robust chance constraints is changed to

$$\mathbb{P}_t\text{-CVaR}_{\varepsilon}(\boldsymbol{a}_t^{\mathrm{T}} \boldsymbol{\omega}_t \leq c_t) \leq 0,\ \forall \mathbb{P}_t \in \mathcal{P}_t^3 \tag{5.4.7}$$

where $\boldsymbol{a}_t = (-\frac{1}{\eta \cdot R}, -\frac{C}{\eta \cdot \Delta t})^{\mathrm{T}}, c_t = q_t^{\text{ref}} - \frac{1}{\eta \cdot R} \cdot \mu_t - \frac{C}{\eta \cdot \Delta t} \cdot \phi_t$ for Eqn. (5.4.6e) and $\boldsymbol{a}_t = (\frac{1}{\eta \cdot R}, \frac{C}{\eta \cdot \Delta t})^{\mathrm{T}}, c_t = q_t^{\max} - q_t^{\text{ref}} + \frac{1}{\eta \cdot R} \cdot \mu_t + \frac{C}{\eta \cdot \Delta t} \cdot \phi_t$ for Eqn. (5.4.6f). Eqn. (5.4.7) is reformulated to be linear based on the theorem below and the proof is similar to the proof of ***Theorem 1***.

Theorem 3: When the ambiguity set $\mathcal{P}_t^3$ is constructed, the distributionally ro-

bust constraint Eqn. (5.4.7) is satisfied if and only if there exist $\boldsymbol{y} \in \mathcal{R}^2$, $\beta \in \mathcal{R}$, and $\lambda_i \in \mathcal{R}, i = 1, \cdots, m$, such that

$$\beta + \frac{1}{\varepsilon} \cdot (\boldsymbol{\rho}_t^{\mathrm{T}} \boldsymbol{y} + \sum_{i=1}^{m} \lambda_i \cdot p_t^i) \leq 0 \tag{5.4.8a}$$

$$\forall i = 1, \cdots, m:$$

$$(l_t^i, \varphi_t^{\min}) \boldsymbol{y} + \sum_{j=i}^{m} \lambda_j \geq 0 \tag{5.4.8b}$$

$$(l_t^i, \varphi_t^{\max}) \boldsymbol{y} + \sum_{j=i}^{m} \lambda_j \geq 0 \tag{5.4.8c}$$

$$(u_t^i, \varphi_t^{\min}) \boldsymbol{y} + \sum_{j=i}^{m} \lambda_j \geq 0 \tag{5.4.8d}$$

$$(u_t^i, \varphi_t^{\max}) \boldsymbol{y} + \sum_{j=i}^{m} \lambda_j \geq 0 \tag{5.4.8e}$$

$$(l_t^i, \varphi_t^{\min}) \boldsymbol{y} + \sum_{j=i}^{m} \lambda_j - ((l_t^i, \varphi_t^{\min}) \boldsymbol{a}_t - c_t - \beta) \geq 0 \tag{5.4.8f}$$

$$(l_t^i, \varphi_t^{\max}) \boldsymbol{y} + \sum_{j=i}^{m} \lambda_j - ((l_t^i, \varphi_t^{\max}) \boldsymbol{a}_t - c_t - \beta) \geq 0 \tag{5.4.8g}$$

$$(u_t^i, \varphi_t^{\min}) \boldsymbol{y} + \sum_{j=i}^{m} \lambda_j - ((u_t^i, \varphi_t^{\min}) \boldsymbol{a}_t - c_t - \beta) \geq 0 \tag{5.4.8h}$$

$$(u_t^i, \varphi_t^{\max}) \boldsymbol{y} + \sum_{j=i}^{m} \lambda_j - ((u_t^i, \varphi_t^{\max}) \boldsymbol{a}_t - c_t - \beta) \geq 0 \tag{5.4.8i}$$

The proposed DROA with $m = 15, \varepsilon = 0.005$ and [60° F, 70° F] as the comfortable temperature zone is tested under 10,000 samples of the outdoor temperature and the effect of users' activities. The effect of users' activities is sampled based on the norm distribution between $\varphi^{\min}$ and $\varphi^{\max}$. $\varphi^{\min}$ and $\varphi^{\max}$ are assumed to be [0.5, 0.5, 0.4, 0.4, 0, 0, 0, 0, 0.3, 0.3, 0.6, 0.6, 0.8, 0.8, 0.8, 0.8, 0, 0, 0, 0, 0, 0, 0, 0] and [1.3, 1.3, 0.8, 0.8, 0.4, 0.4, 0.2, 0.2, 0.5, 0.5, 1, 1, 1.2, 1.2, 1, 1, 0.6, 0.6, 0.2, 0.2, 0.2, 0.2, 0.2, 0.2] in the scheduling horizon. The Cost, Num_VioTem, VioTem, Prob_VioEneL, Prob_VioEneH and Time are \$0.931, 1, 0.0200°F, 0, 0.0001 and 0.9070s, respectively. With the consideration of the effect of users' activities on

the indoor temperature and the uncertainty of outdoor temperature, the room temperature remains in users' comfortable zone with the expectation of electricity cost minimized. Though two dimensional uncertainties are considered, the distributionally robust chance constraints are transferred to linear constraints as well and the computation time is not much increased.

Considering the deviation of users' preferred temperature

Users may not only require the indoor temperature within the comfortable temperature zone but also have their preferred indoor temperature. The deviation of the indoor temperature from the preferred temperature is taken into account in the energy consumption scheduling of HVAC, which is formulated as the same as Eqn. (5.2.6) except that the objective function is changed to

$$\min_{q_t^{\text{ref}}} \mathbb{E}\{\sum_{t=1}^{T} e_t \cdot q_t \cdot \Delta t + \kappa \cdot (\theta_t - \theta^{\text{best}})^2\} \tag{5.4.9}$$

where κ penalizes the deviation of the preferred indoor temperature and θ^{best} denotes users' preferred temperature.

The proposed DROA with $m = 15, \varepsilon = 0.005$, [60° F, 70° F] as the comfortable temperature zone and $\theta^{\text{best}} = 65°$ F is tested under 10,000 samples of the outdoor temperature. The Cost, Num_VioTem, VioTem, Prob_VioEneL, Prob_VioEneH and Time are \$0.925, 0, 0, 0.0008, 0.0011 and 0.7458s, respectively. Compared with the situation where the problem is formulated as Eqn. (5.2.6) with the same m, ε and the comfortable temperature zone, the electricity cost is increased as users' preferred temperature is taken into account and this temperature is lower than the upper limit of the comfortable temperature zone. When there is no preferred temperature, the room temperature can reach the upper limit to save the electricity cost.

5.5 Conclusions

In this chapter, the DROA based on the probabilistic information of subintervals of the outdoor temperature is proposed to schedule the energy consumption of H-

VAC. The simulation results have demonstrated that the proposed DROA reduces the electricity cost compared with the ROA, and that it reduces the electricity cost with approximate 10% of computation time of the DROA based on the mean and the variance of the outdoor temperature. By increasing the number of temperature subintervals, i.e. by taking into account more information about the uncertainty of the outdoor temperature, the electricity cost of the proposed DROA is decreased. The proposed DROA has proved effective in the energy consumption scheduling of HVAC with the consideration of the uncertainty of the outdoor temperature.

Chapter 6

Conclusions and future research

6.1 Conclusions

Demand response (DR) plays an important role in smart grid to meet the balancing between the supply and the demand and it helps improve the reliability of power grid and the penetration of renewable energy sources (RESs). The energy consumption of residential users is one of the major parts of DR, and residential users usually participate in DR through the residential demand side scheduling (RDSS) in response to the electricity price information. To further improve the performance of the RDSS, this thesis deals with the energy consumption scheduling of residential users considering appliances' operational safety and uncertainties of manually operated appliances (MOAs) and the outdoor temperature. The main conclusions are listed as follows.

Chapter 3 considers the operational safety of home appliances as a new objective in the RDSS together with objectives of the electricity cost and the operational delay. The operational safety of appliances is of great concern to users especially when the appliances are in operation without users' monitoring, e.g. in periods when users are not at home or when they are asleep. Based on whether users are at home and awake to monitor the appliances' operations, the operational safety of appliances is taken into account. The approach of finding the Pareto-optimal front is adopted to solve the multi-objective RDSS and it is compared with the Weight approach and

the Constraint approach. Compared with the Weight approach, the Pareto approach clearly presents the relationships between the operational safety and the other two objectives, and compared with the Constraint approach, the solutions of the Pareto approach are better with solutions those dominate the solutions of the Constraint approach, i.e. there exist solutions of the Pareto approach with values of all objectives better than solutions of the Constraint approach. Simulation results have demonstrated the operational safety is improved with the sacrifice of the electricity cost and the operational delay, and that the Pareto approach is effective in presenting comprehensive optimal solutions of the multi-objective RDSS with relationships among objectives presented.

Chapter 4 takes into account the uncertainty of MOAs' energy consumption in the RDSS through the robust optimization approach (ROA) as the uncertainty of MOAs affects the electricity cost and the probabilistic information of MOAs' uncertainty is not easily obtained. The ROA is compared with the approach without considering the MOAs' energy consumption and the approach considering MOAs with a fixed energy consumption. Simulation results have verified that the ROA effectively avoids the risk of a high electricity cost caused by the MOAs' uncertainty and reduces the electricity cost of home appliances compared with the other two approaches.

Chapter 5 considers the uncertainty of the outdoor temperature in the RDSS of the heating, ventilation and air conditioning (HVAC) system through the distributionally robust optimization approach (DROA). The uncertainty of the outdoor temperature should be taken into account as it affects the electricity cost and users' temperature comfort. The proposed DROA constructs the ambiguity set of the outdoor temperature's probability distribution based on the probabilistic information of its subintervals, and the RDSS of HVAC is formulated as a nonlinear problem with distributionally robust chance constraints. These constraints are reformulated to be linear and the energy scheduling problem is solved through linear programming. The simulation results have proved that the proposed DROA reduces the electricity cost with users' comfortable temperature zone satisfied. Compared with the DROA based on the mean and the variance of the outdoor temperature, the pro-

posed DROA reduces the electricity cost with approximate 10% of the computation time. The electricity cost of the proposed DROA is also reduced in the comparison with the ROA.

6.2 Future research

Based on the work of this thesis, the following perspectives can be explored.

- RDSS with users' requirements learned: In the system model of RDSS of this thesis, users are required to input the requirements for the operations of appliances, e.g. the operation time interval and the operation length [152]. To improve users' convenience, a method of learning users' requirements is to be investigated including how to get the original data of users' requirements, how to learn users' requirements from the original data and how to judge the learned results [128].

- The effect of RDSS on power system: This thesis schedules the energy consumption of residential users in response to electricity price [153]. Though users can get benefit from the RDSS, the effect of RDSS on the power system is not investigated. There are several issues to be further studied.

  Firstly, it may cause new peak demand if all users respond to the same electricity price [47]. How to make the decision of electricity price with the consideration of its impact on users' energy consumption can be further studied, or a method of scheduling a number of users' energy consumption to avoid the possible new peak demand should be proposed. Secondly, the methods of reducing the operation cost of the whole power system through the RDSS of a number of users can be explored in future, for example, the method of shaping the aggregate profile of energy consumption of users and the method of providing the reserve service [25]. Thirdly, how to allocate the energy consumption of each user based on the aggregate profile of energy consumption and how to make users cooperate well is another issue to be investigated. To achieve the desired properties of the aggregate profile, the cooperation of

users' energy consumption scheduling has been studied through game theory in [55, 154] without the consideration of uncertainties in each individual house. The cooperation of users taking into account the uncertainties, e.g. the uncertainty of MOAs, can be studied in future through methods including but not limited to game theory.

- RDSS with the consideration of renewable energy: Renewable energy is an important part of smart grid for its ability of reducing the emissions of greenhouse gases [4] and it is not considered in this thesis. Renewable energy can be taken into account in users' houses and in the power system with the consideration of RDSS of a number of users [38], corresponding to the viewpoints of residential users and the power system operator, respectively.

  With the apparatuses of RESs installed in users' houses, the model of the RDSS in this thesis can be extended. The energy consumption of SAs including HVAC can be scheduled in periods when there is renewable energy to help users to reduce the electricity cost. There are still many issues to be solved with the consideration of renewable energy in users' houses. The uncertainty of renewable energy can be studied in the RDSS together with the uncertainties of MOAs [152] and the outdoor temperature [155]. There may also be conflict between the usage of renewable energy and users' concerns. For example, the integration of solar energy in the RDSS may conflict with the operational safety of appliances that has been considered in this thesis [153]. To improve the operational safety, the energy consumption of home appliances is scheduled in periods when users are at home. However, the solar energy distributes in daytime when users are likely not at home. A method of dealing with this conflict can be investigated.

  With the consideration of renewable energy and RDSS of a number of users in the power system, the method of scheduling the energy consumption to maximize the usage of renewable energy is to be investigated. There exist uncertainties in renewable energy and RDSS and the method of tackling these uncertainties can be studied. The proposed method of scheduling energy con-

sumption of HVAC in chapter 5 can be investigated to deal with the uncertainties of renewable energy and RDSS, i.e. the energy consumption is scheduled based on the forecast values of uncertainties and is adjusted in real time based on the actual values of uncertainties.

- RDSS with the consideration of batteries and other energy sources: This thesis schedules the energy consumption of home appliances without the consideration of batteries and other energy sources. The co-optimization of the RDSS, batteries and multiple energy sources brings more benefit to users as well as the whole energy system and it can be explored in future. It can be studied that how to make the best use of batteries which can storage energy when the electricity price is low and can provide energy when the price is high. The cooperation of batteries of a number of users can be studied to provide the reserve service and to reduce the operation cost of power system. The microcombined heat and power system is an energy-efficient technology that simultaneously provides heat and electricity to households [156]. How to make an optimal scheduling of the mircocombined heat and power system and residential energy consumption can be investigated.

References

[1] R. Deng, Z. Yang, M. Y. Chow, and J. Chen, "A survey on demand response in smart grids: Mathematical models and approaches," *IEEE Transactions on Industrial Informatics*, vol. 11, no. 3, pp. 570–582, June 2015.

[2] A. J. Wood and B. F. Wollenberg, *Power generation, operation, and control*. John Wiley & Sons, 2012.

[3] P. Kundur, N. J. Balu, and M. G. Lauby, *Power system stability and control*. McGraw-hill New York, 1994, vol. 7.

[4] A. Barbato and A. Capone, "Optimization models and methods for demand-side management of residential users: A survey," *Energies*, vol. 7, no. 9, pp. 5787–5824, 2014.

[5] J. Aghaei and M.-I. Alizadeh, "Demand response in smart electricity grids equipped with renewable energy sources: A review," *Renewable and Sustainable Energy Reviews*, vol. 18, pp. 64 – 72, 2013.

[6] M. Mazidi, A. Zakariazadeh, S. Jadid, and P. Siano, "Integrated scheduling of renewable generation and demand response programs in a microgrid," *Energy Conversion and Management*, vol. 86, pp. 1118 – 1127, 2014.

[7] F. Wu, X. Li, F. Feng, and H. B. Gooi, "Multi-topology-mode grid-connected inverter to improve comprehensive performance of renewable energy source generation system," *IEEE Transactions on Power Electronics*, vol. 32, no. 5, pp. 3623 – 3633, 2017.

[8] I. Aravena and A. Papavasiliou, "Renewable energy integration in zonal markets," *IEEE Transactions on Power Systems*, vol. 32, no. 2, pp. 1334–1349, Mar. 2017.

[9] FS-UNEP collaborating center, Global trends in renewable energy investment 2016 [Online]. Available: http://fs-unep-centre.org/sites/default/files/publications/globaltrendsinrenewableenergyinvestment2016lowres_0.pdf.

[10] V. C. Gungor, D. Sahin, T. Kocak, S. Ergut, C. Buccella, C. Cecati, and G. P. Hancke, "Smart grid technologies: Communication technologies and standards," *IEEE Transactions on Industrial Informatics*, vol. 7, no. 4, pp. 529–539, Nov. 2011.

[11] X. Fang, S. Misra, G. Xue, and D. Yang, "Smart grid-the new and improved power grid: A survey," *IEEE Communications Surveys Tutorials*, vol. 14, no. 4, pp. 944–980, 2012.

[12] V. C. Gungor, D. Sahin, T. Kocak, S. Ergut, C. Buccella, C. Cecati, and G. P. Hancke, "A survey on smart grid potential applications and communication requirements," *IEEE Transactions on Industrial Informatics*, vol. 9, no. 1, pp. 28–42, Feb. 2013.

[13] A. Iwayemi, P. Yi, X. Dong, and C. Zhou, "Knowing when to act: an optimal stopping method for smart grid demand response," *IEEE Network*, vol. 25, no. 5, pp. 44–49, Sep. 2011.

[14] Y. Cai, Y. Li, Y. Cao, W. Li, and X. Zeng, "Modeling and impact analysis of interdependent characteristics on cascading failures in smart grids," *International Journal of Electrical Power and Energy Systems*, vol. 89, pp. 106 – 114, 2017. [Online]. Available: http://www.sciencedirect.com/science/article/pii/S0142061516322505

[15] M. Davari and Y. A. R. I. Mohamed, "Robust dc-link voltage control of a full-scale PMSG wind turbine for effective integration in dc grids," *IEEE Transactions on Power Electronics*, vol. 32, no. 5, pp. 4021–4035, May 2017.

[16] K. Reddy, M. Kumar, T. Mallick, H. Sharon, and S. Lokeswaran, "A review of integration, control, communication and metering (ICCM) of renewable energy based smart grid," *Renewable and Sustainable Energy Reviews*, vol. 38, pp. 180 – 192, 2014.

[17] F. Y. Xu, T. Zhang, L. L. Lai, and H. Zhou, "Shifting boundary for price-based residential demand response and applications," *Applied Energy*, vol. 146, pp. 353 – 370, 2015.

[18] S. Rahnama, T. Green, C. H. Lyhne, and J. D. Bendtsen, "Industrial demand management providing ancillary services to the distribution grid: Experimental verification," *IEEE Transactions on Control Systems Technology*, vol. 25, no. 2, pp. 485–495, Mar. 2017.

[19] J. Zazo, S. Zazo, and S. V. Macua, "Robust worst-case analysis of demand-side management in smart grids," *IEEE Transactions on Smart Grid*, vol. 8, no. 2, pp. 662–673, Mar. 2017.

[20] F. L. Meng and X. J. Zeng, "A profit maximization approach to demand response management with customers behavior learning in smart grid," *IEEE Transactions on Smart Grid*, vol. 7, no. 3, pp. 1516–1529, May 2016.

[21] J. Wang, H. Zhong, X. Lai, Q. Xia, C. Shu, and C. Kang, "Distributed real-time demand response based on Lagrangian multiplier optimal selection approach," *Applied Energy*, vol. 190, pp. 949 – 959, 2017. [Online]. Available: http://www.sciencedirect.com/science/article/pii/S0306261916319304

[22] Y. M. Ding, S. H. Hong, and X. H. Li, "A demand response energy management scheme for industrial facilities in smart grid," *IEEE Transactions on Industrial Informatics*, vol. 10, no. 4, pp. 2257–2269, Nov. 2014.

[23] L. Gomes, P. Faria, H. Morais, Z. Vale, and C. Ramos, "Distributed, agent-based intelligent system for demand response program simulation in smart grids," *IEEE Intelligent Systems*, vol. 29, no. 1, pp. 56–65, Jan. 2014.

[24] Y. Kim and L. K. Norford, "Optimal use of thermal energy storage resources in commercial buildings through price-based demand response considering distribution network operation," *Applied Energy*, vol. 193, pp. 308 – 324, 2017. [Online]. Available: http://www.sciencedirect.com/science/article/pii/S0306261917301897

[25] N. Lu and Y. Zhang, "Design considerations of a centralized load controller using thermostatically controlled appliances for continuous regulation reserves," *IEEE Transactions on Smart Grid*, vol. 4, no. 2, pp. 914–921, June 2013.

[26] R. Deng, G. Xiao, R. Lu, and J. Chen, "Fast distributed demand response with spatially and temporally coupled constraints in smart grid," *IEEE Transactions on Industrial Informatics*, vol. 11, no. 6, pp. 1597–1606, Dec. 2015.

[27] L. Yao, W. H. Lim, and T. S. Tsai, "A real-time charging scheme for demand response in electric vehicle parking station," *IEEE Transactions on Smart Grid*, vol. 8, no. 1, pp. 52–62, Jan. 2017.

[28] F. Pallonetto, S. Oxizidis, F. Milano, and D. Finn, "The effect of time-of-use tariffs on the demand response flexibility of an all-electric smart-grid-ready dwelling," *Energy and Buildings*, vol. 128, pp. 56 – 67, 2016. [Online]. Available: http://www.sciencedirect.com/science/article/pii/S0378778816305308

[29] H. T. Haider, O. H. See, and W. Elmenreich, "Residential demand response scheme based on adaptive consumption level pricing," *Energy*, vol. 113, pp. 301 – 308, 2016. [Online]. Available: http://www.sciencedirect.com/science/article/pii/S0360544216309768

[30] H. T. Roh and J. W. Lee, "Residential demand response scheduling with multiclass appliances in the smart grid," *IEEE Transactions on Smart Grid*, vol. 7, no. 1, pp. 94–104, Jan. 2016.

[31] U.K. Power, Economy 7 Tariff 2015 [Online]. Available: https://www.ukpower.co.uk/home_energy/economy-7.

[32] Ameren Illinois Power Company, Real-time pricing for residential customers, Aug. 2012 [Online]. Available: http://www.powersmartpricing.org/chart/.

[33] A. H. Mohsenian-Rad and A. Leon-Garcia, "Optimal residential load control with price prediction in real-time electricity pricing environments," *IEEE Transactions on Smart Grid*, vol. 1, no. 2, pp. 120–133, Sep. 2010.

[34] M. Albadi and E. El-Saadany, "A summary of demand response in electricity markets," *Electric Power Systems Research*, vol. 78, no. 11, pp. 1989 – 1996, 2008.

[35] H. Wu, M. Shahidehpour, and A. Al-Abdulwahab, "Hourly demand response in day-ahead scheduling for managing the variability of renewable energy," *IET Generation, Transmission Distribution*, vol. 7, no. 3, pp. 226–234, Mar. 2013.

[36] H. A. Aalami and S. Nojavan, "Energy storage system and demand response program effects on stochastic energy procurement of large consumers considering renewable generation," *IET Generation, Transmission Distribution*, vol. 10, no. 1, pp. 107–114, 2016.

[37] B. Zeng, J. Zhang, X. Yang, J. Wang, J. Dong, and Y. Zhang, "Integrated planning for transition to low-carbon distribution system with renewable energy generation and demand response," *IEEE Transactions on Power Systems*, vol. 29, no. 3, pp. 1153–1165, May 2014.

[38] M. Asensio and J. Contreras, "Risk-constrained optimal bidding strategy for pairing of wind and demand response resources," *IEEE Transactions on Smart Grid*, vol. 8, no. 1, pp. 200–208, Jan. 2017.

[39] A. Arefi, A. Abeygunawardana, and G. Ledwich, "A new risk-managed planning of electric distribution network incorporating customer engagement and

temporary solutions," *IEEE Transactions on Sustainable Energy*, vol. 7, no. 4, pp. 1646–1661, Oct. 2016.

[40] H. Wang and J. Huang, "Joint investment and operation of microgrid," *IEEE Transactions on Smart Grid*, vol. 8, no. 2, pp. 833–845, Mar. 2017.

[41] M. D. Ilic, L. Xie, and J. Y. Joo, "Efficient coordination of wind power and price-responsive demand-part i: Theoretical foundations," *IEEE Transactions on Power Systems*, vol. 26, no. 4, pp. 1875–1884, Nov. 2011.

[42] V. Hamidi, F. Li, and F. Robinson, "Demand response in the UK's domestic sector," *Electric Power Systems Research*, vol. 79, no. 12, pp. 1722 – 1726, 2009. [Online]. Available: http://www.sciencedirect.com/science/article/pii/S0378779609001710

[43] F. Mwasilu, J. J. Justo, E.-K. Kim, T. D. Do, and J.-W. Jung, "Electric vehicles and smart grid interaction: A review on vehicle to grid and renewable energy sources integration," *Renewable and Sustainable Energy Reviews*, vol. 34, pp. 501 – 516, 2014.

[44] A. Anvari-Moghaddam, H. Monsef, and A. Rahimi-Kian, "Optimal smart home energy management considering energy saving and a comfortable lifestyle," *IEEE Transactions on Smart Grid*, vol. 6, no. 1, pp. 324–332, Jan. 2015.

[45] Z. Wu, S. Zhou, J. Li, and X. P. Zhang, "Real-time scheduling of residential appliances via conditional risk-at-value," *IEEE Transactions on Smart Grid*, vol. 5, no. 3, pp. 1282–1291, May 2014.

[46] A. Giusti, M. Salani, G. A. D. Caro, A. E. Rizzoli, and L. M. Gambardella, "Restricted neighborhood communication improves decentralized demand-side load management," *IEEE Transactions on Smart Grid*, vol. 5, no. 1, pp. 92–101, Jan. 2014.

[47] Z. Zhao, W. C. Lee, Y. Shin, and K. B. Song, "An optimal power scheduling method for demand response in home energy management system," *IEEE Transactions on Smart Grid*, vol. 4, no. 3, pp. 1391–1400, Sep. 2013.

[48] Electrical Safety Council, Electrical safety first core data set, 2012 [Online]. Available: http://www.electricalsafetyfirst.org.uk/news-and-campaigns/policies-and-research/statistics/.

[49] U.S. Fire Administration, Residential building fires, causes and dollar loss 2014 [Online]. Available: http://www.usfa.fema.gov/downloads/xls/statistics/residential_nonresidential_fire_loss_estimates.xlsx.

[50] Electrical Safety Council, Electrical safety first, Jun. 2017 [Online]. Available: https://www.electricalsafetyfirst.org.uk/guides-and-advice/electrical-items/washing-machines/.

[51] C. Wang, Y. Zhou, J. Wu, J. Wang, Y. Zhang, and D. Wang, "Robust-index method for household load scheduling considering uncertainties of customer behavior," *IEEE Transactions on Smart Grid*, vol. 6, no. 4, pp. 1806–1818, July 2015.

[52] S. Salinas, M. Li, and P. Li, "Multi-objective optimal energy consumption scheduling in smart grids," *IEEE Transactions on Smart Grid*, vol. 4, no. 1, pp. 341–348, Mar. 2013.

[53] Z. Chen, L. Wu, and Y. Fu, "Real-time price-based demand response management for residential appliances via stochastic optimization and robust optimization," *IEEE Transactions on Smart Grid*, vol. 3, no. 4, pp. 1822–1831, Dec. 2012.

[54] Y. Ozturk, D. Senthilkumar, S. Kumar, and G. Lee, "An intelligent home energy management system to improve demand response," *IEEE Transactions on Smart Grid*, vol. 4, no. 2, pp. 694–701, June 2013.

[55] A.-H. Mohsenian-Rad, V. W. S. Wong, J. Jatskevich, R. Schober, and A. Leon-Garcia, "Autonomous demand-side management based on game-

theoretic energy consumption scheduling for the future smart grid," *IEEE Transactions on Smart Grid*, vol. 1, no. 3, pp. 320–331, Dec. 2010.

[56] Y. Sun, M. Elizondo, S. Lu, and J. C. Fuller, "The impact of uncertain physical parameters on HVAC demand response," *IEEE Transactions on Smart Grid*, vol. 5, no. 2, pp. 916–923, Mar. 2014.

[57] A. Thavlov and H. W. Bindner, "Utilization of flexible demand in a virtual power plant set-up," *IEEE Transactions on Smart Grid*, vol. 6, no. 2, pp. 640–647, Mar. 2015.

[58] S. Li, D. Zhang, A. B. Roget, and Z. O'Neill, "Integrating home energy simulation and dynamic electricity price for demand response study," *IEEE Transactions on Smart Grid*, vol. 5, no. 2, pp. 779–788, Mar. 2014.

[59] Y. Y. Hong, J. K. Lin, C. P. Wu, and C. C. Chuang, "Multi-objective air-conditioning control considering fuzzy parameters using immune clonal selection programming," *IEEE Transactions on Smart Grid*, vol. 3, no. 4, pp. 1603–1610, Dec. 2012.

[60] W. Wei, F. Liu, and S. Mei, "Distributionally robust co-optimization of energy and reserve dispatch," *IEEE Transactions on Sustainable Energy*, vol. 7, no. 1, pp. 289–300, Jan. 2016.

[61] Electrical Study Portal, The structure of power system (2015). Available: https://electricalstudyportal.blogspot.co.uk/2015/05/power-system-topic-sai-saikumar-jn.html.

[62] H. Chen, T. N. Cong, W. Yang, C. Tan, Y. Li, and Y. Ding, "Progress in electrical energy storage system: A critical review," *Progress in Natural Science*, vol. 19, no. 3, pp. 291 – 312, 2009. [Online]. Available: http://www.sciencedirect.com/science/article/pii/S100200710800381X

[63] H. Wu, M. Shahidehpour, A. Alabdulwahab, and A. Abusorrah, "Demand response exchange in the stochastic day-ahead scheduling with variable renew-

able generation," *IEEE Transactions on Sustainable Energy*, vol. 6, no. 2, pp. 516–525, Apr. 2015.

[64] H. T. Nguyen, D. T. Nguyen, and L. B. Le, "Energy management for households with solar assisted thermal load considering renewable energy and price uncertainty," *IEEE Transactions on Smart Grid*, vol. 6, no. 1, pp. 301–314, Jan. 2015.

[65] H. O. R. Howlader, H. Matayoshi, and T. Senjyu, "Distributed generation integrated with thermal unit commitment considering demand response for energy storage optimization of smart grid," *Renewable Energy*, vol. 99, pp. 107 – 117, 2016. [Online]. Available: http://www.sciencedirect.com/science/article/pii/S0960148116305742

[66] N. Li, L. Chen, and S. H. Low, "Optimal demand response based on utility maximization in power networks," in *2011 IEEE Power and Energy Society General Meeting*, July 2011, pp. 1–8.

[67] N. Forouzandehmehr, M. Esmalifalak, H. Mohsenian-Rad, and Z. Han, "Autonomous demand response using stochastic differential games," *IEEE Transactions on Smart Grid*, vol. 6, no. 1, pp. 291–300, Jan. 2015.

[68] L. Yang, X. Chen, J. Zhang, and H. V. Poor, "Cost-effective and privacy-preserving energy management for smart meters," *IEEE Transactions on Smart Grid*, vol. 6, no. 1, pp. 486–495, Jan. 2015.

[69] M. A. A. Pedrasa, T. D. Spooner, and I. F. MacGill, "The value of accurate forecasts and a probabilistic method for robust scheduling of residential distributed energy resources," in *2010 IEEE 11th International Conference on Probabilistic Methods Applied to Power Systems*, June 2010, pp. 587–592.

[70] A. Safdarian, M. Fotuhi-Firuzabad, and M. Lehtonen, "A distributed algorithm for managing residential demand response in smart grids," *IEEE Transactions on Industrial Informatics*, vol. 10, no. 4, pp. 2385–2393, Nov. 2014.

[71] J. H. Yoon, R. Baldick, and A. Novoselac, "Dynamic demand response controller based on real-time retail price for residential buildings," *IEEE Transactions on Smart Grid*, vol. 5, no. 1, pp. 121–129, Jan. 2014.

[72] S. Gottwalt, W. Ketter, C. Block, J. Collins, and C. Weinhardt, "Demand side management—a simulation of household behavior under variable prices," *Energy Policy*, vol. 39, no. 12, pp. 8163 – 8174, 2011, clean Cooking Fuels and Technologies in Developing Economies. [Online]. Available: http://www.sciencedirect.com/science/article/pii/S0301421511008007

[73] S. Datchanamoorthy, S. Kumar, Y. Ozturk, and G. Lee, "Optimal time-of-use pricing for residential load control," in *2011 IEEE International Conference on Smart Grid Communications (SmartGridComm)*, Oct. 2011, pp. 375–380.

[74] A. J. Roscoe and G. Ault, "Supporting high penetrations of renewable generation via implementation of real-time electricity pricing and demand response," *IET Renewable Power Generation*, vol. 4, no. 4, pp. 369–382, July 2010.

[75] A. J. Conejo, J. M. Morales, and L. Baringo, "Real-time demand response model," *IEEE Transactions on Smart Grid*, vol. 1, no. 3, pp. 236–242, Dec. 2010.

[76] N. Yu and J. l. Yu, "Optimal TOU decision considering demand response model," in *2006 International Conference on Power System Technology*, Oct. 2006, pp. 1–5.

[77] A. Agnetis, G. de Pascale, P. Detti, and A. Vicino, "Load scheduling for household energy consumption optimization," *IEEE Transactions on Smart Grid*, vol. 4, no. 4, pp. 2364–2373, Dec. 2013.

[78] M. A. Zehir and M. Bagriyanik, "Demand side management by controlling refrigerators and its effects on consumers," *Energy Conversion and Management*, vol. 64, pp. 238 – 244, 2012. [Online]. Available: http://www.sciencedirect.com/science/article/pii/S019689041200218X

[79] S. Shao, M. Pipattanasomporn, and S. Rahman, "Development of physical-based demand response-enabled residential load models," *IEEE Transactions on Power Systems*, vol. 28, no. 2, pp. 607–614, May 2013.

[80] A. Barbato, A. Capone, G. Carello, M. Delfanti, M. Merlo, and A. Zaminga, "House energy demand optimization in single and multi-user scenarios," in *2011 IEEE International Conference on Smart Grid Communications (SmartGridComm)*, Oct. 2011, pp. 345–350.

[81] K. Ma, T. Yao, J. Yang, and X. Guan, "Residential power scheduling for demand response in smart grid," *International Journal of Electrical Power and Energy Systems*, vol. 78, pp. 320 – 325, 2016. [Online]. Available: http://www.sciencedirect.com/science/article/pii/S014206151500530X

[82] S. Althaher, P. Mancarella, and J. Mutale, "Automated demand response from home energy management system under dynamic pricing and power and comfort constraints," *IEEE Transactions on Smart Grid*, vol. 6, no. 4, pp. 1874–1883, July 2015.

[83] L. Chen, N. Li, L. Jiang, and S. H. Low, *Optimal Demand Response: Problem Formulation and Deterministic Case*. New York, NY: Springer New York, 2012, pp. 63–85. [Online]. Available: http://dx.doi.org/10.1007/978-1-4614-1605-0_3

[84] D. Zhang, S. Li, M. Sun, and Z. O'Neill, "An optimal and learning-based demand response and home energy management system," *IEEE Transactions on Smart Grid*, vol. 7, no. 4, pp. 1790–1801, July 2016.

[85] Y. Y. Hong, C. R. Chen, and H. W. Yang, "Implementation of demand response in home energy management system using immune clonal selection algorithm," in *2015 IEEE Congress on Evolutionary Computation (CEC)*, May 2015, pp. 3377–3382.

[86] C. R. Chen, M. J. Lan, C. C. Huang, Y. Y. Hong, and S. H. Low, "Demand response optimization for smart home scheduling using genetic algorithm,"

in *2013 IEEE International Conference on Systems, Man, and Cybernetics*, Oct. 2013, pp. 1461–1465.

[87] D. M. Han and J. H. Lim, "Design and implementation of smart home energy management systems based on Zigbee," *IEEE Transactions on Consumer Electronics*, vol. 56, no. 3, pp. 1417–1425, Aug. 2010.

[88] Y. H. Lin and M. S. Tsai, "An advanced home energy management system facilitated by nonintrusive load monitoring with automated multiobjective power scheduling," *IEEE Transactions on Smart Grid*, vol. 6, no. 4, pp. 1839–1851, July 2015.

[89] M. Inoue, T. Higuma, Y. Ito, N. Kushiro, and H. Kubota, "Network architecture for home energy management system," *IEEE Transactions on Consumer Electronics*, vol. 49, no. 3, pp. 606–613, Aug. 2003.

[90] M. Erol-Kantarci and H. Mouftah, "Wireless sensor networks for cost-efficient residential energy management in the smart grid," *IEEE Transactions on Smart Grid*, vol. 2, no. 2, pp. 314–325, June 2011.

[91] LG, Smart living has arrived 2017 [Online]. Available: http://www.lg.com/us/discover/smartthinq/thinq.

[92] C. Vivekananthan, Y. Mishra, G. Ledwich, and F. Li, "Demand response for residential appliances via customer reward scheme," *IEEE Transactions on Smart Grid*, vol. 5, no. 2, pp. 809–820, Mar. 2014.

[93] Z. Chen and L. Wu, "Residential appliance DR energy management with electric privacy protection by online stochastic optimization," *IEEE Transactions on Smart Grid*, vol. 4, no. 4, pp. 1861–1869, Dec. 2013.

[94] O. Tan, D. Gunduz, and H. V. Poor, "Increasing smart meter privacy through energy harvesting and storage devices," *IEEE Journal on Selected Areas in Communications*, vol. 31, no. 7, pp. 1331–1341, July 2013.

[95] L. S. d. Oliveira and S. A. F. P. Saramago, "Multiobjective optimization techniques applied to engineering problems," *Journal of the Brazilian Society of Mechanical Sciences and Engineering*, vol. 32, pp. 94 – 105, Mar. 2010.

[96] K. Deb, A. Pratap, S. Agarwal, and T. Meyarivan, "A fast and elitist multiobjective genetic algorithm: NSGA-II," *IEEE Transactions on Evolutionary Computation*, vol. 6, no. 2, pp. 182–197, Apr. 2002.

[97] M. Alipour, B. Mohammadi-Ivatloo, and K. Zare, "Stochastic scheduling of renewable and CHP-based microgrids," *IEEE Transactions on Industrial Informatics*, vol. 11, no. 5, pp. 1049–1058, Oct. 2015.

[98] R. Dufour, P. E. Labeau, P. Henneaux, K. Karoui, and C. Merckx, "Stochastic optimization for reactive power planning problems," in *2016 IEEE International Energy Conference (ENERGYCON)*, Apr. 2016, pp. 1–6.

[99] G. C. Lazaroiu, V. Dumbrava, G. Balaban, M. Longo, and D. Zaninelli, "Stochastic optimization of microgrids with renewable and storage energy systems," in *2016 IEEE 16th International Conference on Environment and Electrical Engineering (EEEIC)*, June 2016, pp. 1–5.

[100] P. Chen, P. Siano, B. Bak-Jensen, and Z. Chen, "Stochastic optimization of wind turbine power factor using stochastic model of wind power," *IEEE Transactions on Sustainable Energy*, vol. 1, no. 1, pp. 19–29, Apr. 2010.

[101] A. Hatami, H. Seifi, and M. K. Sheikh-El-Eslami, "A stochastic-based decision-making framework for an electricity retailer: Time-of-use pricing and electricity portfolio optimization," *IEEE Transactions on Power Systems*, vol. 26, no. 4, pp. 1808–1816, Nov. 2011.

[102] W. B. Powell and S. Meisel, "Tutorial on stochastic optimization in energy-part i: Modeling and policies," *IEEE Transactions on Power Systems*, vol. 31, no. 2, pp. 1459–1467, Mar. 2016.

[103] N. Korolko and Z. Sahinoglu, "Robust optimization of EV charging schedules in unregulated electricity markets," *IEEE Transactions on Smart Grid*, vol. 8, no. 1, pp. 149–157, Jan. 2017.

[104] C. Dai, L. Wu, and H. Wu, "A multi-band uncertainty set based robust SCUC with spatial and temporal budget constraints," *IEEE Transactions on Power Systems*, vol. 31, no. 6, pp. 4988–5000, Nov. 2016.

[105] L. Bai, F. Li, T. Jiang, and H. Jia, "Robust scheduling for wind integrated energy systems considering gas pipeline and power transmission N-1 contingencies," *IEEE Transactions on Power Systems*, vol. 32, no. 2, pp. 1582–1584, Mar. 2017.

[106] H. Ye and Z. Li, "Robust security-constrained unit commitment and dispatch with recourse cost requirement," *IEEE Transactions on Power Systems*, vol. 31, no. 5, pp. 3527–3536, Sep. 2016.

[107] S. Dehghan, N. Amjady, and A. Kazemi, "Two-stage robust generation expansion planning: A mixed integer linear programming model," *IEEE Transactions on Power Systems*, vol. 29, no. 2, pp. 584–597, Mar. 2014.

[108] E. Delage and Y. Ye, "Distributionally robust optimization under moment uncertainty with application to data-driven problems," *Operations Research*, vol. 58, no. 3, pp. 595–612, 2010.

[109] A. Martinez-Mares and C. R. Fuerte-Esquivel, "A robust optimization approach for the interdependency analysis of integrated energy systems considering wind power uncertainty," *IEEE Transactions on Power Systems*, vol. 28, no. 4, pp. 3964–3976, Nov. 2013.

[110] H. Gao, J. Liu, and L. Wang, "Robust coordinated optimization of active and reactive power in active distribution systems," *IEEE Transactions on Smart Grid*, vol. PP, no. 99, pp. 1–1, 2017.

[111] Q. Wang, J. P. Watson, and Y. Guan, "Two-stage robust optimization for N-k contingency-constrained unit commitment," *IEEE Transactions on Power Systems*, vol. 28, no. 3, pp. 2366–2375, Aug. 2013.

[112] X. Bai and W. Qiao, "Robust optimization for bidirectional dispatch coordination of large-scale V2G," *IEEE Transactions on Smart Grid*, vol. 6, no. 4, pp. 1944–1954, July 2015.

[113] B. Chen and L. Wang, "Robust transmission planning under uncertain generation investment and retirement," *IEEE Transactions on Power Systems*, vol. 31, no. 6, pp. 5144–5152, Nov. 2016.

[114] C. Peng, P. Xie, L. Pan, and R. Yu, "Flexible robust optimization dispatch for hybrid wind/photovoltaic/hydro/thermal power system," *IEEE Transactions on Smart Grid*, vol. 7, no. 2, pp. 751–762, Mar. 2016.

[115] Y. Zhang, S. Shen, and J. L. Mathieu, "Data-driven optimization approaches for optimal power flow with uncertain reserves from load control," in *2015 American Control Conference (ACC)*, July 2015, pp. 3013–3018.

[116] B. Li, R. Jiang, and J. L. Mathieu, "Distributionally robust risk-constrained optimal power flow using moment and unimodality information," in *2016 IEEE 55th Conference on Decision and Control (CDC)*, Dec. 2016, pp. 2425–2430.

[117] M. Lubin, Y. Dvorkin, and S. Backhaus, "A robust approach to chance constrained optimal power flow with renewable generation," *IEEE Transactions on Power Systems*, vol. 31, no. 5, pp. 3840–3849, Sep. 2016.

[118] Q. Bian, H. Xin, Z. Wang, D. Gan, and K. P. Wong, "Distributionally robust solution to the reserve scheduling problem with partial information of wind power," *IEEE Transactions on Power Systems*, vol. 30, no. 5, pp. 2822–2823, Sep. 2015.

[119] O. Erdinc, "Economic impacts of small-scale own generating and storage units, and electric vehicles under different demand response strategies for smart households," *Applied Energy*, vol. 126, pp. 142 – 150, 2014.

[120] Ameren, Day ahead pricing used for billing RTP service (2016). Available: https://www2.ameren.com/RetailEnergy/RealTimePrices.

[121] A. D. Giorgio and F. Liberati, "Near real time load shifting control for residential electricity prosumers under designed and market indexed pricing models," *Applied Energy*, vol. 128, pp. 119 – 132, 2014.

[122] H. S. Shih, "A mixed-data evaluation in group TOPSIS with differentiated decision power," *Group Decision and Negotiation*, pp. 1–29, 2015.

[123] C. Guo, J. Zhan, and Q. Wu, "Dynamic economic emission dispatch based on group search optimizer with multiple producers," *Electric Power Systems Research*, vol. 86, pp. 8 – 16, 2012.

[124] B. S. Ahn, "Compatible weighting method with rank order centroid: Maximum entropy ordered weighted averaging approach," *European Journal of Operational Research*, vol. 212, no. 3, pp. 552 – 559, 2011.

[125] D. Olson, "Comparison of weights in TOPSIS models," *Mathematical and Computer Modelling*, vol. 40, no. 7, pp. 721 – 727, 2004.

[126] T. Logenthiran, D. Srinivasan, and T. Z. Shun, "Demand side management in smart grid using heuristic optimization," *IEEE Transactions on Smart Grid*, vol. 3, no. 3, pp. 1244–1252, Sep. 2012.

[127] C. Jiang, X. Han, and G. Liu, "A nonlinear interval number programming method for uncertain optimization problems," *European Journal of Operational Research*, vol. 188, no. 1, pp. 1 – 13, 2008.

[128] D. O'Neill, M. Levorato, A. Goldsmith, and U. Mitra, "Residential demand response using reinforcement learning," in *2010 First IEEE International Conference on Smart Grid Communications*, Oct. 2010, pp. 409–414.

[129] R. Kuo and Y. Han, "A hybrid of genetic algorithm and particle swarm optimization for solving bi-level linear programming problem - a case study on supply chain model," *Applied Mathematical Modelling*, vol. 35, no. 8, pp. 3905 – 3917, 2011.

[130] R. Hassan, B. Cohanim, O. De Weck, and G. Venter, "A comparison of particle swarm optimization and the genetic algorithm," in *Proceedings of the 1st AIAA multidisciplinary design optimization specialist conference*, 2005, pp. 1–13.

[131] M. AlRashidi and M. El-Hawary, "A survey of particle swarm optimization applications in electric power systems," *IEEE Transactions on Evolutionary Computation*, vol. 13, no. 4, pp. 913–918, Aug. 2009.

[132] The MathWorks, Running GA with default options 2015 [Online]. Available: http://uk.mathworks.com/help/gads/options-and-outputs.html.

[133] T. Zhou and W. Sun, "Optimization of battery-supercapacitor hybrid energy storage station in wind/solar generation system," *IEEE Transactions on Sustainable Energy*, vol. 5, no. 2, pp. 408–415, Apr. 2014.

[134] J. Trovao, V. Santos, C. Henggeler Antunes, P. Pereirinha, and H. Jorge, "A real-time energy management architecture for multisource electric vehicles," *IEEE Transactions on Industrial Electronics*, vol. 62, no. 5, pp. 3223–3233, May 2015.

[135] T. Lui, W. Stirling, and H. Marcy, "Get smart," *IEEE Power and Energy Magazine*, vol. 8, no. 3, pp. 66–78, May 2010.

[136] Wholesale Solar, Power for home appliances, Jun. 2014 [Online]. Available: http://www.wholesalesolar.com/StartHere/HowtoSaveEnergy/PowerTable.html.

[137] Ehow, How does an appliance work 2015 [Online]. Available: http://www.ehow.com.

[138] Popular mechanics, How it works: water heater 2015 [Online]. Available: http://www.popularmechanics.com/home/interior-projects/how-to/a153/1275141/.

[139] Family friendly search, How does an electric radiator work 2015 [Online]. Available: http://familyfriendlysearch.com/heating-your-home-but-how-does-an-electric-radiator-work/.

[140] Y. Khan, V. R. Khare, J. Mathur, and M. Bhandari, "Performance evaluation of radiant cooling system integrated with air system under different operational strategies," *Energy and Buildings*, vol. 97, pp. 118 – 128, 2015.

[141] L. Pérez-Lombard, J. Ortiz, and C. Pout, "A review on buildings energy consumption information," *Energy and Buildings*, vol. 40, no. 3, pp. 394 – 398, 2008.

[142] M. Heleno, M. A. Matos, and J. A. P. Lopes, "Availability and flexibility of loads for the provision of reserve," *IEEE Transactions on Smart Grid*, vol. 6, no. 2, pp. 667–674, Mar. 2015.

[143] S. Sarykalin, G. Serraino, and S. Uryasev, "Value-at-risk vs. conditional value-at-risk in risk management and optimization," in *Tutorials in Operations Research INFORMS*, 2008, pp. 270–294.

[144] R. Khodabakhsh and S. Sirouspour, "Optimal control of energy storage in a microgrid by minimizing conditional value-at-risk," *IEEE Transactions on Sustainable Energy*, vol. 7, no. 3, pp. 1264–1273, July 2016.

[145] A. Shapiro and A. Kleywegt, "Minimax analysis of stochastic problems," *Optimization Methods and Software*, vol. 17, no. 3, pp. 523–542, 2002.

[146] B. P. G. V. Parys, D. Kuhn, P. J. Goulart, and M. Morari, "Distributionally robust control of constrained stochastic systems," *IEEE Transactions on Automatic Control*, vol. 61, no. 2, pp. 430–442, Feb. 2016.

[147] Austin Energy Company, Approved rates schedules for city of Austin 2016 [Online]. Available: http://austinenergy.com/wps/portal/ae/rates/approved-rates-schedules/approved-rates-schedules-for-city-of-austin/.

[148] Weather Underground, The outdoor temperature in Austin 2013 [Online]. Available: https://www.wunderground.com/history/airport/KATT/2013/8/6/.

[149] J. Lofberg, "Yalmip : a toolbox for modeling and optimization in MATLAB," in *2004 IEEE International Symposium on Computer Aided Control Systems Design*, Sep. 2004, pp. 284–289.

[150] Jos F. Sturm, *Using SeDuMi, A MATLAB Toolbox for Optimization over Symmetric Cones*, 2015.

[151] S. Zymler, D. Kuhn, and B. Rustem, "Distributionally robust joint chance constraints with second-order moment information," *Mathematical Programming*, vol. 137, no. 1-2, pp. 167–198, 2013.

[152] Y. F. Du, L. Jiang, Y. Z. Li, and Q. H. Wu, "A robust optimization approach for demand side scheduling under energy consumption uncertainty of manually operated appliances," *IEEE Transactions on Smart Grid*, vol. PP, no. 99, pp. 1–1, 2017.

[153] Y. F. Du, L. Jiang, Y. Z. Li, J. Counsell, and J. S. Smith, "Multi-objective demand side scheduling considering the operational safety of appliances," *Applied Energy*, vol. 179, no. Supplement C, pp. 864 – 874, 2016.

[154] S. Maharjan, Q. Zhu, Y. Zhang, S. Gjessing, and T. Basar, "Dependable demand response management in the smart grid: A Stackelberg game approach," *IEEE Transactions on Smart Grid*, vol. 4, no. 1, pp. 120–132, Mar. 2013.

[155] Y. F. Du, L. Jiang, C. Duan, Y. Z. Li, and J. S. Smith, "Energy consumption scheduling of HVAC considering weather forecast error through distributionally robust approach," *IEEE Transactions on Industrial Informatics*, vol. PP, no. 99, pp. 1–1, 2017.

[156] G. K. H. Larsen, N. D. van Foreest, and J. M. A. Scherpen, "Distributed MPC applied to a network of households with micro-CHP and heat storage," *IEEE Transactions on Smart Grid*, vol. 5, no. 4, pp. 2106–2114, July 2014.